Freie Universität Berlin

# Engineering high specificity peptide inhibitors of a promiscuous protein-protein interaction domain with implications in cystic fibrosis.

Inaugural Dissertation

to obtain the academic degree

d o c t o r  r e r u m  n a t u r a l i u m (Dr. rer. nat.)

submitted to the Department of

Biology, Chemistry, and Pharmacy of Freie Universität Berlin

by

Dipl. Biol. Lars Vouillème from Berlin

2012

Dieser Arbeit wurde in der Gruppe "Molekulare Bibliotheken" des Institutes für Medizinische Immunologie der Charité-Berlin unter der Leitung von Dr. Rudolf Volkmer und unter der Betreuung von Dr. Prisca Boisguérin angefertigt.

This work was realized from July 2008 till February 2012 in the "Molecular Libraries and Recognition" group of Dr. Rudolf Volkmer at the Institute of Medical Immumologie of Charité-Berlin and supervised by Dr. Prisca Boisguérin.

1. Gutachter: Dr. Rudolf Volkmer

2. Gutachter: Prof. Dr. Christian Freund

Disputation am: 02.05.2012

# I        Contents

## II List of figures

# III        List of tables

# 1        Summary

Cystic Fibrosis (CF) is one of the most common lethal hereditary diseases among caucasians and affects multiple organs in humans, resulting in an average life expectancy of about 37 years. The most abundant mutation leading to the symptoms of CF is the single deletion of a Phe in the sequence of an ion channel involved in CF ($\Delta$F508-Cystic Fibrosis Conductance Regulator or $\Delta$F508-CFTR) resulting in a reduced ability of epithelial cells to transport $Cl^-$-ions across the plasma membrane. This causes an osmotic imbalance, causing the airway surface mucus in the lung to thicken, which in turn prevents airway cilia from executing effective mucus clearance which leads to the symptoms of CF. Emerging chronic infections with bacteria like *Staphylococcus aureus* and *Pseudomonas aeruginosa* further reduce lung functionality, and are the main reasons for patient mortality. Therefore, a key therapeutic goal to reduced CF-patient morbidity and mortality is the restoration of sufficient mutant CFTR activity to ameliorate chronic lung infections.

Different classes of therapeutic agents are being developed to address the folding defect ('correctors') and the gating defect ('potentiators') of $\Delta$F508-CFTR, but 'stabilizers' that specifically address the half-life deficiency have not yet been identified.

The PDZ containing proteins CAL (CFTR-Associated Ligand) and its antagonists NHERF1 and NHERF2 ($Na^+/H^+$ Exchanger Regulatory Factor 1/2) compete for CFTR binding. CAL contains one (CALP), and each NHERF protein contains two PDZ domains (N1P1, N1P2, N2P1 and N2P2) that control both the activity and the cell surface abundance of CFTR. NHERF proteins increase CFTR activity at the apical membrane, whereas CAL promotes its lysosomal degradation. Thus, to explore novel therapeutic strategies for increasing the cell-surface abundance of CFTR, the goal was to design a selective inhibitor of the CFTR:CAL interaction that does not affect the biologically relevant PDZ competitors NHERF1 and NHERF2.

This work represents the development and execution of a unique SPOT-synthesis approach to engineer selective peptide based inhibitors for CALP, thus increasing $Cl^-$-efflux across the plasmamembrane of human lung epithelial cells

stably expressing ΔF508-CFTR (CFBE-ΔF cells). This approach allowed us to: (I) identify the natural highest affinity ligand of CAL (SSR5; $K_i$ = 21.4 ± 1.7 μM) among 6223 C-terminal peptides, (II) further enhance its CALP affinity beyond the SSR5 binding affinity, and (III) totally abolish NHERF binding. The resulting decamer peptide, ANSRWPTSII (iCAL36; $K_i$ = 17.3 ± 4.3 μM), was validated by NMR studies to act as a competitive inhibitor of the CFTR:CALP interaction, and its biological functionality was ascertained by determination of Cl$^-$-efflux across the plasmamembrane of polarized CFBE-ΔF cell monolayers. Thus, iCAL36 is able to enhance Cl$^-$-efflux by 25 % at 500 μM, and is exhibits additive effects with the small molecule ΔF508-CFTR corrector Corr-4a. This finding was demonstrated by combinatorial treatments in Ussing chambers. However, mass spectrometry and pull down analysis revealed a single off-target effect with the PDZ domain of the Tax-interacting protein-1 (Tip-1 ). To address this undesired peptide binder, we again utilized our peptide engineering approach combined with X-ray analysis. The result was another CALP inhibitor, named iCAL42 (ANSRLPTSII; $K_i$ = 10.8 ± 0.2 μM) with single PDZ-specificity and with a positive effect on Cl$^-$-efflux. iCAL42 was created by a single Trp-Leu substitution, and specificity was demonstrated by LC/MS/MS analysis combined with pull-down assays. For both peptides, cell internalization was initially achieved using the commercially available delivery reagent BioPORTER™ and demonstrated by fluorescence microscopy. However, to test if the internalization rate of our engineered peptide is sufficient for a therapeutic application, we coupled iCAL36 covalently to cell penetrating peptides (CPPs) and tested for: (I) uptake (confocal microscopy), (II) cytotoxicity (CCK-8 assay), and (III) biological functionality (Ussing chamber). We were able to clearly demonstrate that the chosen CPPs (Penetratin and MPG) were able to internalize iCAL36 into CFBE cells without relevant cytotoxicity, up to a concentration of 100 μM. Ussing chamber experiments revealed a Cl$^-$-efflux of 21 % (p = 0.2) at a 5-fold lower concentration (100 μM) of Penetratin-iCAL36 compared to *F*\*-iCAL36 (500 μM):BioPORTER™. This demonstrates the improved effectiveness of therapeutic peptide delivery by this CPP.

These results show that our engineering process of CALP inhibitors may provide a template that is useful for investigating the cell-biological roles and

therapeutic potential of other PDZ domains. Additionally, the may help to explore the prospect of combination approaches aimed at parallel treatment of the biogenesis and stability defects of the most common disease associated CFTR allele ΔF508 with the potential to attenuate the symptoms of patients with cystic fibrosis in future therapeutic applications.

# 2      Zusammenfassung

Mukoviszidose (Cystische Fibrose - CF) ist eine der häufigsten, tödlichen Erbkrankheiten unter Kaukasiern mit einer durchschnittlichen Lebenserwartung von ca. 37 Jahren. CF wird meist durch die Deletion eines Phenylalanins innerhalb eines Chloridkanales (ΔF508-Cystic Fibrosis Transmembrane Conductance Regulator; ΔF508-CFTR) hervorgerufen, was zu einer verminderten Chloridionen-Ausscheidung an der Zellmembran von Epithelzellen führt. Die daraus resultierende Verdickung des durch die Epithelzellen gebildeten Schleims (Mukus), erschwert oder verhindert dessen Abtransport durch die Zilien der Zellen. Die hierdurch entstehenden Infektionen mit Bakterien wie *Staphylococcus aureus* und *Pseudomonas aeruginosa* verringern die schon beeinträchtigte Lungenfunktionalität noch zunehmend, was die hohe Mortalität von CF-Patienten bedingt.

Ein Schwerpunkt heutiger CF-Therapien liegt in der Wiederherstellung der CFTR-Aktivität, um u. A. die chronischen Lungeninfektionen zu verhindern. Diesbezüglich wurden bereits verschiedene Therapeutika entwickelt, die entweder die Fehlfaltung des ΔF508-CFTR verhindern (Korrektoren) oder dessen verminderter Aktivität entgegenwirken (Potenzierer) sollen. Spezifische "Stabilisatoren", welche die CFTR-Halbwertszeit an der Zellmembran und somit deren Aktivität erhöhen können, wurden bisher noch nicht entwickelt.

Im Kontext eben dieser "Stabilisatoren" spielen vor allem die PDZ Proteine CAL (CFTR-Associated Ligand) und seine Antagonisten NHERF1 und NHERF2 ($Na^+/H^+$ Exchanger Regulatory Factor 1/2) ein große Rolle. Sie konkurrieren um die Bindung an den CFTR und kontrollieren sowohl den CFTR-Transport an die Zelloberfläche als auch dessen Aktivität. CAL enthält eine (CALP) und jede der NHERF Proteine zwei PDZ-Domänen (N1P1, N1P2, N2P1 und N2P2), wobei die NHERF Proteine die CFTR-Aktivität und Menge an der apikalen Membran erhöhen, während CAL dessen lysosomalen Abbau fördert. So würde die Entwicklung spezifischer CFTR:CAL Inhibitoren, die keine weiteren Interaktionen zu anderen PDZ Proteinen aufweisen, die CFTR-Menge an der Plasmamembran erhöhen bzw. stabilisieren.

Die hier vorgestellte Arbeit beschreibt die Entwicklung einer neuen Strategie für die Entwicklung von selektiven, peptid-basierten CALP-Inhibitoren. Diese sollen den $Cl^-$-Ausstoß an der Plasmamembran von humanen Lungenepithelzellen, die den ΔF508-CFTR exprimieren (CFBE-ΔF Zellen), erhöhen. Dieser auf der SPOT-Synthese basierende Ansatz erlaubte es uns: (I) den besten natürlichen CALP-Binder unter 6223 humanen C-terminalen Peptiden zu identifizieren (SSR5; $K_i = 21.4 \pm 1.7$ μM), (II) dessen Affinität weiter zu erhöhen und (III) dabei die Bindung zu den NHERF-Proteinen komplett zu unterbinden. Das hierbei entwickelte dekamere Peptid iCAL36 (ANSRWPTSII; $K_i\,CALP = 17.3 \pm 4.3$ μM) agiert nachweislich als kompetitiver Inhibitor der CFTR:CALP Interaktion, was durch NMR-Analysen nachgewiesen werden konnte. In CFBE-ΔF Zellen führt iCAL36 (500 μM) zu einer Erhöhung des $Cl^-$-Ausstoßes um 25 % (Ussing Kammer, $p = 0.0008$). Eine gleichzeitig Anwendung von iCAL36 mit dem CFTR-Korrektor Corr-4a führt zudem zu einer entsprechenden weiteren Erhöhung des $Cl^-$-Ausstoßes an der Zellmembran, was die Kombinierbarkeit von iCAL36 mit "small molecule"-Korrektoren demonstriert.

Jedoch zeigten MS/MS Analysen sowie pull-down Bestimmungen, dass iCAL36 noch eine weitere PDZ-Interaktion mit dem *Tax-interacting protein-1* (TIP-1) eingeht. Mit Hilfe unserer Strategie, kombiniert mit Röntgenstrukturanalysen, konnte auch diese Interaktion eliminiert und ein zweiter CALP Inhibitor (iCAL42; ANSRLPTSII; $K_i\,CALP = 10.8 \pm 0.2$ μM) mit absoluter CALP-Spezifität entwickelt

werden. Dieser weist einen zu iCAL36 vergleichbaren positiven Effekt auf den Cl⁻-Ausstoß auf. Die zelluläre Peptidaufnahme (500 µM) wurde hierbei zunächst durch das kommerziell erhältliche Reagenz BioPORTER™ realisiert. Um die Zell-Internalisation weiter zu effektivieren, wurde unser iCAL36-Inhibitor zudem kovalent an zellpenetrierende Peptide (CPPs) gekoppelt und bezüglich (I) ihrer Aufnahme (konfokale Mikroskopie), (II) ihrer Zytotoxizität (Viabilitätsbestimmung) sowie (III) ihrer biologischen Funktionalität (Ussing-Kammer) in CFBE-ΔF Zellen untersucht. Hierbei konnte eindeutig festgestellt werden, das iCAL36 gekoppelt an Penetratin bis zu einer Konzentration von 100 µM ohne auftretende Zytotoxizität aufgenommen werden kann. Zudem zeigt der an der Zellmembran gemessene Cl⁻-Ausstoß von 21 % ($p$ = 0,02) bei einer 5-fach niedrigeren Konzentration im Vergleich zum BioPORTER™:*F*\*-iCAL (500 µM) System die verbesserte Effektivität der Internalisierung.

Der hier vorgestellte Ansatz zur Entwicklung peptid-basierter Hemmstoffe kann durch seine generelle Anwendbarkeit für die zellbiologische Untersuchung von PDZ Domänen im therapeutischen Kontext von Nutzen sein. Zudem spiegelt der kombinatorische Ansatz zur parallelen Behandlung der Biogenese- und Stabilitätsdefekte des häufigsten CF-assoziierten CFTR Allels (ΔF508-CFTR Mutation) die Nutzbarkeit und das Potential unserer Inhibitoren wieder, die Symptome von CF-Patienten zukünftig schneller und besser lindern zu können.

# 3       Introduction

## 3.1   Cystic fibrosis

Cystic fibrosis (CF) is the most common life-threatening autosomal recessive disease among people of European ancestry. In airway epithelia, loss of activity of the cystic fibrosis transmembrane conductance regulator (CFTR), the chloride channel mutated in patients with CF, leads to the breakdown of mucociliary clearance and facilitates the establishment of persistent and ultimately fatal bacterial infections [1]. The Δ*F508* allele, found in ~90% of patients, results in a CFTR-protein that fails to fold correctly in the endoplasmic reticulum (ER) (Figure **1** A) [2, 3]. However, if the folding defect is overcome, the resulting ΔF508-CFTR retains chloride channel activity, although with reduced open probability (Po) (Figure 1 A) [4].
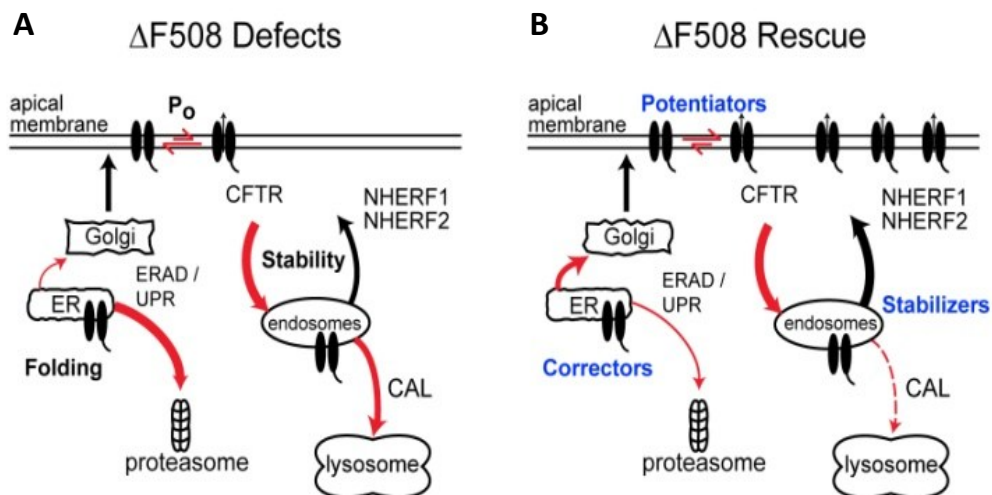


**Figure 1: Defects and strategies to rescue ΔF508-CFTR.**
Endogenous CAL limits ΔF508-CFTR half-life in polarized human airway epithelial cells and represents a potential target for CFTR 'stabilizers.' (**A**) ΔF508-CFTR exhibits three functional defects: (1) a failure to fold properly in the ER, leading to ER associated degradation (ERAD) ("folding"); (2) reduced open probability ("Po") of ΔF508-CFTR channels that are found in the apical membrane; and (3) accelerated breakdown ("stability"). Aberrant flux is highlighted by red arrows. (**B**) Classes of therapeutic agents are being developed to address the folding defect ('correctors') and the gating defect ('potentiators'), but 'stabilizers' that specifically address the half-life deficiency have not yet been identified.

Since only 10-35 % of wild-type channel activity may be required for significant therapeutic benefit [5], our goal is the development of methods to increase the amount of functional ΔF508-CFTR at the apical membrane. Among others CF is characterized by abnormal endocrine and exocrine gland function. In CF, unusually thick mucus leads to chronic pulmonary disease and respiratory infections, insufficient pancreatic and digestive function, and abnormally concentrated sweat. Current treatments for CF generally focus on controlling infections through antibiotic therapy and promoting mucus clearance by use of postural drainage and chest percussion.

## 3.2  Targeting CFTR

Over the past twenty years, 'corrector' and 'potentiator' compounds have been identified, addressing the primary folding and gating defects of ΔF508-CFTR, respectively (Figure 1B) [6, 7]. Potentiator compounds like Genistein [8] that have been widely used in research assays and are as important as compounds, like CFpot-532 [7, 9], that have been developed by the pharmaceutical industry for clinical use. Furthermore, several classes of small molecule correctors like Corr-4a [6] or VRT325 [7] have been identified, and there is now a growing prospect that the maturation and ion-channel activity of ΔF508-CFTR can be pharmacologically enhanced. However, the rescued CFTR-protein is comparatively unstable at physiological temperatures [10-12]. Optimal restoration of ΔF508-CFTR function is therefore likely to require combinatorial treatment of each of its three defects: folding, open probability, and stability (Figure 1 A).

To identify a new class of 'stabilizers' extending the apical-membrane half-life of ΔF508-CFTR, we targeted a key regulator of its post-endocytic trafficking and degradation: CFTR-associated ligand (CAL). CAL negatively regulates ΔF508-CFTR cell-surface abundance through its PDZ (PSD-95, Dlg, and ZO-1) domain [13]. However, CFTR interacts not only with CAL, but also with the $Na^+/H^+$ exchanger regulatory factors NHERF1 and NHERF2. These proteins counteract CAL's effect,

enhancing the activity and the abundance of ΔF508-CFTR at the apical membrane [14-16].

## 3.3 PDZ-Domains

Within a cell, the activity of an individual protein is determined not only by its abundance and stereochemical identity, but also by its localization to specific compartments and its regulatory interactions with other proteins. As a result, the processes of protein trafficking and assembly are carefully regulated by networks of partners, generally expressing combinations of modular protein-protein interaction domains (PPIDs). With more than 200 representatives, the human PDZ domains – characterized by homology to the founding members PSD-95, Dlg, and ZO-1 – are among the most common PPIDs [17-19]. PDZ domains usually consist of approximately 90 amino acid residues that form one or two α-helices (αA-αB) as well as six β-sheets (βA–βF) [17, 20, 21]. The conserved elements can vary in their linking sequences but a highly conserved fold always remains intact (Figure 2). One characteristic element of PDZ domains is the GLGF-loop, a binding motif between the βA and βB sheets whose side chains form a hydrophobic cavity for the C-terminal amino acid of the ligand.
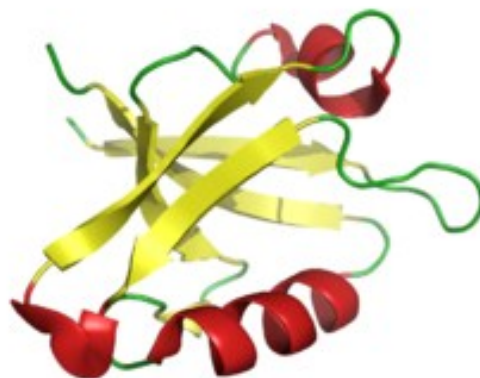


**Figure 2: Structure example of the CAL PDZ domain.**
The structure of the CFTR Associated Ligand protein (CAL; GOPC) PDZ domain [22] clearly reveals the canonical folding consisting 6 β-sheets and two α–helices.

Found either singly or in tandem arrays in over 100 proteins, PDZ domains generally bind to the extreme C-terminal residues of their cognate partners, facilitating the assembly of molecular scaffolds that organize the complex physiological functions of highly differentiated cells. Thus, PDZ proteins are key elements in assembling functional protein complexes and controlling cellular activities. However, the multivalent structure of PDZ proteins and the sequence promiscuity of PDZ:target interactions have complicated efforts to decipher their cell biological roles or to exploit them as sites of therapeutic intervention.

In epithelial tissues, PDZ proteins are essential for the organization of tight junctions between cells and for the establishment and maintenance of apical-basolateral polarization. In particular, a cluster of epithelial PDZ proteins that share overlapping binding motifs regulates the apical membrane abundance and functional activity of the CFTR, the chloride channel mutated in CF-patients [1].

## 3.4   Protein-Protein interactions - PPIs

One way to modulate cell properties is to disrupt or change natural protein-protein interactions (PPIs) by developing selective inhibitors of specific protein domains that permit an interaction to the target domain with even higher affinity than the naturally occurring PPI.A PPI is an interaction between two or more proteins that is mainly based on non-covalent interactions such as van der Waals forces, hydrogen bonds, and electrostatic interactions of near surface protein-domain amino acid residues. PPIs play a key role in virtually all biological protein based processes like signal transduction and transport functions of the cytoskeleton, and have therefore been one of the main topics of life science research over the past years. The entirety of human protein-protein interactions is a network of approximately 650,000 interactions [23] and is commonly denoted as "interactome".

The functional unit of a PPI is the protein-protein interaction domain (PPID), and the variety and complexity of PPIDs are immense. PPIDs are involved in

modulating and controlling the vast majority of signal transduction pathways in humans.

Consequently, the development of new biomolecules to target PPID interactions is of major interest, and has the potential to illuminate cellular functionality and new therapeutic targets. The study and modulation of PPIDs is very challenging, and there is a great diversity of different biochemical and biophysical methods involved in PPI-research. These include SPOT-Synthesis, yeast two-hybrid, and phage-display.

## 3.5  Screening PPIs with peptide/protein libraries

Since protein–protein interactions are key players to understand biological events there are a multitude of methods to detect them. Each of the approaches has its own strengths and weaknesses, especially with regard to the sensitivity and specificity of the method. The first challenge is always the identification of a suitable interaction partner for a particular protein of interest. The three primarily used methods for discovering PPIs are SPOT-Synthesis [24], yeast two-hybrid system (Y2H) [25], and phage display (PD) [26]. However, combination of different methods can also be of great value for the identification of PPIs, e.g. by the combination of pull down techniques and LC/MS/MS analyses [27].

The Y2H approach allows the study of protein-protein or protein-peptide interactions in *Saccharomyces cerevisiae* with posttranslational modifications occurring in eukaryotes such as glycosylation, palmitoylation or folding by chaperones (Figure 3). The robustness and low costs of yeast also allows for high throughput screening of many interaction partners.

However, the interaction with a particular protein takes place in the nucleus where transcription occurs. This can be problematic due to fact that proteins can behave differently in the environment where they usually occur. The appearance of different folding behavior, the fact that fusion proteins are overexpressed and may not usually occur in the same cell compartment, and the partly different modifications in yeast compared to other eukaryotic organisms can lead to false

positive results. Thus, there is a necessity for strict validation using other methods, such as   fluorescence resonance energy transfer (FRET), co-immunoprecipitation, surface plasmon resonance, fluorescence spectroscopy, X-ray analysis, or nuclear magnetic resonance (NMR) spectroscopy.
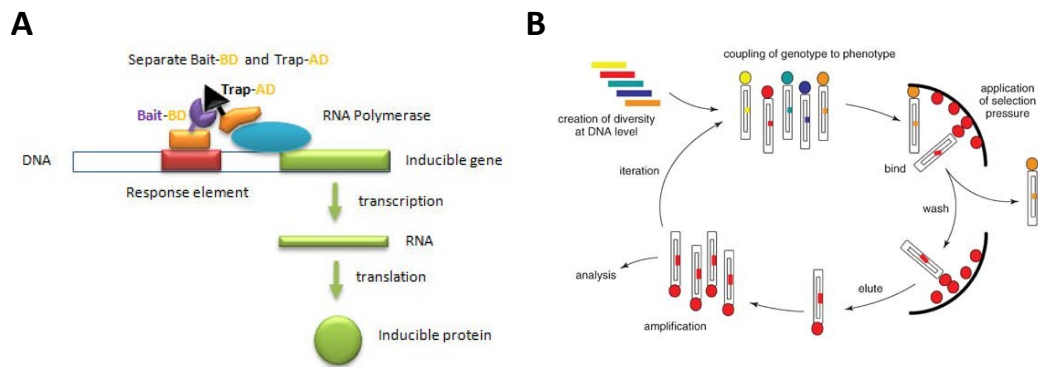


**Figure 3: Yeast two-hybrid system and Phage Display to screen PPIDs.**
**(A) Yeast-two-hybrid:** Transcription factors are often separated into distinct domains interacting with- and activating the transcription machinery. The DNA Binding Domain (DNA-BD) mostly contains motifs that are necessary for DNA-binding whereas the Activation Domain (AD) is necessary for the binding to effector proteins like the RNA-Polymerase. The genetic fusion of a "bait" protein to the DNA-BD as well as a "trap"(or "prey") protein to the AD allows transcription only if a PPI occurs. For this purpose, separate plasmids for BD and AD genes of choice are added to yeast. If both fusion genes are transcribed and translated into the respective proteins, then the transcription of the inducible gene can occur with the PPI as absolute necessity. Figure source:http://employees.csbsju.edu/hjakubowski/classes/ch331/bind/olbindtransciption.html
**(B) Phage display**: The creation of diversity at the DNA level, e.g. by cDNA libraries is the first step of the general phage display cycle and is later translated into phenotypic diversity by displaying proteins or peptides on the phage surface. An interaction molecule coupled to a solid phase reflects the selection pressure (*in vitro* selection). After eliminating unspecific binding events by several washing steps the interacting phage can be eluted and amplified for further analysis. Figure source: Curr. Protoc. Neurosci.51:5.12.1-5.12.27. © 2010 by John Wiley & Sons, Inc.

PD is another way to study PPIs for antibody selection, protein modification, or the investigation of signal transduction pathways. Generally, a filamentous phage (most often M13 phage) is used to display a peptide or protein on their surface by genetic fusion to one of the coat proteins (most often pIII) followed by transformation to *Escherichia coli* (*E.coli*). The resulting coat protein unifies the phenotype and the genotype, which is a very important feature of PD. Thus, a simultaneous polypeptide presentation on the phage surface as well as genetic isolation of the respective peptide or protein occurs, allowing analysis and amplification of the target protein (*in vitro* selection; Figure 3 B). Display techniques have allowed the preparation and characterization of many new

human antibodies and other proteins [28]. The fact that their affinities can be increased by mutagenesis also reflects PD as an approach capable of engineering new binding partners. Several companies now offer to produce virtually any antigen from large, sometimes semi synthetic, PD antibody libraries. This demonstrates the potential for the growth of biotechnology that results in the production of these products once the DNA libraries are produced.

The underlying principal of Y2H as well as of PD is the creation of diversity at the DNA level, e.g. by the production of cDNA libraries. This is an important fact distinguishing these methods from the third method suitable for screening and more importantly for engineering PPIs: SPOT-Synthesis.

## 3.6   SPOT Synthesis

The SPOT synthesis is a robust technique for parallel chemical synthesis of peptides on membrane supports. It was first published in 1992 by Ronald Frank [29], and has become a highly recognized method for the investigation and engineering of protein ligands over the last two decades. In general, spatially addressable immobilization of putative ligands by solid phase peptide synthesis (SPPS) is followed by the incubation with a biological, tagged sample [30] (Figure 4). Therefore, SPOT synthesis is one player on the array technology field, and fulfils the main characteristics of an array technology. Software supported data read-out of the miniaturized array identifies signals or "spots" as places where interactions occur. As previously mentioned, SPOT synthesis is independent of the creation of genetic diversity, making it suitable especially for engineering of new peptide based ligands with desired properties.
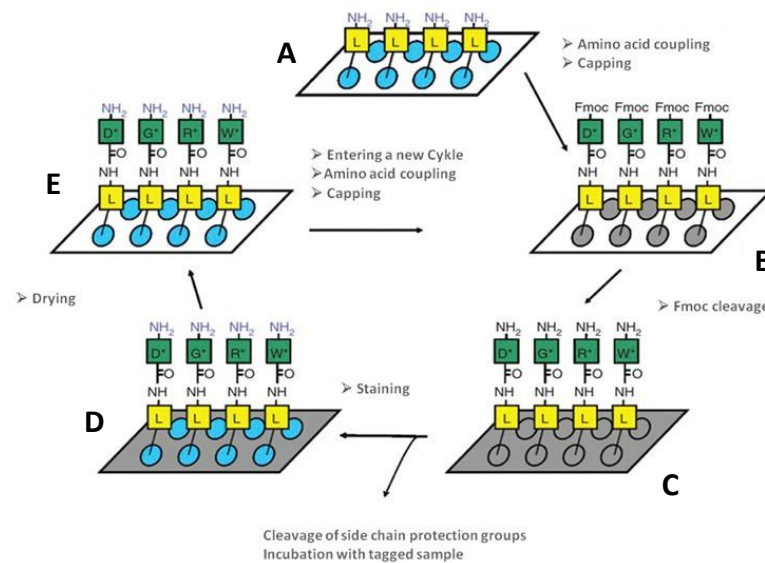
**Figure 4: Principle of SPOT synthesis on membrane supports.**
(**A**) First, a ß-alanine-linker is coupled on the solid phase, e.g. cellulose ("L" within a yellow box). (**B**) Coupling of the desired Fmoc-protected and OpfP activated amino acid (green box). The star reflects the side chain protection groups that are necessary to exclusively permit N-terminal elongation. Gray Spots indicate wet areas on the solid phase. (**C**) Fmoc cleavage under basic condition (piperidine) in order to get free amino groups for the next coupling cycle. The grey color shows solvent treatment of the solid phase. (**D**) The free amino groups are stained with bromophenol blue (BPB; blue dots). (**E**) Dried solid phase while the spots remain stained. Figure source: [30]

The possibility to directly change the capture molecule by substitutional analysis (single mutations) double or triple permutations, the introduction of D- or non natural amino acids, as well as peptoid building blocks [24, 31] within the peptide sequence favors the SPOT-synthesis over Y2H and PD for many applications.

## 3.7   Crossing biological membranes – Penetratin and MPG

Effective delivery of therapeutic agents into the cytosol of target cells remains a major obstacle in the medical field. The use of cell penetrating peptides (CPPs) has become one of the most important tools for the internalization of a wide range of molecules, including pharmaceuticals [32-34]. They are generally rich in basic amino acid residues, and are often derived from proteins involved in signal transduction. Today, due to their high potential to efficiently cross membranes

and transport cargoes, characterizing and optimizing CPPs has become a major goal over the last decade [34-39].

Despite the high number of biological applications using CPPs, there is no generalizable protocol for their use. As a result it is difficult to select a specific CPP for a distinct application. Based on our knowledge regarding CPP-uptake in different cell lines [40, 41], we have selected two CPPs to internalized the putative CAL PDZ inhibitors: MPG [42] and Penetratin [43].

MPG contains a C-terminal hydrophilic region consisting of a lysine rich motif derived from the nuclear localization sequence (NLS) of the SV40 large T antigen (KKKRKV), and an N-terminal hydrophobic domain from the fusion sequence of the HIV protein gp41 (GALFLGFLGAAGSTMGA). The hydrophilic domain is important for the solubility of the carrier peptide, as well as the intracellular trafficking and interaction with nucleic acids. The hydrophobic domain is mainly required for initial interactions with the plasma membrane prior to uptake [42, 44, 45].

MPG is one of the most extensively characterized CPPs. It was originally created for the delivery of small nucleic acids by the formation of peptide based nanoparticles (PBNs) through non covalent electrostatic or hydrophobic interactions [42].

The use of a specific mechanism of cellular uptake of PBNs depends on their ability to form stable nanoparticles with the cargoes, their structural polymorphism, and on their interaction with membrane components. Most PBNs enter the cell independent of endosomal events, and were used with a large variety of different cell types and animal models [46, 47].

Penetratin is a CPP derived from the homeodomain of *Drosophila* Antennapedia homoeprotein [48]. It was extensively investigated by Alain Prochiantz and colleagues, and it was found to be a peptide with the ability to form different structures depending on its environment which should also be true for almost all CPPs investigated later. Thus, the lipid interaction of Penetratin seems to be a reciprocal process affecting both partners. For example, in the presence of anionic phospholipids, the peptide exhibits a coiled structure, but becomes disordered in an aqueous environment. Depending on

concentration, Penetratin tends to adopt an α-helical [43] (peptide/lipid ratio: 1/325) or anti-parallel ß-sheet conformation (peptide/lipid ratio 1/10) [49, 50]. The heterogenic nature of Penetratin is not only shown by its dependence on concentration, but also on pH and temperature, as well as the presence of tags. In contrast to MPG, the cargoes were mostly covalently bound to Penetratin, showing their different uptake mechanisms.

The behavior of CPPs depends on the used cell line [40]. This means it is necessary to analyze each selected CPP in the desired disease related cell type. New insight into the trafficking of CPPs with their cargoes into human bronchial epithelial cell lines will provide essential information to develop new tools for biological approaches, as well as for the treatment cystic fibrosis.

Today, the number of CPPs that reach clinical trials is constantly growing, and the applications are pervasive. Their potential of application extends over a wide variety of diseases including keloid scarring, myocardial infarction, pain, hearing loss, stroke, and cancer [51].

# 4        Objectives and Strategy

PDZ domains are highly conserved throughout all domains of life: from bacteria to humans [52]. Consistent with their structural homology, PDZ domains exhibit overlapping recognition sequences, meaning that a given partner typically can interact with multiple domains. Eight years ago, a general and efficient procedure for profiling PDZ-peptide interactions was proposed. The specificity and selectivity covering the complete PDZ-ligand sequence space were evaluated by combining SPOT synthesis and $K_d$ prediction [53]. As predicted, there was substantial overlap of ligand sequences among the three PDZ domains analyzed (AF6, ERBIN and SNA1). Additionally, all of these peptide sequences bound with $K_d$ values between 50- 100 µM. Although recent studies have revealed encouraging diversity among PDZ sequence preferences [54, 55], it is not yet possible to predict a peptide inhibitor for a single PDZ domain while the target may have overlapping recognition motifs with other PDZ domains.

Therefore, the synthesis of selective peptide based inhibitors for a unique PDZ domain and its biochemical characterization are main objectives of this work. Due to the fact that PDZ domains have a well-defined binding pocket, they are promising targets for drug discovery. A suitable system to address this question is the intracellular trafficking of CFTR in the context of CF. CFTR is mainly regulated via three PDZ domain containing proteins (CAL, NHERF1 and NHERF2). The PDZ containing proteins CAL (also called GOPC) [1, 56] and its antagonists NHERF1 and NHERF2 [1, 57] compete for the binding to CFTR. CAL contains one PDZ domain (CALP), and each NHERF protein has two (N1P1, N1P2, N2P1 and N2P2). Through these domains, CAL NHERF1, and NHERF2 control both the activity and the cell surface abundance of CFTR. NHERF family members increase CFTR activity at the apical membrane, whereas CAL promotes its lysosomal degradation. Thus, to explore novel therapeutic strategies for increasing the cell-surface abundance of CFTR, the goal was to design a selective inhibitor of the CFTR:CAL interaction that does not affect the biologically relevant PDZ competitors NHERF1 and NHERF2 [1, 57].
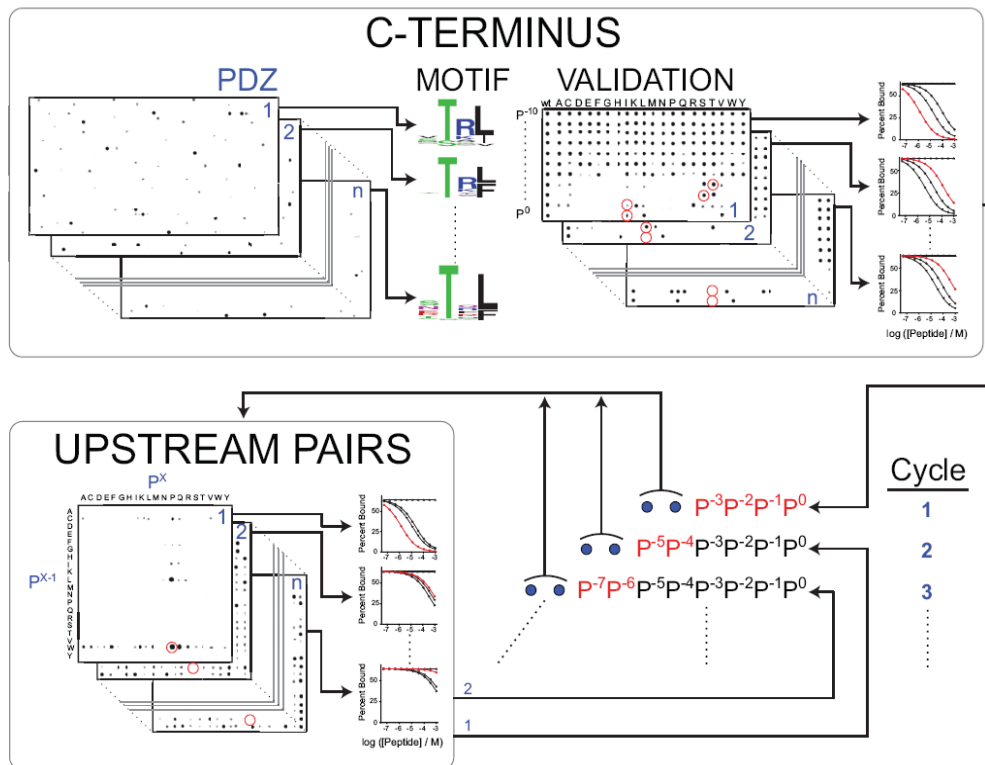
**Figure 5: An iterative approach for engineering selective PDZ inhibitors.**
Upper panel: Inverted HumLib arrays of human C-terminal sequences were incubated with individual PDZ domains, and immunoblotted with antibody to detect bound PDZ protein as a function of peptide sequence. Top binding sequences were aligned (motifs), and arrays of individual side-chain substitutions were synthesized (validation) to establish C-terminal sequence motifs with affinity for the target, but not the counter-target domains. Candidate peptides were synthesized and tested via FP inhibition assay for binding to all five domains. Lower panel: Once a selective C-terminal sequence was established for positions P-3 to P0, combinatorial libraries were prepared, adding all possible combinations of the next two N-terminal amino acids to the core sequence. After PDZ domain incubation, pairs of amino acids were selected for further analysis based on strong binding to the CAL PDZ domain and weak or reduced binding to the NHERF domains. FP inhibition was used to validate the solid-state binding data, and once a residue pair was added to the core sequence, the pairwise N-terminal extension process was iterated.

Here, a strategy for the parallel evolution of inhibitor affinity and selectivity by optimizing binding determinants distributed along the length of a decameric sequence is presented. The general approach [58] involves the synthesis of a variety of different cellulose-bound peptide libraries with the method of inverted peptides (see materials and methods section) based on SPOT technology [24] – a simple and robust technique for the parallel synthesis of up to 6000 peptides with free C-termini on planar surfaces (spot diameter 1.2 mm) [31]. Promising peptide extensions or sequence modifications are identified, and fluorescence

polarization (FP) assays [59] are later used to determine binding constants. FP also allows us to examine the relative affinity for all five PDZ domains relevant to CFTR trafficking. Each modification is then evaluated for its contribution to the affinity with regards to CAL, and to the loss of affinity for the NHERF PDZ domains.

We employed this general strategy to develop CAL PDZ inhibitors (iCAL) on a time scale relevant to industrial drug target discovery. "First generation" iCAL peptides will be validated by affinity capture, followed by Western blot or LC/MS/MS analyses. If off-targets are observed, we will then iterate the SPOT synthesis approach to develop iCAL of "second generation".

Few peptides are able to freely cross biological membranes. Therefore, therapeutic peptides are generally administered in association with cell penetrating peptides (CPPs). For drugs targeted to function within the cytosol, their successful localization must be evaluated side by side with its biological functionality. The final goal of this PhD-thesis will be the validation of an intracellular delivery and drug efficacy strategy by measurement of $Cl^-$-efflux post-treatment of polarized CFBE-$\Delta$F508 cells with CPP-iCAL conjugates. Since CPPs has been shown to deliver different cargoes including peptides into cells - without disrupting cell integrity - such an approach seems to be promising for a future therapeutical development.

# 5       Materials and methods

## 5.1   Protein Expression and Purification

NHERF1 (SwissProt accession #O14745; N1P1; residues 1 139; N1P2; residues 133-234) and NHERF2 (SwissProt accession #Q15599; N2P1; residues 1 151; N2P2 residues 143-230) constructs were subcloned as described previously [13]. The vectors encoding the wild-type CAL PDZ domain (SwissProt accession #Q9HD26-2; CALP; residues 278-362) have also been described previously [59]. All constructs were verified by DNA sequencing at the Dartmouth Molecular Biology Core Facility. All PDZ constructs were expressed, harvested, and lysed. The lysates were clarified as previously described [13], except that NHERF1 and NHERF2 PDZ domains were expressed in Rosetta 2 (DE3) cells (Novagen). Immobilized metal-affinity and size-exclusion chromatographic (SEC) purification of the PDZ domains of NHERF1, NHERF2 and CAL was performed essentially as previously described for CALP [13, 59]. Proteins were concentrated using Amicon Ultra-15 5000 MWCO (NHERF1 and NHERF2 PDZ domains) or YM-3 concentrators (CAL PDZ domain constructs) (Millipore). Following concentration, proteins were dialyzed into storage buffer: 25-50 mM $NaH_2PO_4$, pH 7.4 (N1P1, N1P2, and N2P1), 25 mM Tris, pH 7.5 (N2P2) or 25 mM Tris, pH 8.5 (CAL PDZ).

TIP-1 (accession # O14907) was expressed and purified similarly except that an N-terminal 10-His tag was used with a modified HRV-3C protease recognition sequence (LEVLFQ*G) upstream of the full-length protein sequence. Following TIP-1 purification via immobilized metal-affinity chromatography, the protein was applied to a Superdex S75 gel filtration column (GE Healthcare) and eluted in 50 mM Tris pH 8.5, 150 mM NaCl, 0.1 mM TCEP, 0.02 % $NaN_3$. Human rhinovirus 3C protease (Novagen) was added to the pooled protein fractions at a 1:30 mass ratio and incubated at 4 °C for 48 hr. Following cleavage the protein was passed through a 1mL HisTrapHP column (GE Healthcare) equilibrated in 20 mM imidazole, 25 mM Tris pH 8.5, 150 mM NaCl, 0.1 mM TCEP, 0.02 % $NaN_3$. The protein was further purified on a Superdex S75 column as described above.

Following gel filtration the protein was dialyzed into gel filtration buffer with 5 % glycerol. Thermal stability of all constructs was confirmed at temperatures previously used for *in vitro* binding measurements [59].

**Table 1:** PDZ domains

| PDZ domain | amino acids # | molecular weight (g / mol) | protein name / UniProt ID | ε (L·mol$^{-1}$·cm$^{-1}$) |
|------------|---------------|----------------------------|---------------------------|----------------------------|
| N1P1 | 162 | 17556.6 | NHERF1 / O14745 | 3105 |
| N1P2 | 208 | 23128.5 | NHERF1 / O14745 | 1615 |
| N2P1 | 173 | 19591.9 | NHERF2 / Q15599 | 12615 |
| N2P2 | 160 | 17671.6 | NHERF2 / Q15599 | 3105 |
| CALP | 131 | 14632.2 | CAL / Q9HD26 | 2980 |
| TIP-1 | 143 | 16081.2 | TIP-1 / O14907 | 8480 |

Calculation of ε was done according to the ProtParam tool of the Expasy website.

Sequence of N1P1
==============

MGHHHHHHHH   HHSSGHIEGR   HMMSADAAAG   APLPRLCCLE   KGPNGYGFHL

HGEKGKLGQY   IRLVEPGSPA   EKAGLLAGDR   LVEVNGENVE   KETHQQVVSR

IRAALNAVRL   LVVDPETDEQ   LQKLGVQVRE   ELLRAQEAPG   QAEPPAAAEV

QGAGNENEPR EA

Sequence of N1P2
==============

MGHHHHHHHH   HHSSGHIEGR   HMNENEPREA   DKSHPEQREL   RPRLCTMKKG

PSGYGFNLHS   DKSKPGQFIR   SVDPDSPAEA   SGLRAQDRIV   EVNGVCMEGK

QHGDVVSAIR AGGDETKLLV VDRETDEFFK KCRVIPSQEH LNGPLPVPFT NGEIQKENSR

EALAEAALES PRPALVRSAS SDTSEELNSQ GDPKETAAAK FERQHMDS

Sequence of N2P1
==============

MGHHHHHHHH   HHSSGHIEGR   HMMAAPEPLR   PRLCRLVRGE   QGYGFHLHGE

KGRRGQFIRR   VEPGSPAEAA   ALRAGDRLVE   VNGVNVEGET   HHQVVQRIKA

VEGQTRLLVV   DQETDEELRR   RQLTCTEEMA   QRGLPPAHDP   WEPKPDWAHT

GSHSSEAGKK DVSGPLRELR PRL

Sequence of N2P2

MGHHHHHHHH   HHSSGHIEGR   HMPLRELRPR   LCHLRKGPQG   YGFNLHSDKS

RPGQYIRSVD   PGSPAARSGL   RAQDRLIEVN   GQNVEGLRHA   EVVASIKARE

DEARLLVVDP ETDEHFKRLR VTPTEEHVEG PLPSPVTNGT SPAQLNGGSA CSSRSDLPGS


Sequence of CAL

MGHHHHHHHH   HHSSGHIEGR   HMENLYFQGI   RKVLLLKEDH   EGLGISITGG

KEHGVPILIS EIHPGQPADR CGGLHVGDAI LAVNGVNLRD TKHKEAVTIL SQQRGEIEFE

VVYVDPKETA AAKFERQHMD S


Sequence of TIP-1

MGHHHHHHHH   HHLEVLFQGM   SYIPGQPVTA   VVQRVEIHKL   RQGENLILGF

SIGGGIDQDP   SQNPFSEDKT   DKGIYVTRVS   EGGPAEIAGL   QIGDKIMQVN

GWDMTMVTHD QARKRLTKRS EEVVRLLVTR QSLQKAVQQS MLS


All proteins contain the about 80 amino acids long PDZ domains (grey) flanked by parts of the native protein (white). The histidin-tag is shown in yellow.


## 5.2   Protein and peptide binding experiments


Native, fluoresceinated and biotinylated peptides were synthesized by the Molecular Libraries and Recognition Group as reported previously [40] (Charité-Berlin).

In detail, the peptides used for the binding studies were automatically syntheziced (Syro II, MultiSynTech) using the Fmoc standard protocol. Peptides with a C-terminal carboxyl group were generated using TentaGel S PHB-aa-Fmoc (Rapp Polymere) and with a C-terminal carboxyamide group using TentaGel S Ram resin (Rapp Polymere). For standard synthesis Fmoc-aa-OH were used with the following side-chain protections: E-, D-(OtBu); S-, T-, Y-(tBu); K-, W-(Boc); N-, Q-, H-(Trt); R-(Pbf) (Novabiochem; Bachem). (5,6)-carboxyfluorescein (*F*\*-, Fluka)

coupling was achieved using 1 equiv. N-hydroxybenzotriazole (HOBt) and 1 equiv. di-isopropylcarbodiimide (DIC) as activators, as reported in [60]. The crude peptides were purified to > 95 % by preparative high-performance liquid chromatography (HPLC; Waters) and their identity was determined by analytical reversed phase-HPLC (Waters) and MALDI TOF (matrix-assisted laser desorption/ionization - time of flight) mass spectrometry (LaserTec BenchTopII, PerSeptive Biosystems).

Biotin ("*BT*") was N-terminally coupled via a WrFKK linker sequence (lower-case = D-amino acid). These peptides were synthesized by the Tufts University Core Facility, Yale Keck Biotechnology Resource.

## 5.3   Synthesis and incubation of peptide libraries.

All peptide libraries were generated by a MultiPep SPOTrobot (INTAVIS Bioanalytical Instruments AG, Software LISA, in-house software). As reported previously, all peptide libraries were prepared using an optimized method for generating inverted peptides [61] and incubated with all five PDZ domains. All amino acids that have been used for SPOT-sythesis were purchased from Merck, BACHEM, or PerSeptive Biosystems GmbH.

Library definition: 6223HumLib = 6223 C-termini (11 mers) of human proteins; SubAna = substitutional analyses [each residue of the ligand was substituted by 20 L-amino acids]; ProLibs = profile library [permutation of the four C-terminal ligand positions based on a limited amino acid set]; CombLib = combinatorial library of the type B1-B2-(X)n [B1 and B2 are the positions which will be permuted and "X" represents sequence specific amino acids which were held constant].

Peptide array binding studies were incubated as previously reported [59]. Briefly, membranes were incubated with polyhistidine-tagged PDZ domain (10-20 µg/mL) in blocking buffer overnight at 4 °C. His-tagged PDZ domains were detected using a mouse anti-polyHis antibody (Sigma; 1:2,600 in blocking buffer,

2 hr at RT) followed by horseradish-peroxidase conjugated anti-mouse antibody (Calbiochem; 1:2,000 in blocking buffer, 1 hr at RT).

## 5.4  Fluorescence anisotropy binding experiments

Fluorescence polarization data were measured on a Spectramax M1000 microplate reader (Molecular Devices) at 24 °C. For $K_d$ measurements with a given fluorescently labeled peptide, a stock solution of protein was incubated for 10-30 min at room temperature in FP buffer (storage buffer, supplemented to a final concentration of 0.1 mg/mL bovine IgG (Sigma) and 0.5 Mm Thesit (Fluka) containing 30 nM fluorescent peptide). The pre-equilibrated protein:reporter peptide mixture was then serially diluted into FP buffer containing 30 nM fluorescent peptide and allowed to incubate for 10 min. 40 µL aliquots were transferred to HE low-volume, black 96-well plates (Molecular Devices). Fluorescence polarization was determined at an excitation wavelength of 485 nm and an emission wavelength of 525 nm as depicted in ref. [59]. For competition experiments, a single stock solution was prepared in FP buffer containing fixed concentrations of both fluorescently labeled reporter peptide and protein. This mixture was allowed to equilibrate for 20-60 min at RT. Unlabelled competitor peptide was dissolved and serially diluted in DMSO (Fluka). Each serial dilution was aliquoted at 1/20 final volume, to which was added 19/20 volume of the protein:reporter mixture. The final reporter peptide concentration was 30 nM and the final protein concentration was 0.25 $K_d$ - 3.0 $K_d$, depending on the measurement. Plates were mixed by vibration, centrifuged and allowed to incubate for an additional 15 min at 24 °C in the microplate reader before measurement. For weakly interacting peptides, $K_i$ values were estimated as follows: theoretical fluorescence anisotropy values were calculated for inhibitor $K_i$ based on the known reporter:peptide fluorescence anisotropy (FPPL), free reporter anisotropy (FPL), and the known $K_d$ of the reporter:peptide complex. The estimated $K_i$ value was increased until the theoretical fluorescence anisotropy value (with assumed equal variance) at the 1 mM concentration significantly increased ($p < 0.05$) above experimental fluorescence anisotropy.

## 5.5   NMR studies

Isotopically labeled [15]N- or ^{15}N,[13]C-CAL (UniProt accession number Q9HD26-2) was prepared using published protocols [59, 62], and dialyzed into 10 mM D11-Tris pH 7.8, 150 mM NaCl, 0.02 % NaN3, 0.1 mM TCEP. NMR experiments were conducted at 25 °C on a Bruker 600 MHz spectrometer, equipped with a TCI cryogenic probe. CALP (480 µM) backbone assignment was achieved through two-dimensional ^{1}H-^{15}N HSQC an three-dimensional HNCA, HN(CO)CA, HNCACB, and CBCA(CO)NH experiments. 78 of 82 (95 %) backbone amides from the CALP core PDZ domain were successfully assigned. A peptide-bound assignment was performed similarly with 470 µM ^{15}N,[13]CCALP and 810 µM (*F*\*-WrFKK-iCAL36) using ^{1}H,^{15}N HSQC, HNCA, HN(CO)CA, and HNCACB experiments. iCAL36 (ANSRWPTSII) ^{1}H,^{15}N HSQC backbone crosspeaks were assigned by comparison with the CALP apo and F\*-WrFKK-iCAL36 spectra. Labeled crosspeaks exhibited a normalized chemical shift offset $\Delta \geq 0.15$, where $\Delta = [(\Delta^1 H)^2 + (\Delta^{15} N/6)^2]^{1/2}$. Protein surface depictions of CAL (PDB ID 2DC2 [22] were prepared using PYMOL [63].

## 5.6   Pull-down assays

Native and biotinylated peptides were commercially synthesized. Biotin (*"BT"*) was N-terminally coupled via a WrFKK linker sequence. The control peptide SCR (SPTINSAIWR) represents a scrambled version of the iCAL36 sequence. Streptavidin paramagnetic beads (Promega) were incubated with buffer (control) or N-terminally biotinylated peptides corresponding to the CFTR and SSR5 C-termini and iCAL36 and washed to remove unbound peptide. CFBE41o- cells [64] cells stably expressing ΔF508-CFTR under the control of a cytomegalovirus promoter [65] (CFBE-ΔF cells) were cultured to confluence, serum starved for 24 hr, and lysed at 4 °C. Clarified supernatants were pooled and incubated with peptide-treated beads. Following washing, bound proteins were eluted on ice with buffer (control) or with 0.5 mM peptide inhibitor or 0.5 mM scrambled

peptide in 2.5 % DMSO. Proteins were resolved by SDS-PAGE and analyzed by Western blotting.

## 5.7   Cell culture

Caco-2 cells were a generous gift from Prof. Dr. Theuring (Center for Cardiovascular Research – Charité Berlin). Cells were maintained in DMEM High Glucose (4.5 g/L), with L-glutamine without phenolred (PAA) completed by 1:100 MEM non essential amino acids (100x; PAA), 1:100 penicillin / streptomycin (100x; PAA) and 20 % fetal bovine serum (Biochrom AG) (Caco-2 medium). Cells were grown at 37 °C in 5 % $CO_2$. All cells used in experiments were between passages 10 and 70.

CFBE-ΔF cells were a generous gift of Dr. J.P. Clancy (University of Alabama, Birmingham). Cells were maintained in MEM with 2 mM L-glutamine, 10 % fetal bovine serum (FBS), 50 units/mL penicillin (Sigma), 50 µg/mL streptomycin (Sigma), 2 µg/mL puromycin (Invitrogen), and 5 µg/ml plasmocin (Invivogen) (ΔF-medium). Cells were grown at 37 °C in 5 % $CO_2$. Cells were switched to MEM with only penicillin and streptomycin 24 hr before experiments. All cells used in experiments were between passages 12 and 25.

## 5.8   Immunostaining and microscopy

CFBE-ΔF confocal microscopy: Confocal images were acquired with a Nikon TE2000 swept field confocal microscope equipped with a QuantEM:512SC EMCCD camera (Photometrics, Tucson, AZ) and a 100× (N.A. 1.49) oil-immersion objective at 25 °C. The red Draq5 fluorescence was excited with a 638 nm diode laser. The green (5,6) carboxyfluorescein fluorescence was excited with the 488 nm laser line of a diode laser. The system was run in sequential scanning mode, where only one laser was active at a time, to avoid spectral overlap. The emission of FITC was recorded using a 525/50 nm filter. For Draq5, the emission was recorded using a 700/75 nm filter. The images were analyzed using the

Nikon NIS-Element software. All measurements of peptide uptake were performed with living, non-fixed cells grown in a coverlips (MakTek). Cells were seeded at a density of $1 \times 15^5$/well 3 days before the experiment and cultured in ΔF-medium. Prior to Microscopy, cells were washed twice with 1 ml PBS followed by a 3.5 hr incubation with 1 mL peptide solutions in ΔF-medium without FBS (5 µM). After peptide incubation, cells were washed three times with ΔF-medium without FBS. Nuclei were stained by adding 1 mL prediluted (1:1,000 in ΔF-medium without FBS) Draq5 dye (Cell signaling) for 3 min at 37 °C.

CFBE-ΔF fluorescence microscopy: CFBE ΔF508 cells were seeded at $10^5$ cells per coverslip (MatTek) and 6 days later treated with PBS, BioPORTER™ reagent (Sigma) and DMSO, BioPORTER™ and peptide, or CPP and peptide as described for Ussing chamber experiments. The immunostaining protocol was described by Swiatecka-Urban et al. [12] except that Alexa 568 goat anti-rabbit antibody was used.

## 5.9   Cellular uptake

Caco-2 cell layers were seeded ($6 \times 10^4$) and subsequently cultivated for 14 days in 6 well plates (Falcon) until they were differentiated. Cells were cautiously rinsed twice with 1 mL PBS to completely remove the medium. One mL of a peptide solution in Caco-2 medium without FBS was applied for 3.5 hr at 37 °C, 5 % $CO_2$. Afterwards, 1 mL PBS was added and cells were transferred to a 2 mL reaction tube (Eppendorf) followed by a centrifugation step for 10 min at 4 °C and 4,000 RPM. The cells were trypsinated for 10 min at 37 °C with 300 µL trypsin (0.05 % trypsin /0.02 % EDTA (w/v) solution (Biochrom AG). Then, cells were washed with 1 mL PBS buffer, and centrifuged at 4000 RPM at 4 °C for 10 min (2x). Lysis and BCA assay was performed as described previously [40].

## 5.10 Cell viability assay

**Caco-2:**

100 µl containing $6 \times 10^4$ cells were seeded in 96-well microtiter plates (Falcon) and cultivated overnight. One day (80 % confluence), three days (100 % confluence) or 14 days (differentiated) after cultivation, cells were rinsed twice with PBS, and subsequently, 100 µL Caco-2 medium without FBS was added. Then, 10 µL of different peptide solution concentrations were applied, and cells were incubated for 3.5 hr at 37 °C. Subsequent addition of 50 µL Caco-2 medium with 20 % FBS was followed by an incubation overnight at 37 °C and 5 % $CO_2$. The next day, 10 µL of CCK-8 solution (Fluka) was added for 4 hr, and cell viability was determined by measuring the absorbance of each sample due to the formazan product at 570 nm using a microplate reader (FLUOstar Optima).

**CFBE cells:**

100 µl containing $1 \times 10^5$ cells were seeded in 96-well microtiter plates (Falcon) and cultivated 5 days until they have reached confluence. Afterwards, cells were rinsed twice with ΔF-medium, and subsequently, 100 µL ΔF-medium without FBS was added. Then, 10 µL of different peptide solution concentrations were applied, and cells were incubated for 3.5 hr at 37 °C. Subsequent addition of 50 µl ΔF-medium with 10 % FBS was followed by an incubation overnight at 37 °C and 5 % $CO_2$. The next day, 10 µL of CCK-8 solution (Dojindo) was added for 4 hr, and cell viability was determined by measuring the absorbance of each sample due to the formazan product at 570 nm using a microplate reader (BioTek Synergy).

## 5.11 Ussing chamber chloride efflux experiments

Ussing chamber measurements were performed 12 days after seeding CFBE ΔF508 cell monolayers on 12 mm Snapwell™ (Corning) filter supports with a density of $1 \times 10^5$ cells. Peptide delivery was performed either by BioPORTER™ (Sigma) reagent or cell penetrating peptides covalently bound to inhibitor peptides of the CAL PDZ domain. In case of the BioPORTER™ delivery the peptide inhibitors were dissolved in DMSO, diluted in PBS to 1.25 mM, and then 100 µL of diluted peptide was added to lyophilize BioPORTER™. 150 µl MEM was added to reaction tubes. CFBE-ΔF polarized monolayers were treated apically with the resulting 500 µM iCAL36 solution for 3.5 hr and washed to remove non-internalized peptide. Depending on experimental design, 20 µg/mL cycloheximide (CHX) was applied for the final 2 h or at the completion (0 hr baseline) of peptide treatment, after which the cells were washed. CPP-iCAL36 delivery was realized by dissolving the peptide in DMSO and adding it to 250 µL MEM followed by apical treatment of CFBE-ΔF cells with the peptide solution for 3.5 hr. The DMSO concentration did not exceed 0.03 % in peptide-only treatments or 0.14 % in combined treatments with corr-4a. Short circuit current ($I_{SC}$) measurements were performed as described [13], except that all measurements were performed at 37 °C. In general, 50 µM amiloride (Sigma) was initially applied apically to inhibit epithelial sodium channel (ENaC) activity. $I_{SC}$ was stimulated with 20 mM forskolin (Sigma) added to the apical and basolateral bath solution to increase cellular cAMP levels followed by 50 mM genistein (Sigma) added only to the apical bath solution to increase the open probability of ΔF508-CFTR Cl channels. Once maximal activation was achieved, CFTR-specific chloride efflux was computed as the $I_{SC}$ current change ($\Delta I_{SC}$) following application of CFTR$^{inh172}$ which reversibly inhibits CFTR $I_{SC}$. Resistances were monitored throughout each experiment to ensure monolayer integrity. For small molecule corrector experiments, 3 µM corr-4A or DMSO was added to cells 24 hr before experiments.

## 5.12 CFTR stability assay

CFBE cells were transfected using 200 nM siCAL (siGOPC3, Qiagen) or control siNEG (Qiagen) as described [13]. Seven days post-transfection, cells were switched to 27 °C, and 8-12 hr later, complete medium was replaced with MEM. Following >24 h low temperature rescue, MEM was replaced with 37 °C MEM containing 20 µg/mL CHX (Sigma). At $t = 0$ h and $t = 2$ hr, CFTR surface biotinylations were performed as described [13]. CAL and CFTR were detected in whole-cell lysates (WCL) and biotinylated fractions as described [66]. ß-actin was used as a loading control.

## 5.13 Statistical analysis

Values are reported as mean ± SD except for Ussing chamber experiments where mean ± SEM is reported. Student's one-tailed t-test was used for peptide selectivity profiles by fluorescence anisotropy in addition to CFTR stability assays. Student's one-tailed paired t-test was used for analysis of Ussing chamber experiments to account for current drifts during the course of the experiments. The magnitude of the currents reproducibly became smaller as a function of experiment length.

# 6 Results

## 6.1 Engineering "first generation" peptide inhibitors

This project was initiated with the synthesis of a peptide library containing 6223 different peptide sequences representing the C-termini of human proteins (6223-HumLib) [59, 61]. For each PDZ domain involved in the regulation of CFTR (CALP, N1P1, N1P2, N2P1, and N2P2) a 6223-HumLib was synthesized and peptide:PDZ interactions were revealed by immunoblotting (see materials and methods section). Beside new interaction partners such as the somastotatin receptor type 5 (SSR5) [59], published interactions could be detected, thereby demonstrating the robustness of our method. For example, known N1P1 binding partners such as the platelet-derived growth factor [67], β2-adrenergic receptor [68], CFTR [68], and the N2P2 partner β-catenin [69] were all found (see appendix Tables A2- A6).

### 6.1.1 Engineering the four C-terminal positions

The 80 best binding sequences of the respective 6223-Humlib incubations determined by evaluation of spot intensities were analyzed using the WebLogo algorithm [70], revealing clear C-terminal binding motifs (Figure 6). Consistent with their shared affinity for the CFTR C-terminus, the resulting consensus motifs are very similar, especially for ligand positions 0 ($P^0$: ligand positions are numbered in reverse from the C-terminal ligand residue, which is denoted as 0) and $P^{-2}$ requiring Leu and Ser/Thr, respectively. We also found distinctions in the alternative side-chain preferences at $P^0$, with CAL sequences containing Ile or Val, and NHERF sequences containing Phe. A similar N1P1 binding motif corresponding to Xxx-Ser/Thr-Arg-Phe was reported by Joo and Pei [71]. Generally, it appears that CALP only tolerates aliphatic-hydrophobic amino acids whereas the NHERF domains prefer Leu and aromatic-hydrophobic amino acids at these positions.
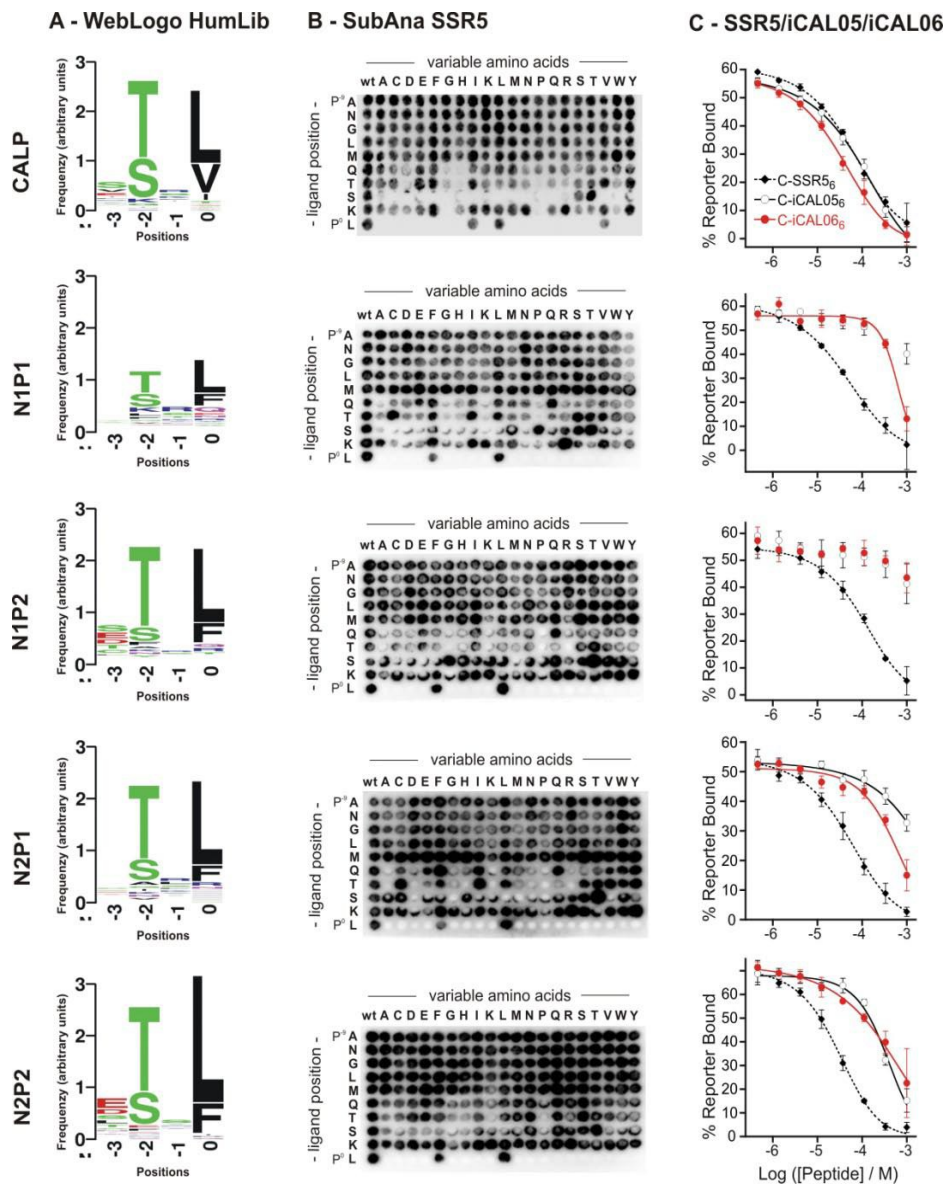
Figure 6: **Consensus motifs of the five PDZ domains involved in CFTR binding.**

(**A**): Five 6223-HumLibs were generated by the method of inverted peptides (SPOT synthesis), each containing 6223 human C-terminal peptides, which were incubated with the CAL and the four NHERF PDZ domains, respectively. The most frequent amino acids were plotted for the four C-terminal residues using WebLogo (http://weblogo.berkeley.edu/) analysis of the 80 best binding sequences. (**B**): Substitutional analyses (SubAna) of the C-terminal SSR5 sequence demonstrate the interaction determinants of the CALP and the NHERF PDZ domains. (**C**): FP measurements comparing $SSR5_6$ (MQTSKL) with $iCAL06_6$ (MQTSKI) and with $iCAL05_6$ (MQTSII) clearly revealed that I at $P^0$ does not disturb the interaction with CALP, but increases the $K_i$-values of the NHERF PDZ domains. Values shown are mean ± SD, n=3.

To investigate the context dependence of the amino-acid preferences, we performed substitutional analyses (SubAna) on a series of peptides from the 80 best 6223-HumLib-peptides. This selection included the C-terminus of the somatostatin receptor type 5 ($SSR5_{10}$), which has the highest known affinity for

CALP [59]. SubAnas are single-substitution peptide libraries in which each residue of a given ligand is sequentially replaced by each of the 20 gene-encoded L-amino acids. SubAnas are suitable peptide libraries to determine key positions of the ligand for a given protein or protein domain. The SubAnas confirm the difference in the amino-acid preferences at $P^0$ between the five PDZ domains (Figure 6 B). Taken together, CALP shows a clear tolerance for Ile at $P^0$ as shown in the SubAna of SSR5 (Figure 6 B), as well as with other ligands (Figure 7). In contrast, NHERF PDZ domains show weak or absent binding for Ile at these positions (Figure 6 B). As determined by FP measurements, the single $P^0$ Leu/Ile substitution generates a ~7-fold increase in the selectivity index for CALP compared to the NHERF PDZ domains (from 0.4 for $SSR5_6$ to 2.7 for $iCAL05_6$) (Table 2). SubAna data also reveal a modest preference of CALP for Ile at $P^{-1}$ (Figure 6 B, red circles in Figure 7). With the double substitution at $P^0$ and $P^{-1}$ we increase the selectivity index ~25-fold (from $SSR5_6$ to $iCAL06_6$, Table 2).

Although the motif and SubAna data on $P^{-2}$ and $P^{-3}$ were ambiguous, previous FP measurements had shown that the Thr-Ser sequence provided ~5-fold more selectivity versus N1P2 compared to the Ser-Thr sequence (data not shown).
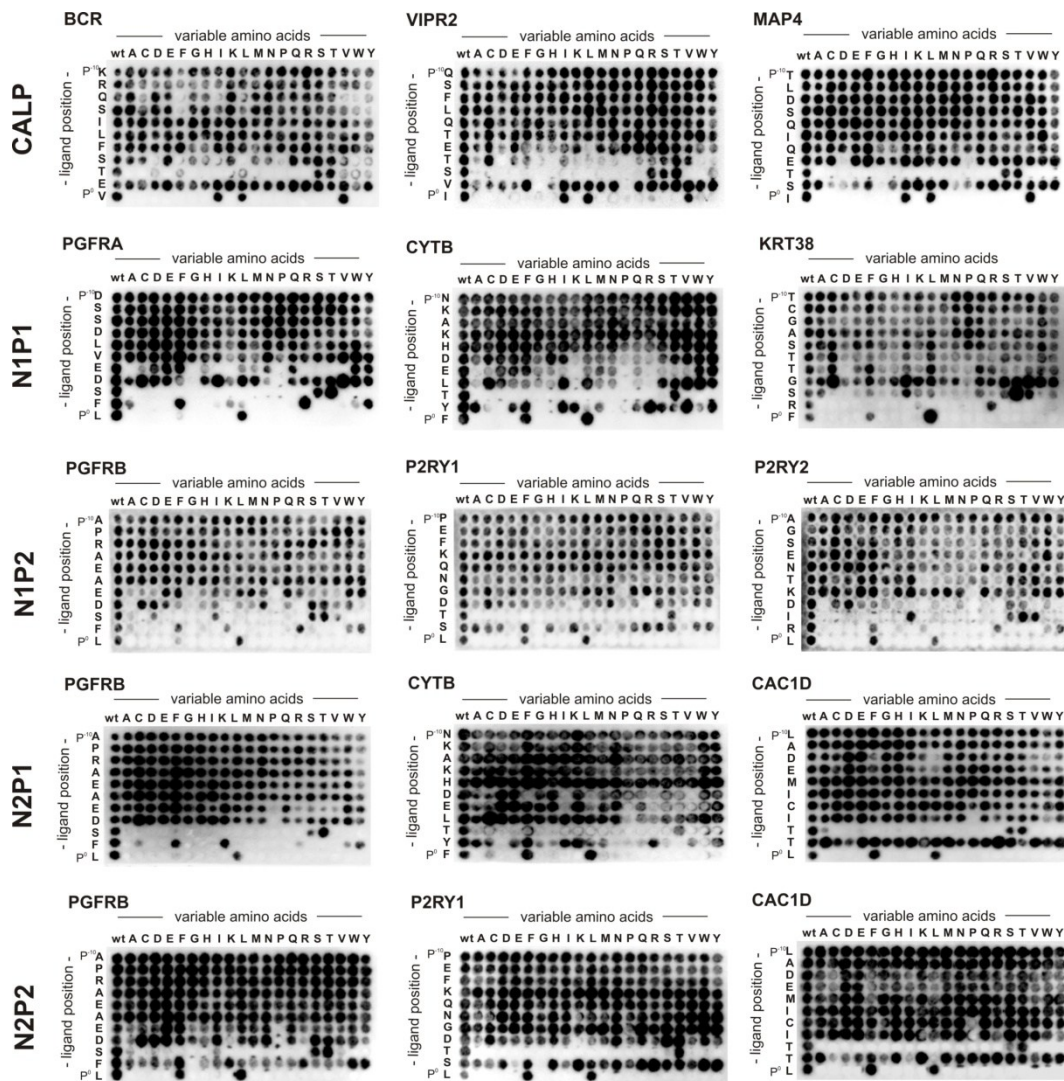
**Figure 7: SubAna incubations of different C-termini with the PDZ domains of the CAL, NHERF1 and NHERF2 protein.**

**(CALP)** The SubAna of the breakpoint cluster region protein (BCR), the vasoactive intestinal polypeptide receptor 2 (VIPR2) and the microtubulin-associated protein 4 (MAP4) were incubated with CALP

**(N1P1)** The SubAnas of the alpha-type platelet-derived growth factor receptor (PGFRA), the cystatin-B (CYTB) and the keratin, type I cuticular Ha8 (KRT38) were incubated with N1P1.

**(N1P2)** The SubAnas of the beta-type platelet derived growth factor receptor (PGFRB), the P2Y purinoceptor 1 (P2RY1) and the P2Y purinoceptor 2 (P2RY2) were incubated with N1P2.

**(N2P1)** The SubAnas of PGFRB, CYTB and the voltage-dependent L-type calcium channel subunit alpha-1D (CAC1D) were incubated with N2P1.

**(N2P2)** The SubAnas of PGFRB, P2RY2 and CAC1D were incubated with N2P2.

Amino acid substitutions to Ile on $P^{-1}$ are mostly not tolerated by the NHERF PDZ domains. Each residue of the ligand was substituted by 20 naturally occurring L-amino acid residues. The resulting peptides were generated by SPOT synthesis of inverted peptides. All spots in the left-hand columns are identical and represent the wild-type (wt) peptide. All other spots are single substitution analogues, with the rows defining the sequence position that is substituted and the columns defining the amino acid used as a replacement.

**Table 2:** Evaluation of $K_i$ values for peptide engineering

| Peptide | Sequence | CALP | N1P1 | N1P2 | N2P1 | N2P2 | Select.[a] |
|---|---|---|---|---|---|---|---|
| CFTR$_{10}$ | TEEEVQDTRL | 390±20 | 0.45±0.02 | 1.9±0.1 | 1.1±0.1 | 0.10±0.02 | 0.00026 |
| SSR5$_{10}$ | ANGLMQTSKL | 21.4.±1.7 | 24.5±1.9 | 130±48 | 38.6±7.7 | 19.8±2.7 | 0.93 |
| SSR5$_6$[b] | MQTSKL | 25.3±3.4 | 19.3±5.6 | 50.2±9.1 | 31.7±8.9 | 10.0±0.6 | 0.40 |
| iCAL05$_6$[b] | MQTSKI | 40.8±10.3 | 914±186 | 1700±1300 | 806±84 | 109±10 | 2.7 |
| iCAL06$_6$[b] | MQTSII | 16.9±1.6 | 245±71 | 2400±1400 | 245±26 | 166±104 | 9.8 |
| iCAL35$_6$[b] | WQTSII | 16.3±2.1 | 430±109 | >5,000 | 496±151 | 246±186 | 15 |
| iCAL36$_6$[b] | WPTSII | 32.8±0.3 | >5,000 | >5,000 | >5,000 | >5,000 | 150 |
| iCAL36$_8$ | SRWPTSII | 20.3±2.6 | >5,000 | >5,000 | 516±183 | 433±154 | 21 |
| iCAL36$_{10}$ | ANSRWPTSII | 17.3±4.3 | >5000 | >5000 | >5000 | >3000 | 170 |

Footnotes: $K_i$ ± SD values are given in µM.
[a] Selectivity index (Select.) = min($K_i$N1P1,$K_i$N1P2,$K_i$N2P1,$K_i$N2P2)/$K_i$CAL.
[b] Peptides include an N-terminal Cys to permit labeling. N = 3 for all experiments

## 6.1.2   Engineering the ligand positions P$^{-4}$ and P$^{-5}$

Beyond the P$^{-3}$ position (Figure 6 B and Figure 7) it is difficult to determine any differences between the binding patterns of the five PDZ domains based on the SubAna results. However, other studies have shown that upstream residues can contribute to PDZ binding affinity [59]. Our hypothesis was that different C-terminal anchor sequences might have distinct upstream preferences, washing out signals in a global motif analysis. To detect context-dependent preferences, we generated combinatorial libraries (CombLib). CombLibs allow the addition of all possible combinations of two N-terminal amino acids to the core sequence (Figure 1, cycle 1). Due to chemical restriction during library synthesis, the core sequence must have a minimum of 4 residues to allow cyclization and the generation of free a C-terminus. The advantage of CombLib double permutation over SubAnas is the opportunity to identify cross-talk between adjacent amino acid positions. As the starting point for our investigations, we selected B1-B2-TSII (B1 and B2 were permuted simultaneously with the 20 gen-encoding L-amino acids, whereas the other positions were held constant) to elucidate the preferences of P$^{-4}$ and P$^{-5}$.

With this peptide library, we were able to determine that Gln or Pro at P$^{-4}$ and Trp at P$^{-5}$ gave the highest signal intensities for CALP (Figure 8 A). To establish the affinity contribution of the single substitutions rigorously, we analyzed the

sequences WQTSII (iCAL35$_6$) and WPTSII (iCAL36$_6$) compared to MQTSII (iCAL06$_6$) by FP measurements (Figure 8, B-F; Table 2).
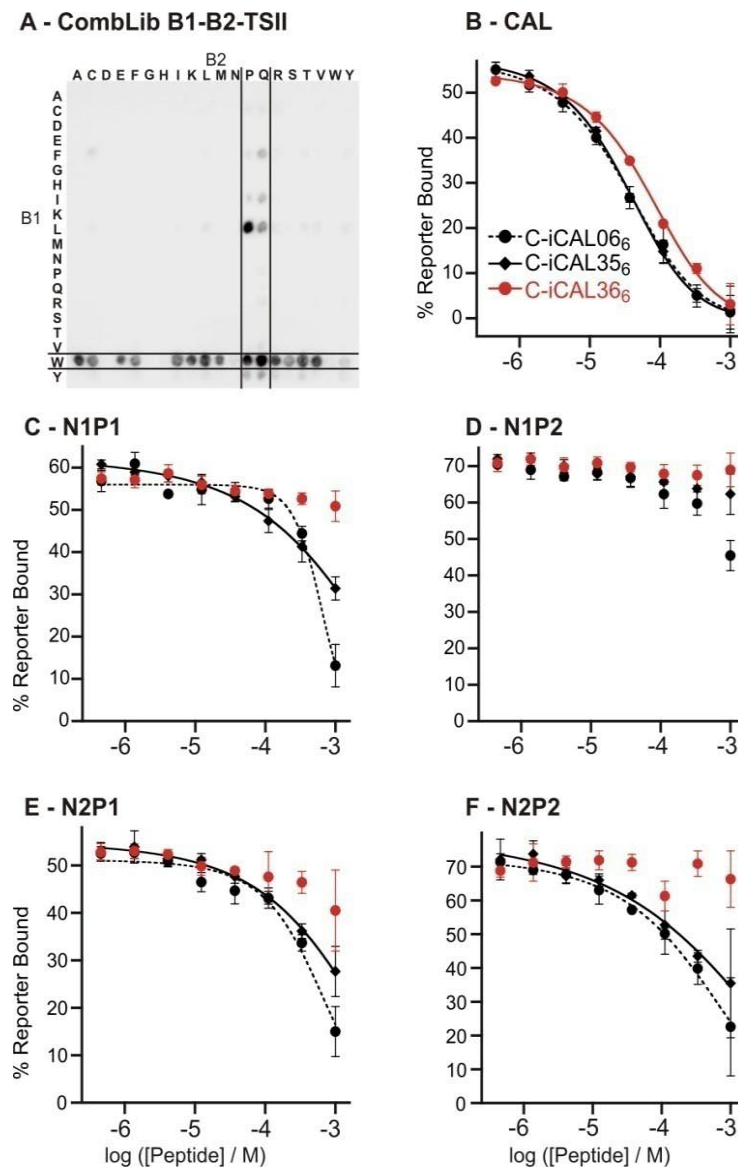


**Figure 8: Enhancing CAL PDZ selectivity by amino-acid substitution.**
(**A**): The recognition pattern of the CombLib incubation shows a clear preference for the combination of Q and W as well as P and W for the P$^{-4}$ and P$^{-5}$. (**B-F**): The three peptides iCAL06$_6$, iCAL35$_6$ and iCAL36$_6$ were measured with the five different PDZ domains.

The substitution of Trp for Met at P$^{-5}$ (iCAL06$_6$ → iCAL35$_6$) has only a minimal effect on CALP affinity, but further weakens peptide interactions with all of the NHERF domains, increasing the selectivity index from 9.8 to 15 (Table 2). The additional substitution of Pro for Gln at P$^{-4}$ (iCAL35$_6$ → iCAL36$_6$) abolished interactions with the NHERF PDZ domains (all >5000 µM), consistent with

CombLib data showing that NHERF domains bind poorly to peptides containing Pro at P$^{-4}$ in multiple sequence contexts (Figure 9).
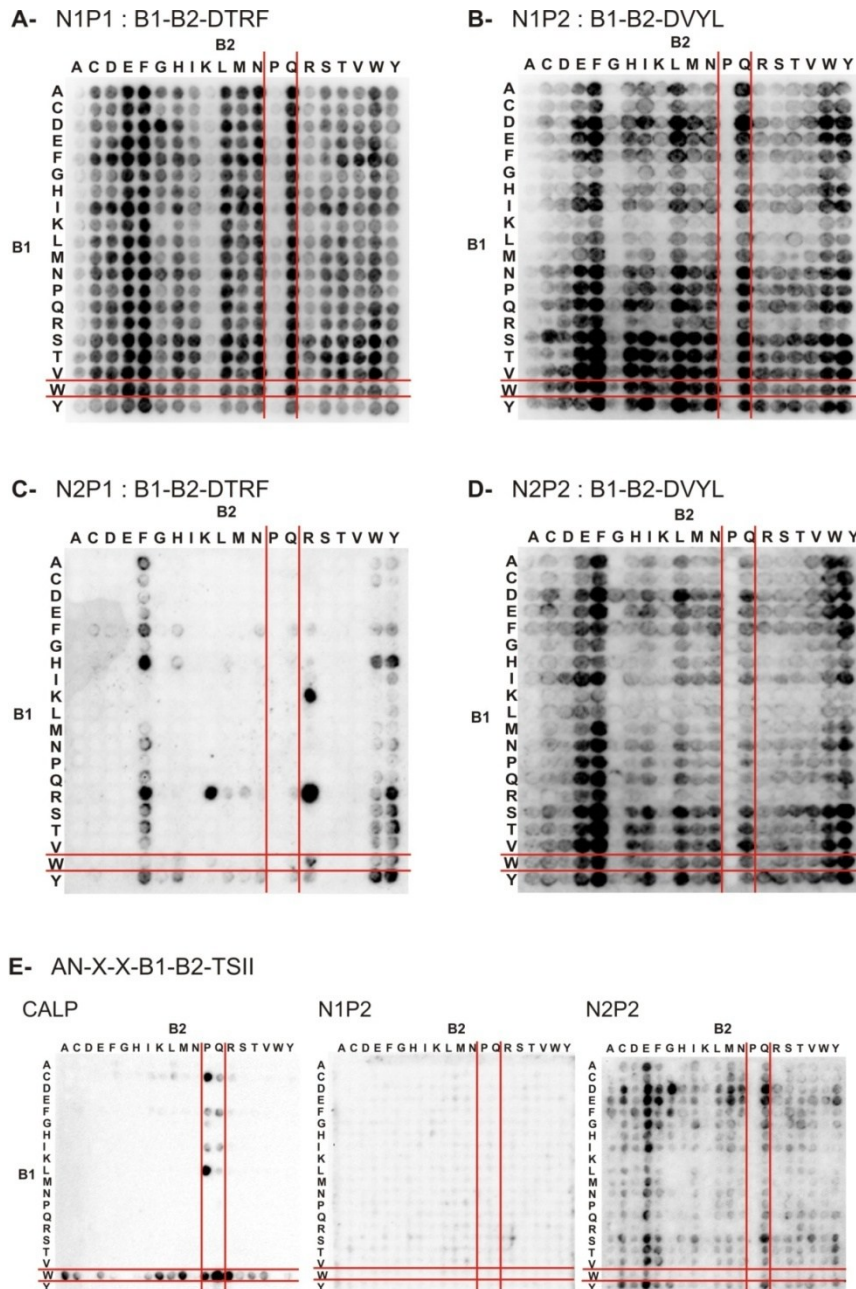


**Figure 9: Combinatorial libraries of ligand positions P$^{-4/-5}$.**
For N1P1 (**A**) and N2P1 (**C**) we used the CombLib B1-B2-DTRF and for N1P2 (**B**) and N2P2 (**D**) the CombLib B1-B2-DVYL. The fixed amino acids in P$^{-3}$ to P$^0$ are selected based on the results of the HumLibs and SubAnas. Cross-validation of the AN-X-X-B1-B2-TSII CombLib previously incubated with CALP, N1P2 and N2P2 (**E**). In all Comlibs, we could observe that Pro in P$^{-4}$ is not tolerated in all NHERF PDZ domains. B1/B2: Permutation of the 20 L-amino acids, X = mixture of all L-amino acids (Cys, Met and Trp omitted), other positions with the one-letter code are fixed.

The ability to visualize negative contributions to peptide affinity represents another important advantage of the CombLib approach over WebLogo-based

motif analysis. Even though affinity for CAL is also reduced by nearly 2-fold, the resulting peptide iCAL36$_6$ (WPTSII) has a selectivity index of 150 (Table 2).

## 6.1.3    Engineering upstream positions (P$^{-6}$ till P$^{-9}$)

Based on our knowledge about the importance of the C-terminal peptide length on CALP affinity [59], we decided to elongate the iCAL36$_6$ sequences N-terminally to further optimize the peptide specificity. CombLibs of the type B1-B2-WQTSII and B1-B2-WPTSII were incubated with CALP to determine the amino acid preferences at P$^{-6}$ and P$^{-7}$, but reflected little specificity at either position (Figure **10**).
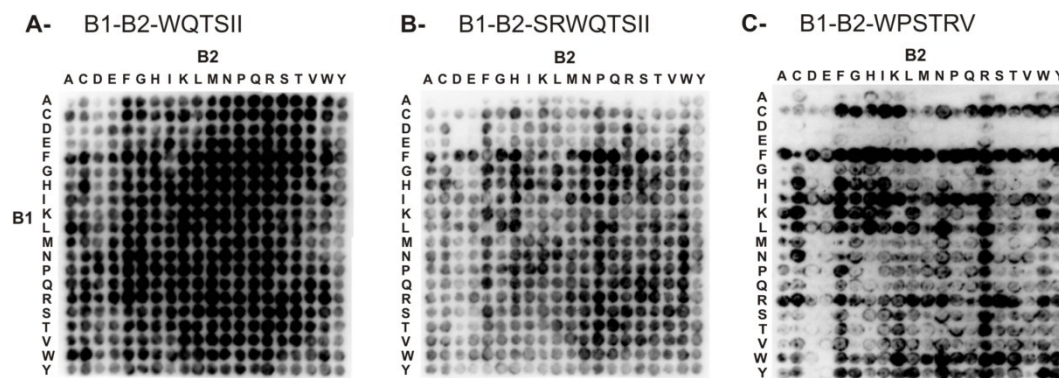


**Figure 10: Combinatorial libraries of of ligand positions P$^{-6}$ till P$^{-9}$.**
ComLibs of the type: B1-B2-WQTSII (**A**) and B1-B2-SRWQTSII (**B**) were incubated with CALP to determine N-terminal amino acid preferences. Using these both libraries no specificity could be detected. Fortunately, the CombLib B1-B2-WPSTRV (**C**) clearly demonstrates a preference for Arg at P$^{-5}$. B1/B2: Permutation of the 20 L-amino acids, X = mixture of amino acids (C, M and W omitted), other positions with the one-letter code are fixed.

This apparent un-specificity correlates with SubAna incubations, which revealed no specificity upstream of P$^{-6}$ (Figure 7). Nevertheless, B1-B2-WPSTRV CombLib incubated with CALP demonstrates a slight preference for Arg at P$^{-6}$ (Figure 10). Addition of a Ser-Arg pair at P$^{-7}$ and P$^{-6}$ enhanced CALP affinity, but also reduced selectivity versus NHERF2 PDZ domains. Selectivity was restored without loss of CAL affinity by a further addition of an Ala-Asn pair at P$^{-9}$ and P$^{-8}$. As the CombLibs also did not reveal any clear side-chain preference at these positions (Figure 10 B), these affinity effects are presumably mediated primarily

by peptide main-chain interactions. Altogether, these extensions of the peptide sequences resulted in the peptide sequence iCAL36$_{10}$ (ANSRWPTSII). Retrospective sequence analysis of iCAL36$_{10}$ using a SubAna library shows a similar binding pattern for CALP with $P^0$, $P^{-2}$ and $P^{-5}$ as key residues (Figure 11).
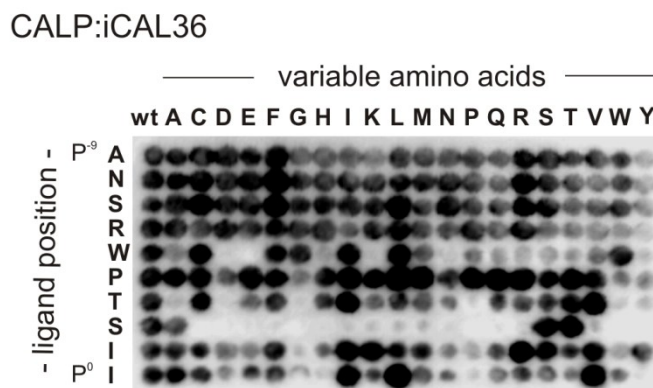


**Figure 11: Substitutional analyses of iCAL36 incubated with the CAL PDZ domain.** SubAna peptide array incubated with CAL confirms that $P^0$, $P^{-2}$, $P^{-5}$ are critical residues for CAL binding.

Our final modification involved the N-terminal attachment of (5,6)-carboxyfluorescein (*F*\*-) to a decamer sequence, which previous studies had shown to enhance CALP binding more than NHERF1 binding [59]. As expected, the resulting *F*\*-iCAL36$_{10}$ sequence exhibits substantially improved affinity for the CAL PDZ domain ($K_d$ = 1.3 ± 0.1 µM). Titrations with NHERF PDZ domains did not reveal significant binding at concentrations as high as ~100 µM, indicative of $K_d$ values >1 mM. As a result, the selectivity index for *F*\*- iCAL36 exceeds 750. Compared to the non-selective SSR5 sequence, *F*\*-iCAL36$_{10}$ has 16-fold higher affinity for CALP and a >830-fold higher selectivity index. Compared to the CFTR C-terminus, its target for competitive displacement, *F*\*-iCAL36$_{10}$ has 300-fold higher affinity for CAL and greater than 3×10$^6$-fold increase in selectivity.

## 6.2   Biochemical characterization of iCAL36:CALP

This chapter deals with the newly engineered iCAL36 as a CAL-PDZ inhibitor, and its subsequent biochemical and structural characterization. To simplify the nomenclature, the denominated iCAL36 peptide from here on will be referring to the 10-mer sequence.

### 6.2.1      Structural analyses of the iCAL36:CALP interaction

To visualize the iCAL36 binding site on CALP, NMR heteronuclear single quantum coherence (HSQC) analyses in the presence and absence of iCAL36 were performed (Figure 12 A). When assigned and mapped to the surface of the PDZ domain, the chemical shift perturbations associated with peptide binding show that the iCAL36 binding site is superimposed on that of the CFTR C-terminal peptide, confirming a competitive mode of displacement (Figure **12** B, C). Furthermore, compared to the octameric peptide sequence used in CFTR-binding studies [62], the decameric iCAL36 peptide exhibits additional interactions at the distal end of the peptide-binding groove (Figure 12 B, arrow). This is consistent with the contributions of N-terminal extensions to peptide affinity and selectivity.
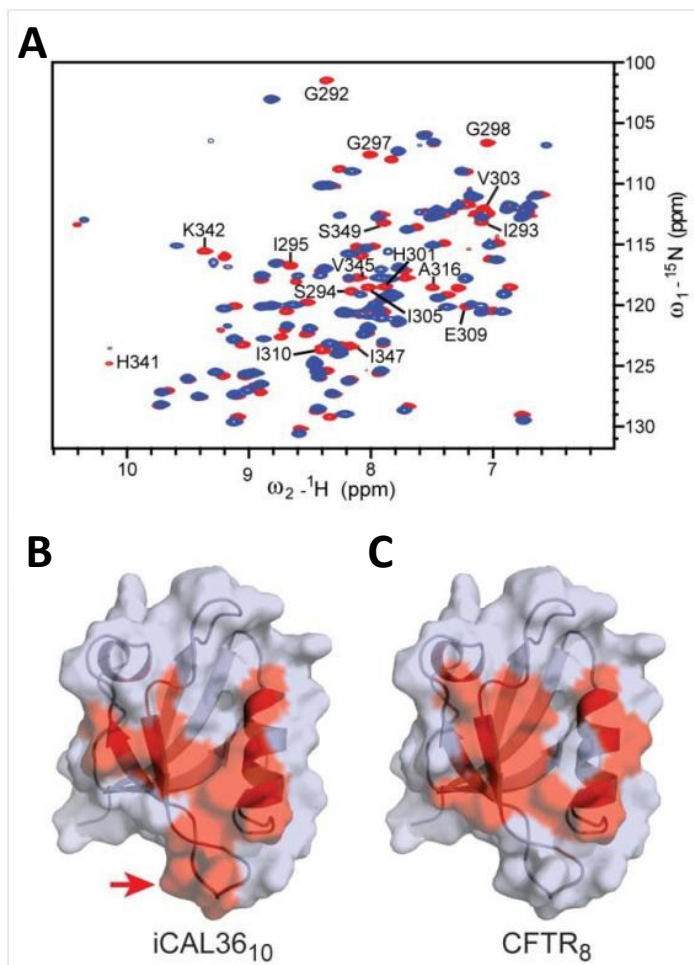
**Figure 12: iCAL36 acts as a competitive inhibitor.**
(**A**) HSQC spectra of 15N-CALP were determined in the absence (red) and in the presence (blue) of 800 µM iCAL36. Protein backbone cross-peaks that are perturbed by addition of iCAL36 are labeled. (**B, C**) Surface representations of the CAL PDZ domain are shown, highlighting in red residues that are perturbed in complex with the iCAL36 decamer (**B**) or with the CFTR C-terminal octamer (**C**). iCAL36 binds in the same pocket occupied by the CFTR C-terminal peptide, with additional interactions in the distal region that accommodates the N-terminal residues (**B, arrow**).

### 6.2.2        *In vitro* validation of iCAL36 with endogenous CAL protein

We next investigated the ability of our PDZ domain-based approach to predict peptide interactions with endogenous full-length proteins in the presence of other cellular factors, across the spectrum of CAL/NHERF selectivity. To facilitate a pull-down assay, N-terminally biotinylated (*BT*-) versions of three peptides were synthesized: the CFTR C-terminus (*BT*-CFTR), which preferentially binds NHERF PDZ domains; the somatostatin receptor type 5 C-terminus (*BT*-SSR5), which binds the CAL domain more tightly than CFTR, but also the NHERF PDZ

domains; and *BT*-iCAL36, which binds CAL with the highest affinity and exhibits no appreciable affinity for the NHERF PDZ domains. Fluorescence polarization (FP) analysis confirmed that the biotinylated peptides retain the relative binding profiles of the core sequences (Table 3).

**Table 3:** Affinity values for peptide inhibitors.

| Protein | *BT*-CFTR (*BT*-WrFKKTEEEVQDTRL)[a] $K_i \pm SD$ (µM) | *BT*-SSR5 (*BT*-WrFKKANGLMQTSKL)[a] $K_i \pm SD$ (µM) | *BT*-iCAL36 (*BT*-WrFKKfNSRWPTSII)[a] $K_i \pm SD$ (µM) |
|---|---|---|---|
| CAL PDZ | 110 ± 8 | 3.4 ± 0.2 | 0.8 ± 0.1 |
| NHERF1 PDZ1 | 0.4 ± 0.1 | 11.0 ± 0.3 | >5000 |
| NHERF1 PDZ2 | 1.9 ± 0.6 | 160 ± 10 | >5000 |
| NHERF2 PDZ1 | 1.0 ± 0.1 | 17 ± 1 | >5000 |
| NHERF2 PDZ2 | 0.1 ± 0.1 | 19.0 ± 0.9 | >5000 |

**Footnotes**: n = 3 for all titrations.
[a] *BT* denotes amino-terminal biotin moiety; lower case letters denote D-amino acids

Following immobilization on streptavidin beads, each sequence was incubated with whole-cell lysates of CFBE-ΔF cells. Bound proteins were eluted with free peptide and probed by Western blotting with antibodies specific for CAL, NHERF1, and NHERF2 (Figure 13). In each case, the FP affinity data with single PDZ domains faithfully predict the interactions with full-length proteins in cell lysates. Our experiments confirm that iCAL36 is selective for endogenous CAL protein, whereas the high-affinity SSR5 C-terminal sequence is not.
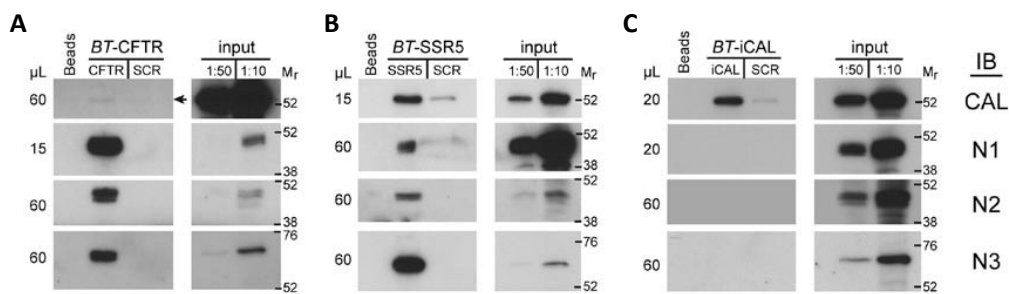
**Figure 13: Pull-down binding assays validate the specificity profiles of PDZ inhibitors for endogenous full-length target proteins.**
(**A**) *BT*-CFTR, (**B**) *BT*-SSR5, and (**C**) *BT*-iCAL36 (iCAL) peptides were conjugated to streptavidin beads. Control experiments were performed with unconjugated beads (Beads). Following incubation with CFBE-ΔF cell extracts, bound proteins were eluted with the corresponding unlabeled peptide or scrambled control peptide, and the indicated volumes were immunoblotted (IB) with CAL-, NHERF1 (N1)-, NHERF2 (N2)-, and NHERF3 (N3)-specific antibodies. Dilutions of cell extracts were blotted on the same membrane as positive controls. Arrowhead indicates the position of the CAL band in (A). Representative blots are shown, with M_r standards at right. n=3.

We also tested the ability of the various peptides to interact with the tetra-PDZ protein NHERF3, which has been shown to interact functionally with CFTR in intestinal epithelia [72]. Although NHERF3 domains were not included in the engineering phase, the iCAL36 sequence also exhibits no interaction with NHERF3 in the pull-down assay, whereas the CFTR and SSR5 C-termini clearly do (Figure 13). Thus, iCAL36 is selective for CAL, thereby abolishing the interactions to all NHERF variants known to interact with CFTR.

## 6.3 Inhibition of CALP and *in vitro* effect on CFTR

### 6.3.1 CAL as a regulator of the post-maturational stability of ΔF508-CFTR

To evaluate iCAL36 as an apical-membrane stabilizer of chloride efflux activity, patient-derived bronchial epithelial cells (CFBE-ΔF cells) were used for *in vitro* evaluation of the iCAL36 effects. CFBE-ΔF cells were allowed to form polarized monolayers and were then treated with iCAL36 peptide and BioPORTER™ delivery reagent. In order to best mimic physiological conditions, cells were maintained at 37 °C throughout the experiments. N-terminally fluoresceinated

(*F\**-) peptides were used, which have somewhat higher affinity for the CAL PDZ domain (1.3 µM) and comparable selectivity [58]. Short-circuit currents ($I_{SC}$) were monitored in Ussing chambers under conditions of low apical chloride. Following channel activation by forskolin which elevates the cAMP level, and genistein which is a selective CFTR activator (details are given in Chapter 5.11), ΔF508-CFTR-mediated chloride efflux was determined. This was accomplished by monitoring the change in short-circuit current ($\Delta I_{SC}$) associated with acute, specific inhibition of CFTR channels with $CFTR_{inh}172$ [73, 74]. CFBE-ΔF monolayers treated with a scrambled control peptide (*F\**-SCR) in combination with BioPORTER™ did not exhibit significant shifts in chloride efflux ($\Delta I_{SC} \leq 4$ %) as compared to untreated cells.

Having established an electrophysiological assay for peptide-mediated ΔF508-CFTR rescue, CFBE-ΔF monolayers were treated with *F\**-iCAL36 or *F\**-SCR (with 0.03 % DMSO). Both peptide uptakes were confirmed by fluorescence microscopy (Figure **14** A,B). Monolayers treated with each peptide were also treated with cycloheximide (CHX), to block *de novo* protein synthesis for the final 2 hr before measurement of $\Delta I_{SC}$ (Figure 14 C) in order to demonstrate that iCAL36 acts as a stabilizer. When normalized to the baseline values obtained from corresponding monolayers washed immediately after treatment with CHX, residual $\Delta I_{SC}$ values were 25 % higher for monolayers treated with *F\**-iCAL36 than for control monolayers (0.75 ± 0.02 vs. 0.60 ± 0.03, p = 0.0005; Figure 14 D). Thus, iCAL36 rescues functional ΔF508-CFTR by extending the half-life of mature ΔF508-CFTR at the apical membrane. To confirm that rescue involved an increase in ΔF508-CFTR abundance, surface biotinylation and Western blotting were used to detect ΔF508-CFTR following CAL knockdown. At the end of 2 hr CHX treatment, CAL knockdown is clearly associated with an increase in the residual amount of ΔF508-CFTR channels present at the apical membrane, compared to cells treated with control siRNA (Figure 14 E). Together, these data clearly establish CAL as a regulator of the post-maturational stability of ΔF508-CFTR, thereby demonstrating that iCAL36 can have potentially therapeutic effects on CFTR levels.
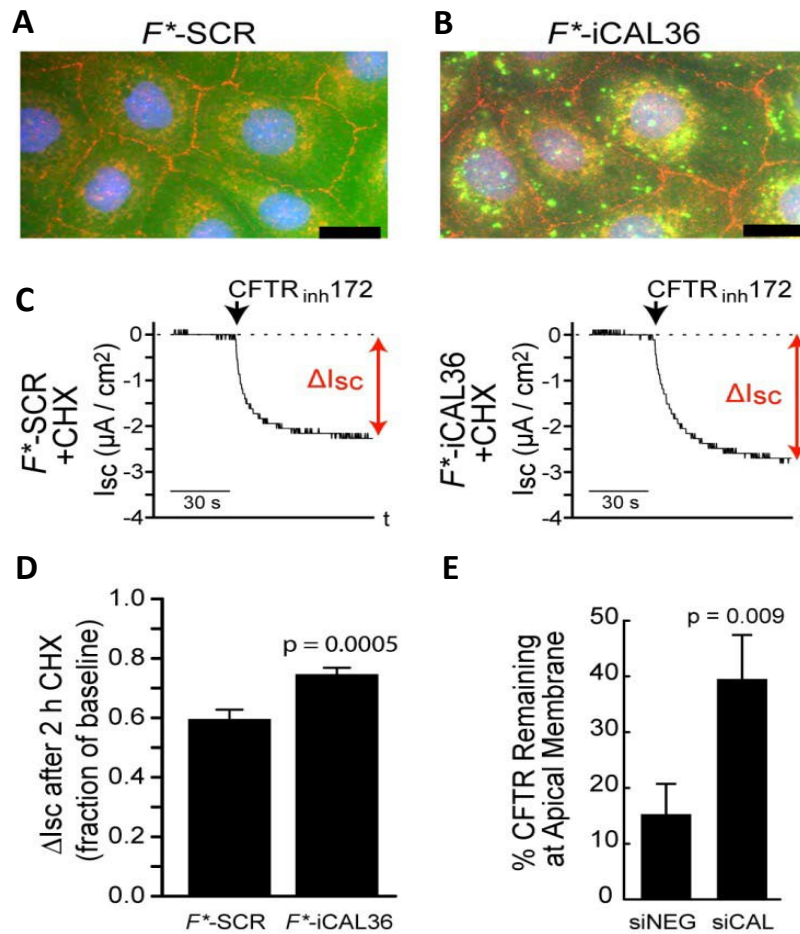
**Figure 14: CAL inhibitors target ΔF508-CFTR stability at the apical membrane.**
(**A, B**) Interior sections of a Z-stack are shown for CFBE-ΔF cells incubated with fluorescent control (**A**; *F\**-SCR) or inhibitor (**B**; *F\**-iCAL36) peptides. Cells grown on cover slips were fixed and immunostained with a polyclonal α-ZO-1 Ab (red). Cell nuclei were stained with Hoechst 33342 (blue). Peptide internalization was monitored via the N-terminal fluorescein moiety (green). Scale = 20 μm. (**C, D**) Following treatment with *F\**-iCAL36 or *F\**-SCR, polarized CFBE-ΔF cells were treated with CHX for 0 h or 2 hr, and chloride efflux ($I_{SC}$) was measured. (**D**) The residual $\Delta I_{SC}$ values after 2 hr exposure to CHX are plotted as a fraction of the corresponding 0 h starting value. CAL-specific inhibition increased residual $\Delta I_{SC}$ from 60 % to 75 % of baseline (n = 9). (**E**) Cell-surface retention of ΔF508-CFTR is enhanced by CAL knockdown. CFBE-ΔF cells were treated with CAL-specific (siCAL) or control (siNEG) siRNAs. Post-maturational stability of ΔF508-CFTR was determined by incubating CFBE-ΔF cells in CHX and measuring the cell-surface abundance of ΔF508-CFTR at t = 2 hr as a fraction of the amount present at t = 0 hr. siCAL-treated cells exhibited 71 % CAL knockdown and retain 40 % of ΔF508- CFTR, compared to 15 % retention seen in siNEG-treated cells (n = 12 for siNEG and n = 8 for siCAL). Values shown are mean ± SEM.

## 6.3.2    Effects of CAL inhibtion on ΔF508-CFTR maturation

In order to determine whether CAL inhibition also has a substantial effect on ΔF508-CFTR maturation, CFBE-ΔF monolayers were treated with *F\**-iCAL36 in the absence of CHX. The resulting highly significant 26 % increase in $\Delta I_{SC}$ (Figure 15) is

close to the 25 % increase observed in the presence of CHX (Figure 14 D), indicating that the effect of iCAL36 is largely independent of biogenesis. Furthermore, the magnitude and significance of the functional rescue directly correlates with the affinity and selectivity of peptide inhibitors for the CAL PDZ domain. In these studies, we also tested our NHERF-selective CFTR C-terminal mimetic ($CFTR_{16}$) and the non-specific decameric CAL inhibitor *F\*-SSR5* (ANGLMQTSKL). $CFTR_{16}$ did not significantly increase the magnitude of $CFTR_{inh}172$ $\Delta I_{SC}$ relative to the scrambled control. Treatment with *F\*-SSR5* however, also increased $CFTR_{inh}172$-specific $\Delta I_{SC}$ by 15 % relative to the control. This effect is intermediate between those of the NHERF-selective $CFTR_{16}$ and the CAL-selective iCAL36 inhibitors (Figure 15).
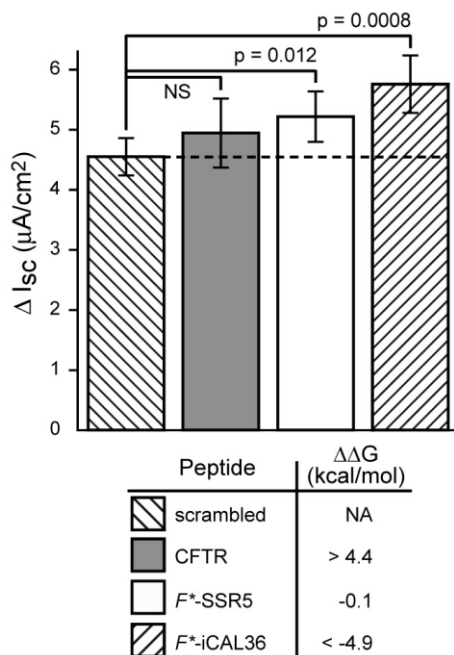


**Figure 15: CAL selectivity improves the efficacy of ΔF508-CFTR rescue.**
Polarized monolayers were treated with a scrambled control peptide (SCR), or with the CFTR, SSR5, or iCAL36 peptides in the presence of BioPORTER™. Following channel activation, the change in short-circuit currents ($\Delta I_{SC}$) was monitored upon application of the CFTR-specific inhibitor $CFTR^{inh172}$. The differential free energy of binding ($\Delta\Delta G$) for the CAL PDZ domain vs. the NHERF1 PDZ domain is shown below the graph for each inhibitor peptide. Rescue ($\Delta I_{SC}$) increases with selectivity ($\Delta\Delta G$). P-values are shown for pair wise comparisons (n ≥ 5). Values shown are mean ± SEM.

The efficacy seen with the *F\*-SSR5* inhibitor peptide may reflect the fundamental pharmacological susceptibility of the CAL:CFTR interaction. Although non-specific, the SSR5 affinities are simultaneously stronger for CAL and weaker for the NHERF proteins than are those of CFTR (Table 3). As a result, SSR5 appears able to displace CFTR from its deleterious interaction with CAL without interfering with its favorable interactions with the NHERF proteins.

### 6.3.3    The potential of complementary action of CAL inhibitors and CFTR correctors

Apical-membrane stabilization of ΔF508-CFTR should act in concert with enhanced ΔF508-CFTR biosynthesis. Some studies have indicated that corrector compounds have ΔF508-CFTR stabilizing properties [75], although this effect has not been demonstrated using corr-4a in primary human airway epithelial cells [10]. To assess the potential for additive action, we tested whether CAL inhibition can augment the effect of chemical correctors of the primary folding defect with the CFBE-ΔF cell line. Cells were treated with either the first-generation corrector corr-4A or DMSO and either *F*-iCAL36 (*F*- ANSRWPTSII) or *F*-SCR (*F*-SPTINSAIWR) (0.14 % final DMSO concentration).
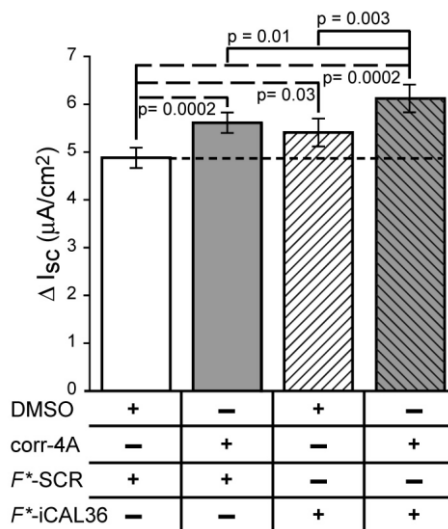


**Figure 16: iCAL36 and corr-4a represent complementary rescue strategies.**
CFBE-ΔF monolayers were treated with DMSO or with corr-4a for 24 h, and were subsequently treated with BioPORTER™ and either *F*-SCR or *F*-iCAL36. Chloride efflux values ($\Delta I_{SC}$) were determined, showing enhancements for both iCAL36 (11 %) and corr-4a (15 %), with nearly additive effects upon co-application (25 %). p-values are shown for pairwise comparisons (n ≥ 9). Values shown are mean ± SEM.

Relative to the double negative control (*F*-SCR and DMSO), *F*-SCR and corr-4A enhanced CFTR$_{inh}$172 $\Delta I_{SC}$ by 15 %. In this experiment, cells treated with *F*-iCAL36 and vehicle exhibited an 11 % increase in the magnitude of CFTR$_{inh}$172 $\Delta I_{SC}$. When *F*-iCAL36 and corr-4A were combined, a 25 % increase in CFTR$_{inh}$172 $\Delta I_{SC}$ was observed (Figure 16), demonstrating that the effects of small-molecule correctors and CAL inhibitors are essentially additive. In this side-by-side comparison, it is clear that iCAL36 treatment independently provides a level of rescue comparable to that seen with the first generation corrector corr-4a

(Figure 16). Furthermore, our knockdown experiments demonstrate the magnitude of rescue potentially accessible to more efficacious CAL inhibitors: 71 % CAL knockdown is associated with a 2.7-fold increase in cell-surface ΔF508-CFTR (Figure 14 E).

## 6.4   Engineering single PDZ specificity: a "second generation" CALP inhibitor.

By exploiting an iterative design approach, a peptide (iCAL36) that inhibits the PDZ domain of CAL but not those of the NHERF proteins [76] was successfully engineered. When applied to human airway epithelial cells that express the most common disease-associated mutant (ΔF508-CFTR), iCAL36 significantly enhanced chloride secretion across polarized monolayers [77].

Despite this success, the initial negative design efforts were restricted to two other known CFTR regulators, NHERF1 and NHERF2. As a result, it remained unclear whether iCAL36 can inhibit PDZ domains other than CAL. Since off-target interactions could potentially confound our understanding of CAL-mediated CFTR rescue and complicate therapeutic applications, the main objective was to target CAL specifically. However, there is no precedent for an inhibitor that can target a single PDZ domain, and it was unclear whether such specificity could be achieved. Based on the well-known promiscuity of PDZ-domain interactions, a major concern was that additional sequence modifications would simply yield an ever-changing cast of off-target PDZ interactions. However, with our engineering approach we were also able to create an optimized sequence with true PDZ selectivity for CAL, thereby eliminating all off-target interactions found by pull-down/mass spectrometry. Finally, resulting "second generation" CAL inhibitors were tested in their ability to enhance CFTR activity in human airway epithelial cells.

### 6.4.1   iCAL36 is a highly selective PDZ inhibitor.

To determine the full spectrum of PDZ domains inhibited by iCAL36 (sequence: ANSRWPTSII) in our target epithelial cells, pull-down/mass-spectrometry assays for iCAL36 interactors were performed. As bait, N-terminally biotinylated (*BT*-) version of iCAL36 were used, which has been shown to retain the binding profile of the decamer [77]. *BT*-iCAL36 was coupled to streptavidin beads and incubated with whole-cell lysates (WCL) from human cystic fibrosis bronchial epithelial cells expressing ΔF508-CFTR (CFBE-ΔF cells). Mass spectrometry revealed only two PDZ proteins that were enriched in iCAL36 versus control eluates (Figure 17 A).
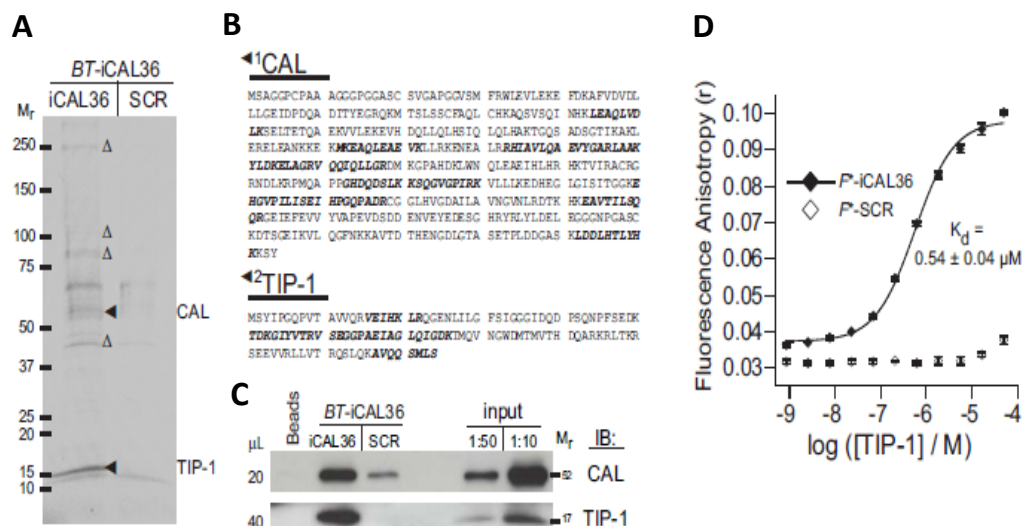


**Figure 17: iCAL36 exhibits a single off-target PDZ interaction in airway epithelial cell lysates**.
(**A**) Endogenous proteins were captured from CFBE-ΔF lysates using immobilized *BT*-iCAL36 as bait, eluted with iCAL36 or a scrambled control peptide (SCR) and visualized by SDS-PAGE. A representative gel is shown (n=3). (**B**) Bands enriched in the iCAL36 elution (Δ) were digested and sequenced by LC/MS/MS. Peptide sequences (bold italic) were identified for two PDZ proteins: CAL (♦1) and TIP-1(♦2). (**C**) α-CAL or α-TIP-1 immunoblots (IB) confirm the enrichment of endogenous CAL and TIP-1 proteins in iCAL36 pulldowns. (D) Fluorescence anisotropy was measured for *F*\*-iCAL36 and a scrambled control peptide (*F*\*-SCR) in the presence of increasing concentrations of purified TIP-1 PDZ domain protein, demonstrating a specific and high-affinity ($K_d$ = 0.54 µM) interaction with iCAL36 (n = 3).

CAL was identified with good peptide coverage (Figure 17 B). The second PDZ sequence identified by mass-spectrometry was the Tax-interacting protein-1 (TIP-1; Figure 17 B). Both interactions were validated using WCL pull-downs and immunoblotting (Figure 17 C). Thus, although initially engineered to avoid

interactions only with the NHERF1 and NHERF2 PDZ domains, iCAL36 also robustly engage only a single "off-target" protein. Significant enrichment of the iCAL36-eluted bands over the inputs, especially in the case of TIP-1, is consistent with a potent interaction. To quantify its strength relative to the on-target binding of CAL, recombinant expression and purification of the TIP-1 PDZ domain were performed to monitor its interaction with $F^*$-iCAL36 by means of FP assays. Titration reveals a strong, dose- and sequence-dependent binding isotherm, with a fitted $K_d$ of 0.54 µM (Figure 17 D; Table 1). Consistent with the strong pull-down signal, TIP-1 actually binds $F^*$-iCAL36 2.5-fold more tightly than does CAL ($K_d$ = 1.3 µM, ref. [76]), and its submicromolar interaction places it at the high-affinity end of the spectrum of PDZ:peptide interactions [54]. As a result, in earlier cell-based studies using $F^*$-iCAL36 [77], TIP-1 may have been inhibited at least as potently as CAL.

TIP-1 is an unusual protein composed almost entirely of a single PDZ domain, which has been implicated in negatively regulating the Wnt signaling pathway by sequestering β-catenin [78]. Recent reports also suggest TIP-1 may play a role in regulating the surface expression of membrane proteins, including the $K^+$-channel Kir 2.3 [79]. Thus, despite the excellent overall specificity of iCAL36, its off-target interaction with TIP-1 could potentially have contributed to its reported effects on CFTR stability [77]. To resolve this target ambiguity, and to test our ability to achieve true single-PDZ specificity, we sought to design CAL inhibitors without TIP-1 affinity.

### 6.4.2   Sequence determinants of the iCAL36:TIP-1 interaction

As a basis for eliminating the off-target interaction, we undertook parallel structural and biochemical approaches to understand the contributions of individual iCAL36 side chains to TIP-1 binding. To visualize the stereochemistry of binding, we determined the X-ray crystallographic structure of the complex of iCAL36 with human TIP-1 (for parameters see Table A1). The TIP-1 protein adopts a standard PDZ domain fold (e.g., rmsd = 0.38 Å vs. PDB entry 3DIW;[80]), and the iCAL36 peptide adopts a canonical PDZ-binding conformation, forming standard

C-terminal carboxylate, $P^0$ and $P^{-2}$ interactions in the binding pocket (Figure 18 A). Away from the C-terminus, the $P^{-5}$ side chain is bound within a deep, hydrophobic pocket that provides excellent stereochemical complementarity to the planar Trp conjugated ring system (Figure 18 B). In comparison, the structure of the CAL PDZ domain shows no equivalent hydrophobic pocket even though CAL binds iCAL36 [76]. If superimposed on the CAL PDZ domain, the $P^{-5}$ Trp of the TIP-1:iCAL36 structure exhibits steric clashes, and no alternative hydrophobic pockets are found in the vicinity (Figure 18 C).
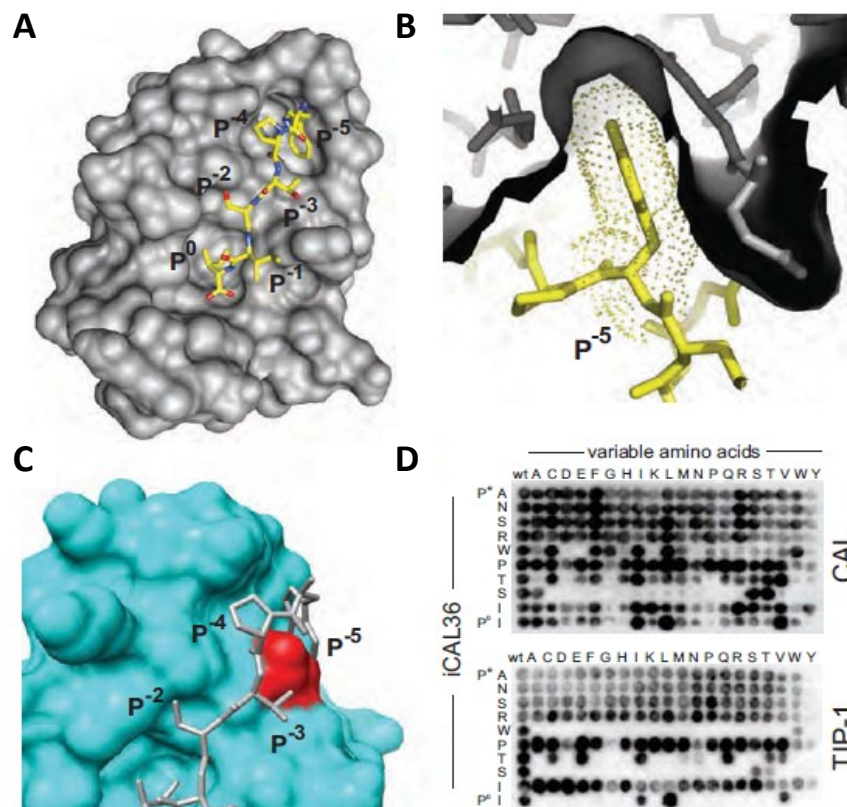


**Figure 18: Targeting the iCAL36:TIP-1 interation.**
(**A**) The structure of the complex of TIP-1 (grey, surface representation) with the iCAL36 peptide (stick figure) reveals a canonical PDZ binding interaction involving residues $P^0$ through $P^{-5}$. TIP-1 surface pockets are seen at either end of the binding groove, which interact with the $P^0$ and $P^{-5}$ side chains. Carbon, oxygen and nitrogen atoms are colored yellow, red and blue, respectively. Data collection and refinement statistics are given in the appendix, Table A1. (**B**) The van der Waals surface of the $P^{-5}$ Trp-binding pocket of TIP-1 is shown in cross section (grey surface), together with stick and dot-surface models of the bound iCAL36 Trp side chain, illustrating the tight packing of the planar ring system. (**C**) The CAL PDZ domain was superimposed on the TIP-1 domain. The CAL surface (blue) is shown in the same orientation as in (**A**). When the TIP-1 bound conformation of iCAL36 is superimposed (grey stick figure), substantial steric clashes (red) are observed at the distal $P^{-5}$ end of the CAL peptide-binding pocket, which lacks the deep pocket seen in TIP-1. (**D**) Binding of CAL and TIP-1 PDZ proteins to iCAL36 SubAna arrays reveals differential sequence preferences at non-motif positions, including in particular the requirement of Trp at $P^{-5}$ for TIP-1 binding.

Thus, it is likely that when iCAL36 is bound to CAL, the $P^{-5}$ Trp side chain adopts a more surface-exposed conformation. In order to assess the free-energy contribution of each side chain to the interaction, we performed SubAnas of the iCAL36 sequence. Consistent with the stereochemistry of the interaction, the binding patterns of the CAL and TIP-1 PDZ domains also highlighted the importance of the $P^{-5}$ Trp side chain to the off-target binding affinity of iCAL36. $P^{-5}$ substitution with any other natural amino acid abrogated TIP-1 binding, whereas multiple substitutions were tolerated at other positions along the iCAL36 sequence. In contrast, CAL binding was retained for multiple substitutions at both the $P^{-5}$ position and elsewhere in the sequence (Figure 18 D). Both the biochemical and structural data thus suggested that the affinity of TIP-1 for iCAL36 was tightly focused on the $P^{-5}$ position, whereas CAL's affinity is more broadly distributed along the length of the peptide.

Since iCAL36 was derived by iterative optimization from the somatostatin receptor subtype 5 (SSR5) C-terminal peptide (ANGLMQTSKL) [76], we wanted to establish whether its affinity for TIP-1 was encoded by residual elements of the starting sequence. Using *F\*-*iCAL36 as a high-affinity reporter peptide, an FP displacement assay revealed that the SSR5 sequence interacts with TIP-1 even though it has a Met at the $P^{-5}$ position, a substitution that abrogates TIP-1 binding in the context of the iCAL36 sequence (Figure 18 D). In comparison to unlabeled iCAL36, which binds TIP-1 with a $K_i$ of 1.8 µM, unlabeled SSR5 peptide shows an important decrease of affinity with a $K_i$ value of 130 µM (Table 4). Taken together, these data suggest that both the baseline affinity of the SSR5 starting sequence and the $P^{-5}$ Trp represent potential contributors to the high affinity of the off-target interaction.

**Table 4:** $K_d$ and $K_i$ values for engineered peptide inhibitors

| Peptide | Sequence | $K_i/K_d \pm SD$ (µM) | | | | | |
|---|---|---|---|---|---|---|---|
| | | CAL | TIP-1 | N1P1 | N1P2 | N2P1 | N2P2 |
| C-βCAT | CNQLAWFDTDL | $1,100 \pm 500^a$ | $0.43 \pm 0.02$ | $ND^b$ | $ND^b$ | $ND^b$ | $ND^b$ |
| CFTR | TEEEVQDTRL | $390 \pm 20^c$ | $>1,000$ | $0.45 \pm 0.02^a$ | $1.9 \pm 0.1^a$ | $1.1 \pm 0.1^a$ | $0.10 \pm 0.02^a$ |
| SSR5 | ANGLMQTSKL | $21 \pm 2^c$ | $130.1 \pm 0.4$ | $25 \pm 2^c$ | $130 \pm 50^c$ | $39 \pm 8^c$ | $20 \pm 3^c$ |
| iCAL36 | ANSRWPTSII | $17.3 \pm 4.3$ | $1.82 \pm 0.09$ | $> 5,000^c$ | $> 5,000^c$ | $> 5,000^c$ | $> 3,000^c$ |
| iCAL41 | ANSRAPTSII | $183 \pm 19$ | $> 3,000$ | $> 5,000$ | $> 5,000$ | $> 1,000$ | $> 3,000$ |
| iCAL42 | ANSRLPTSII | $53 \pm 4$ | $> 3,000$ | $> 5,000$ | $> 5,000$ | $> 4,000$ | $> 5,000$ |
| *BT*-iCAL36 | *BT*-WrFKKfNSRWPTSII$^d$ | $0.767 \pm 0.006^e$ | $1.1 \pm 0.1$ | $> 5,000^e$ | $> 5,000^e$ | $> 5,000^e$ | $> 5,000^e$ |
| *BT*-iCAL42 | *BT*-WrFKKANSRLPTSII$^d$ | $9.2 \pm 0.9$ | $> 4,000$ | $> 5,000$ | $> 5,000$ | $> 5,000$ | $> 5,000$ |
| *F\**-iCAL36 | F\*-ANSRWPTSII$^f$ | $0.6 \pm 0.05$ | $0.54 \pm 0.04$ | $DNS^g$ | $DNS^g$ | $DNS^g$ | $DNS^g$ |
| *F\**-iCAL42 | F\*-ANSRLPTSII$^f$ | $10.8 \pm 0.2$ | $DNS^g$ | $DNS^g$ | $DNS^g$ | $DNS^g$ | $DNS^g$ |

**Footnotes**: n ≥ 3 for all titrations.
$^a$ Cushing et al. 2008, $^b$ Not determined, $^c$ Vouilleme et al. 2010
$^d$ *BT*-, biotin moiety; lower case letters denote D-amino acids.
$^e$ Cushing et al. 2010, $^f$ *F\**- fluorescein coupled via an aminohexanoic acid linker.
$^g$ Titrations did not achieve saturation.

### 6.4.3    A stereochemical Achilles' heel

In a next step of inhibitor improvement in terms of a pharmacological application, our combinatorial peptide-array/FP counterscreening paradigm is again used to increase the iCAL selectivity profile. Hexamer CombLib peptide arrays, in which all 400 possible pairs of amino acids were inserted into positions $P^{-5}$ and $P^{-4}$, had already been evaluated for binding to the CAL and NHERF PDZ domains [76]. A comparable CombLib was now prepared and surveyed for TIP-1 binding, which was found to require an aromatic residue at $P^{-5}$ (Figure 19 A). Comparison with published arrays identified a number of combinations that bound CAL, but did not bind TIP-1 or any of the NHERF domains previously studied [76, 77]. Among these was a Leu/Pro combination. To control for the possible influence of upstream residues, this preference was verified by additional CombLibs synthesized in the framework of the full iCAL36 sequence (Figure 19 A, B). Our SubAna arrays showed that the CAL-binding signal of the $P^{-5}$ Leu substitution was comparable to those of the strongest Trp/Xxx combinations

(Figure 18 D). Separate SubAna arrays based on the new sequence (iCAL42; ANSRLPTSII) confirmed that the CAL PDZ binding preferences were largely retained. Underscoring the critical contribution of the $P^{-5}$ Trp side chain, no additional single substitution can compensate for its loss: TIP-1 binding was abrogated for all single substitutions of the Leu-based iCAL42 sequence except for the Leu/Trp exchange (Figure 19 C).

Among previously identified TIP-1 ligands, the β-catenin C-terminus (NQLAWFDTDL) also contains a $P^{-5}$ Trp side chain [78]. However, compared to the >1500-fold loss of affinity achieved by a Trp/Leu substitution in iCAL36, a $P^{-5}$ Trp/Ala substitution in the β-catenin C-terminus caused only a 100-fold loss of TIP-1 affinity [80]. The greater sensitivity of the iCAL36 sequence could be due to the orientation of its Trp side chain within the TIP-1 binding pocket, which differs from that observed in the TIP-1:β-catenin complex [80] (Figure 19 D). Alternatively, the differential free-energy change could be due to the different replacement side-chains (Ala vs. Leu). In particular, analysis of the TIP-1 $P^{-5}$ pocket suggests that it could not readily accommodate the larger branched Leu side chain at this position (Figure 19 B). To determine the relative contributions of Trp affinity and/or Leu incompatibility to the iCAL42 binding energy, we also synthesized a $P^{-5}$ Ala mutant of iCAL36 and tested its binding by FP displacement. The ANSRAPTSII sequence (iCAL41) exhibits a similar lack of affinity for TIP-1 as does iCAL42 (Table 4). Thus, it appears that the thermodynamic impact of the $P^{-5}$ substitution on the iCAL36:TIP-1 interaction primarily reflects the loss of the Trp side chain in stabilizing this complex, rather than a specific incompatibility of Leu.
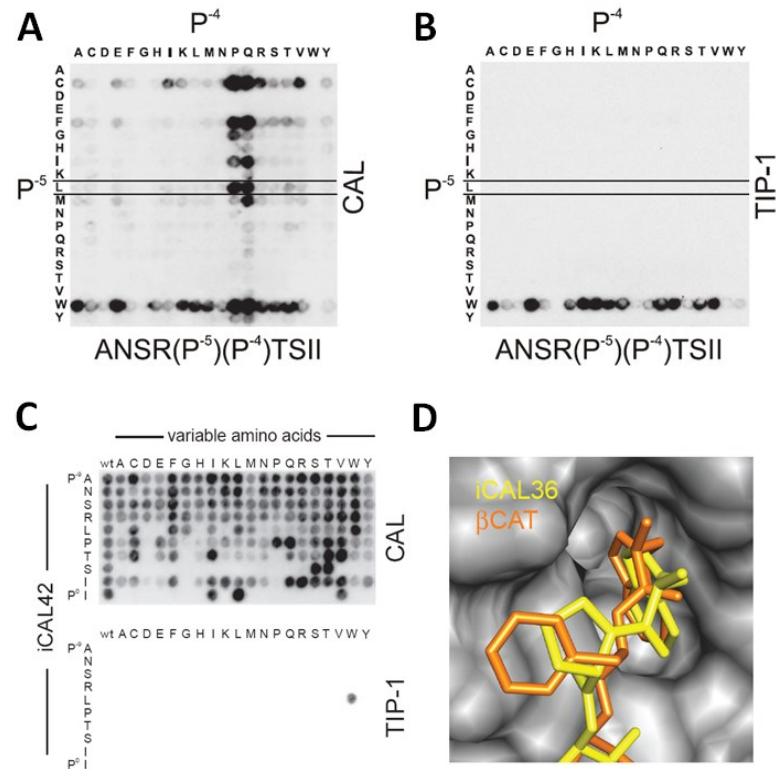
**Figure 19: Identification of a CAL-selective sequence substitution.**
CombLib peptide arrays varying two positions (P-5, P-4) of the iCAL36 sequence were incubated with either CAL (**A**) or TIP-1 (**B**) PDZ domains. Luminescent detection of bound protein revealed interacting sequences (dark spots). Only peptides with a Trp residue at $P^{-5}$ bound TIP-1, including iCAL36 (WP). Incubation with CAL shows higher redundancy at this position. Of peptides with Pro at $P^{-4}$, those with Leu, Phe or Cys at $P^{-5}$ bound CAL most strongly, but did not bind TIP-1. (**C**) To test for potential alternative sources of TIP-1 affinity, SubAna arrays based on the iCAL42 sequence were incubated with CAL (top) and TIP-1 (bottom) PDZ domains. While the CAL binding pattern remained similar to that of iCAL36, TIP-1 showed no binding except for the Leu->Trp revertant at $P^{-5}$. (**D**) The $P^{-5}$ Trp side chain of the iCAL36 peptide (stick figure, yellow) interacts with a deep hydrophobic pocket at the distal end of the peptide-binding groove that is also occupied by the $P^{-5}$ Trp in the TIP-1 complex with the β-catenin peptide (stick figure, orange; PDB code 3DIW).

In order to quantify the impact of the $P^{-5}$ Leu substitution and to assess inhibitory potential at high peptide concentrations, we performed FP displacement assays. Consistent with the qualitative peptide-array data, CAL displacement isotherms showed that iCAL42 retains robust CAL PDZ affinity, with a fitted $K_i$ value of 53 µM (Figure 20 A), only three-fold weaker than unlabeled iCAL36. The NHERF CombLib preferences were also validated: iCAL42 fails to bind any of the four NHERF1 or NHERF2 PDZ domains with appreciable affinity (Figure 1 appendix). Critically, the iCAL42 displacement isotherm for TIP-1 was also essentially indistinguishable from the vehicle control up to millimolar

peptide concentrations, representing a >1500-fold decrease in binding affinity (Figure 20 B). Thus, in the context of the iCAL36 sequence, the $P^{-5}$ side chain acts as a single-site TIP-1 affinity switch.
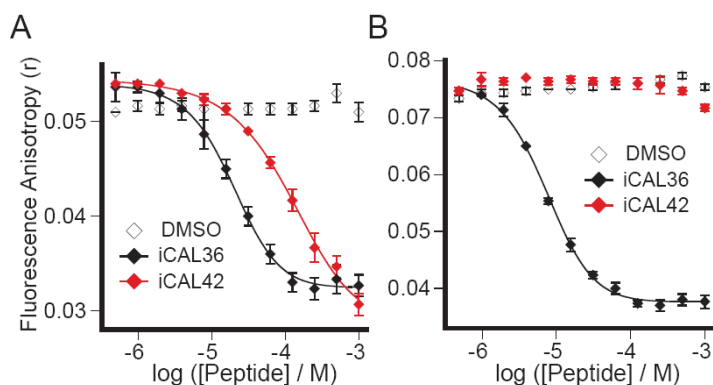


**Figure 20: Affinity measurements of iCAL36 versus iCAL42.**
Fluorescence anisotropy values are shown for a fluorescent reporter incubated with CAL (**A**) or TIP-1 (**B**) PDZ domain in the presence of increasing concentrations of iCAL36 (black) or iCAL42 (red), compared to DMSO (open). A four-parameter logistic fit is shown to reflect $IC_{50}$ values (n = 3).

### 6.4.4  iCAL42 is a single-PDZ inhibitor of endogenous CAL

Exploiting the localized vulnerability of the TIP-1 binding site for iCAL36, we were able to dramatically increase the inhibitor selectivity against known off-target interactions, as measured by the difference between the free energy of a given peptide binding to the CAL PDZ domain and the free energy of the same peptide binding to the highest affinity alternative among the NHERF and TIP-1 PDZ domains ($\Delta\Delta G$) (Figure 21). The SSR5 starting sequence binds CAL almost exactly as tightly as the closest NHERF1 or NHERF2 domain, N2P2 ($\Delta\Delta G_{CAL-best}$ = +0.1 kcal/mol). While the binding free energy of iCAL36 for CAL is much more favorable than for the NHERF PDZ domains ($\Delta\Delta G$ = -3.3 kcal/mol), it is actually 1.0 kcal/mole less favorable than for TIP-1 ($\Delta\Delta G$ = +1.0 kcal/mol). iCAL42 reverses this trend, binding CAL with a free energy that is substantially more favorable than any of the other partners ($\Delta\Delta G$ = -2.5 kcal/mol). Thus, the reward for a five-fold reduction in CAL binding affinity is a 60-fold difference relative to the $K_i$ of the PDZ domain with the next highest affinity.
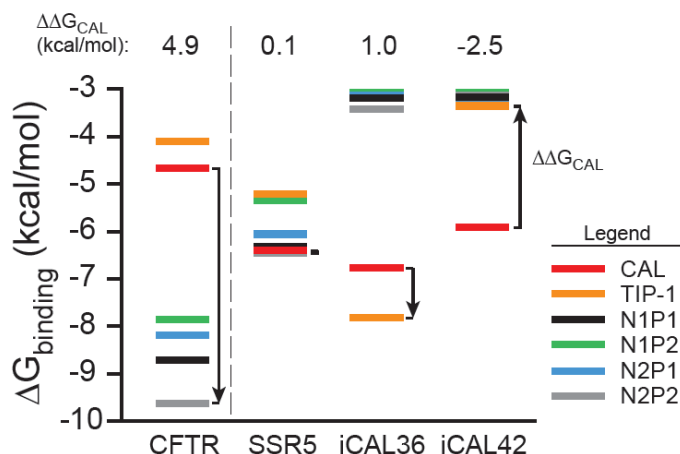
**Figure 21: Enhanced PDZ selectivity.**
ΔG⁰ values calculated from fluorescence anisotropy competition experiments are shown for the indicated peptide sequences against NHERF1, NHERF2, CAL, and TIP-1 PDZ domains. The ΔΔG value from CAL to the highest affinity off-target interaction is indicated by an arrow for each sequence.

To validate these observations for full-length proteins in the presence of potential physiological accessory proteins, we utilized the previously described WCL pull-down assay, together with a biotinylated analog of iCAL42 (*BT*-iCAL42). The FP competition assay was used to ensure that the selectivity profile was not compromised by the addition the N-terminal biotin linker. As expected, *BT*-iCAL42 bound CAL robustly ($K_i$ = 9.2 μM), but exhibited no appreciable binding for the NHERF and TIP-1 PDZ domains (Table 4). In a WCL pull-down immunoassay, *BT*-iCAL42 was used as bait, and captured prey proteins were eluted by displacement with unlabeled iCAL42. When probed by Western blotting, full-length CAL was clearly identified, but neither NHERF proteins, nor TIP-1 were observed (Figure 22 A).
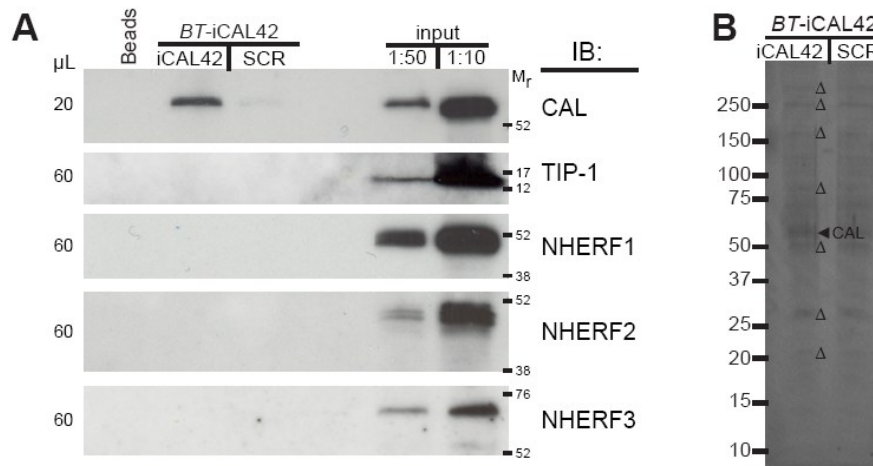
**Figure 22: iCAL42 a specific inhibitor for CAL PDZ domain.**
(**A**) A PDZ pull-down assays reveal that iCAL42 is selective for endogenous CAL over NHERF proteins and TIP-1 in an immunoblot assay (**B**) SDS-PAGE analysis (followed by LC/MS/MS) confirms that iCAL42 does not exhibit any high-affinity off-target PDZ interactions, but confirm its retention of affinity for CAL.

To assess the possibility that the Trp/Leu substitution might have generated unanticipated off-target interactions, in analogy to that originally seen for iCAL36 with TIP-1, we repeated the *BT*-iCAL42 pull-down assay and resolved putative interactors by silver stained SDS-PAGE (Figure 22 B). Aside from a modest enrichment of CAL, no protein bands were enriched in the iCAL42 cognate-peptide eluate compared to the scrambled-peptide control. Nevertheless, all major bands were submitted for mass-spectrometric analysis (Figure 22 B, triangles) and consistent with Western blotting, only endogenous CAL was again clearly identified (Figure 22 B, arrow). However, even by reducing the stringency of the pull-down assay and analyzing bands that were only marginally enriched relative to control eluates, we were unable to identify any other PDZ-domain containing protein, instead finding highly abundant and presumably non-specific interactors (e.g. cytoskeletal components). Based on these data, among the PDZ proteins expressed in CFBE-ΔF epithelial cells, CAL is the only one with appreciable affinity for iCAL42.

### 6.4.5  *F\*-iCAL42* enhances CFTR-mediated Cl⁻ secretion

Finally, we exploited the strict selectivity of iCAL42 to test the hypothesis that the off-target TIP-1 interaction might have contributed to the ΔF508-CFTR rescue seen with iCAL36. For these studies, the enhanced CAL selectivity of decapeptides carrying an N-terminal fluorescein moiety was exploited, which had been seen previously in comparison of the fluoresceinated ($K_d$) and unlabeled ($K_i$) affinities of iCAL36. For TIP-1, the affinity of *F\*-iCAL36* is only three-fold stronger than that of unlabeled iCAL36 (Table 4), compared to a 13-fold increase previously reported for CAL [76]. We therefore synthesized an N-terminally fluoresceinated version of iCAL42 (*F\*-iCAL42*) and tested it for binding against both CAL and TIP-1. In the context of the iCAL42 sequence, the addition of the N-terminal fluorescein moiety produces a five-fold enhancement in CAL affinity (Table 4). Conversely, the fluoresceinated peptide stills shows no appreciable binding to TIP-1: at the highest protein concentration tested (150 µM), *F\*-iCAL42* is essentially indistinguishable from a fluoresceinated scrambled control peptide *F\*-SCR* (Table 4). Having validated the affinity profile of our fluoresceinated probe, the ability of *F\*-iCAL42* to rescue ΔF508-CFTR chloride-channel activity was tested in comparison to the one of *F\*-iCAL36*. In Ussing chamber measurements [77] *F\*-iCAL36* and *F\*-iCAL42* were tested in head-to-head measurements for efficacy versus the scrambled control peptide, *F\*-SCR* (Figure 23). Consistent with previous measurements, *F\*-iCAL36* increased the CFTR$_{inh}$-172-sensitive $\Delta I_{sc}$ by 10.7 % (p = 0.0016; n=10). Treatment of CFBE-ΔF cells with *F\*-iCAL42* yielded a 12.5 % increase (p = 0.0013; n=10) in $\Delta I_{sc}$. Thus, *F\*-iCAL42* was at least as efficacious as *F\*-iCAL36*, suggesting that TIP-1 inhibition is not a substantial component of iCAL-mediated chloride-channel rescue.
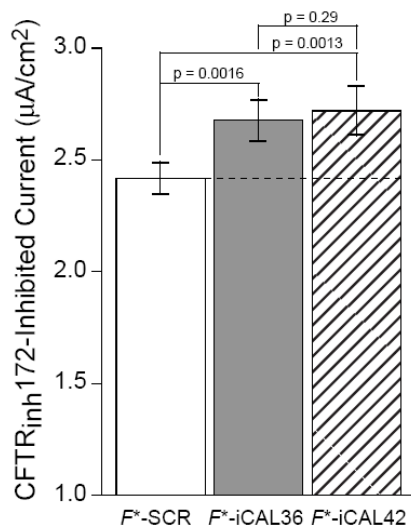
**Figure 23: A globally selective CAL inhibitor increases CFTR-mediated Cl⁻ efflux.**
Ussing chamber measurements confirm that iCAL42 retains efficacy for ΔF508-CFTR rescue. Polarized CFBE-ΔF cells were treated with *F*-SCR, *F*-iCAL36, or *F*iCAL42. CFTR-specific short-circuit currents ($\Delta I_{sc}$) were measured following addition of CFTR$_{inh}$-172. Mean $\Delta I_{sc}$ values are shown ± SEM (n=10).

## 6.5 Crossing biological membranes

Developing peptide based inhibitors for future therapeutic applications is a promising endeavor but another problem still remains: their poor ability to cross biological membranes. Since peptides do not cross biological barriers, they have been delivered as CPP (cell penetrating peptides) conjugates in most studies [32].

It has been shown in a recent study that CPPs behave differently as a function of (I) the type of CPP, (II) their type of N- and C-termini (e.g. carboxyamidaded , carboxylated, tags), (III) their concentrations, and (IV) the cell type that is used [40, 41, 81]. It is therefore necessary to test different types of CPPs in different cell lines preferably related to the target cell type of the future therapeutical application. Due to the fact that cystic fibrosis is a multi organ disease, the CPPs and/or CPP-effector conjugates should be tested first *in vitro* for cytotoxicity, uptake, affinity to the target molecule, and the biological function in different cell lines expressing the wt-CFTR or ΔF508-CFTR.

In this study, mainly two different cell lines have been used. The Caco-2 cell line is a continuous line of heterogeneous human epithelial colorectal adenocarcinoma cells and has been used as a model cell line of the colon expressing wt-CFTR [82, 83]. The second cell line are transformed human epithelial cells (CFBE41o- cells) [64] stably expressing ΔF508-CFTR under the control of a

cytomegalovirus promoter (CFBE-ΔF cells) [65]. These cells are commonly used as model system for lung cells expressing ΔF508-CFTR.

### 6.5.1   Coupling of iCAL36 to CPPs

Based on previous results [40], two CPPs were selected due to their high potential to penetrate biological membranes in different cell lines. The CAL PDZ domain inhibitor iCAL36 is covalently conjugated to the C-terminus of MPG and Penetratin (MPG-iCAL36 and Pen-iCAL36). Additionally, a control sequence representing a scrambled version of iCAL36 that is coupled to both CPPs (MPG-SCR and Pen-SCR) was synthesized. The CPP-conjugates are available as unlabeled peptides for viability assays and as (5,6)-carboxyfluorescein (*F*\*-) labelled version for uptake and microscopy analyses.

However, before testing the CPP-conjugates *in vitro*, they were analyzed in terms of their ability to target the CAL PDZ domain by FP measurements (Table **5**). As previously shown (Table 4), the extension of iCAL36 by fluorescein causes a 29-fold increase in binding affinity to CALP ($K_i$ = 17.3 ± 4.4 µM versus $K_d$ = 0.6 ± 0.1 µM). The same phenomenon is observed with the Pen-elongation of iCAL36 for the $K_i$ values (8-fold increase) and to a lower extent for the $K_d$ values (1.5-fold increase). Thus, the elongation of the iCAL36 sequence with Penetratin has a positive impact on peptide interaction with the CAL PDZ domain but the effect is less pronounced compared to the *F*\*-labeling alone ($K_i$ = 2.2 ± 0.3 µM versus $K_d$ = 0.6 ± 0.1 µM). Furthermore, the relatively weak improvement of CALP affinity from Pen-iCAL36 to *F*\*-Pen-iCAL36 suggests, that a possible effect on binding affinity to CALP is related to domain:peptide interactions upstream of the iCAL36 N-terminus. This is consistent with the observation that N-terminal extensions contribute to peptide affinity and selectivity. As previously shown, compared to the octamer used in CFTR-binding studies [62], the decameric iCAL36 peptide exhibits additional interactions at the distal end of the peptide-binding groove (Figure 12 B, arrow). This is consistent with the fact that *F*\*-Pen-iCAL36 has a slightly lower CALP affinity than *F*\*-iCAL suggesting that the *F*\*-labeling of *F*\*-Penetratin contributes less to binding affinity than Penetratin.

**Table 5:** Evaluation of $K_i$ / $K_d$ values (in μM) - influence of a N-terminal CPP-elongation sequence on binding affinity

| Peptide | Sequence | $K_i$ (μM) | $K_d$ (μM) |
|---------|----------|------------|------------|
| iCAL36$_{10}$ | ANSRWPTSII | 17.3 ± 4.3 | |
| F*-iCAL36$_{10}$ | F*-ANSRWPTSII | | 0.6 ± 0.1 |
| Pen-iCAL36$_{10}$ | RQILIWFQNRRMKWKKANSRWPTSII | 2.2 ± 0.3 | |
| F*-Pen-iCAL36$_{10}$ | F*-RQILIWFQNRRMKWKKANSRWPTSII | | 1 ± 0.1 |
| F*-MPG-iCAL36$_{10}$ | F*-GALFLGWLGAAGSTMGAWSQPKKKRKVANSRWPTSII | | 3.6 ± 0.1 |

F* Peptides include an N-terminal 5,6 Carboxyfluorescein to permit $K_d$ determination. Values ± SD. n=3 for all experiments.

A direct comparison between the $K_i$ of iCAL36 and the $K_i$ of MPG-iCAL36 was not possible due to increasing total fluorescence values during fluorescence anisotropy determination of MPG-iCAL36. However, the elongation of iCAL36 sequence to *F\**-MPG-iCAL36 seems to have an less pronounced effect on CALP affinity showing a 4-fold decrease of binding affinity compared to *F\**-Pen-iCAL36. his suggests that the effect of a MPG-elongation without *F\** would also be less pronounced compared to the Pen-elongation without *F\**.

In conclusion, the addition of MPG or Penetratin at the N-terminus of the iCAL36 sequence barely influences the binding affinity to CALP resulting in $K_d$ values in the low micromolar range (3.6 μM till 1 μM) which was also seen for *F\**-iCAL36 ($K_d$ = 0.6 ± 0.1 μM). These results are encouraging with regards to an *in vitro* application as well as to a potential *in vivo* development of a drug.

### 6.5.2 Internalization of MPG-iCAL36 and Pen-iCAL36 in Caco-2 cells

Having confirmed that the CPP-iCAL36 conjugates have a similar affinity for CALP as iCAL36 alone, the peptide effect on cell viability was determined using the Cell Counting Kit-8 (CCK-8) on Caco-2 cells. Measurement of cell viability (or toxic effects) is based on the principle, that WST-8 produces a water-soluble formazan dye upon reduction in the presence of an electron carrier. Therefore, WST-8 is reduced in cells by dehydrogenases to give a yellow colored product (formazan), which is soluble in the tissue culture medium. The amount of the formazan dye generated by the activity of dehydrogenases in cells is directly proportional to

the number of living cells. In general and for all further assays, we held a constant incubation time of about 3.5 hr to ensure comparability to previous experiments (see chapters 6.3.3 and 6.4.5 and ref. [84]).

In a first step, a tripartite approach using Caco-2 cells at different growing states (80 % confluent, 100 % confluent or polarized) was applied to determine the putative toxic impact of CPP-iCAL36 conjugates and their scrambled versions (MPG-iCAL36, MPG-SCR, Pen-iCAL36, Pen-SCR) on Caco-2 cells at concentrations between 1 µM to 500 µM. As shown in Figure 24, a value of 100 % ± 20 % corresponds to a non-toxic effect of the peptides, whereas values lower than 80 % viability represent a toxic effect.

Looking on 80 % confluent Caco-2 cells, the cell viability constantly decreases from 10 µM to 500 µM with a residual viability of about 5 % at 500 µM for all peptides. If cells reach 100 % confluence, this effect is clearly diminished – cells are still viable after incubation with 50 µM peptide. Cytotoxic effects at 100 µM are even smaller (80 % - 90 % viable cells) than those observed at 80 % confluence (40 % - 60 % viable cells). However, the residual viability at 500 µM is similar to the level observed for 80 % confluent cells (Figure 24 A, B).

In contrast, differentiated Caco-2 cells clearly show the slightest susceptibility for cytotoxic effects of CPP-iCAL conjugates. There is no reduction in cell viability up to concentrations of 100 µM. Only at a concentration of 500 µM a cytotoxic effect appears, however, to a lesser extent (20 % - 70 % viable cells dependent on the used CPP; Figure 24 C).

Generally, the cytotoxic effect of the different CPP-iCAL conjugates is quiet similar, showing a toxic effect at 500 µM in all state of Caco-2 cells. However, peptide concentration of 100 µM shows less toxicity especially in 100 % confluent and differentiated Caco-2 cells. In the differentiated one, mostly all CPP-iCAL conjugates are not toxic, which represent a good starting point for the further applications.

Knowing, that the CPP-iCAL36 conjugates have no influence on cell viability at concentrations between 1 µM and 100 µM, this range was used for internalization experiments with *F*\*-tagged CPP-iCAL conjugates.
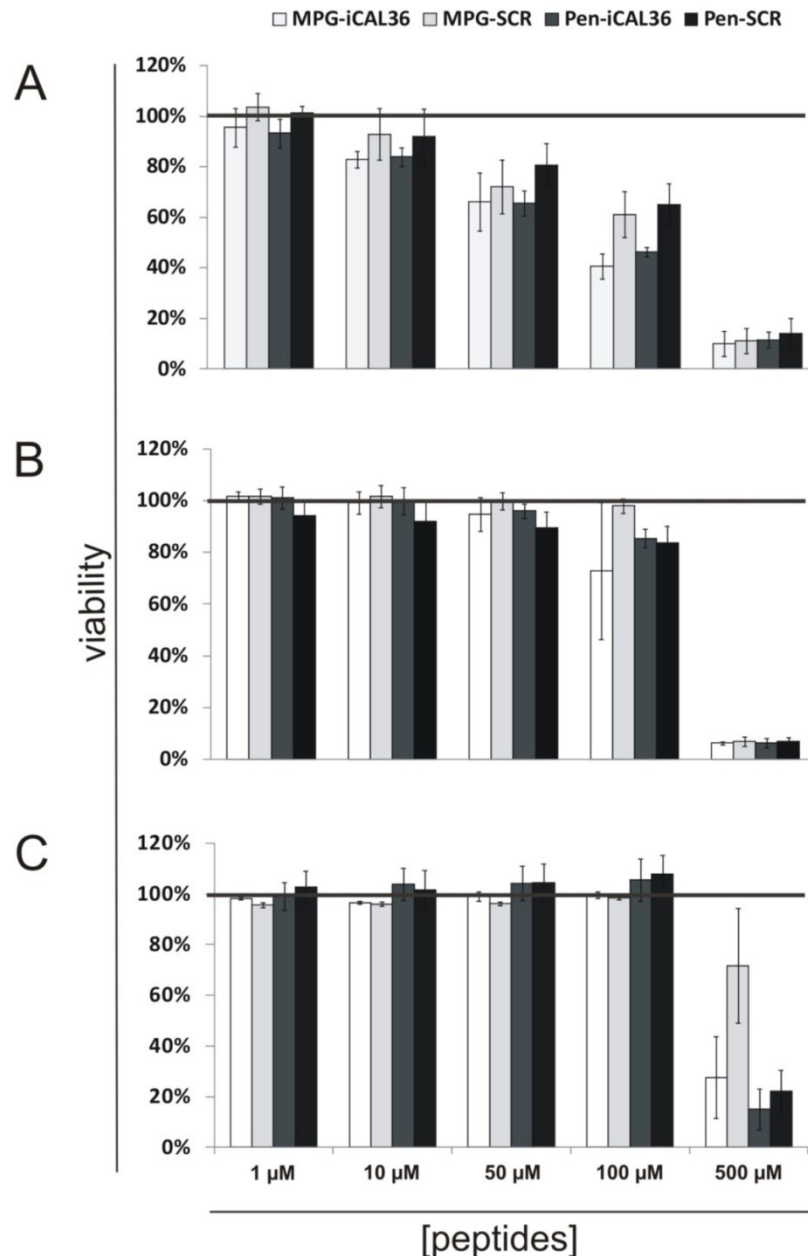
**Figure 24: Influence of CPP-iCAL conjugates on cell viability in Caco-2 cells.**
Cell viability was monitored after 3.5 hr incubation of different concentrations of CPPs by detecting the level of dehydrogenases released by Caco-2 cells. Values are normalized to an untreated control (100 %). The influence of CPP-iCAL constructs was monitored for (**A**) 80 % confluent, (**B**) 100 % confluent, and (**C**) differentiated cells. The CPP-peptide constructs show dose dependency that decreases when cell density increases. In differentiated cells, the highest concentration that does not evoke cytotoxicity is at 100µM whereas it is at 1-5 µM for 80 % confluent cells. n=4 for all experiments. Values shown are mean ± SD.

The *F\**-CPP-conjugates (MPG-iCAL36, MPG-SCR, Pen-iCAL36 and Pen-SCR) show similar internalization rates at 1 µM which are about 2.5 fold higher than *F\**-iCAL36, and 3.5-fold higher than the background level (Figure 25 A) (no significant difference between *F\**-iCAL36 and background). 80 % confluent

Caco-2 cells were incubated with conjugates at low concentration (1 µM) to evaluate differences in uptake between them (Figure 25 A). After 3.5 hr incubation, cells were trypsinized to remove exceed of membrane-bound CPP-iCAL. Thereafter, cells were lyzed and fluorescence is determined by spectrometry in relation to the total protein concentrations in the cell lysates (Signal intensities (SI)/mg protein).
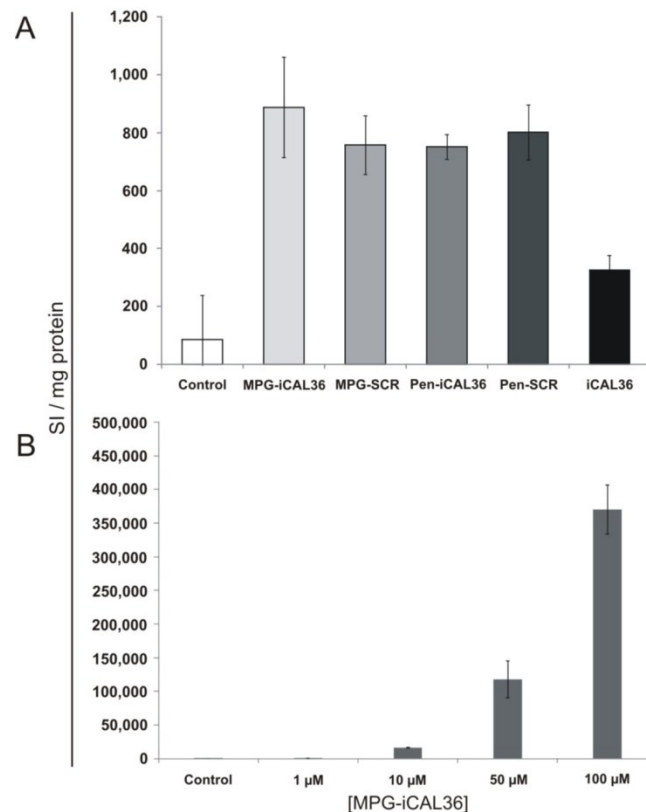


**Figure 25: Cellular uptake of different CPP-iCAL conjugates for differentiated Caco-2 cells.**
(5,6)-carboxyfluorescein (*F\**) was used for the detection of internalized peptide. After 3.5 hr incubation with a peptide followed by a trypsinization step, the internalized peptide was monitored and normalized to the total protein concentration of the cells. (**A**) Different CCP-iCAL36 and CPP-SCR conjugates with a concentration of 1 µM were used to compare the cellular uptake. Unlabeled iCAL36 and *F\** iCAL36 was used as negative controls. MPG and Penetratin conjugates show an increased cellular uptake compared to negative controls. (**B**) Cellular uptake of different concentrations of MPG-iCAL36 was monitored showing dose dependency. n=2 for all experiments. Values shown are mean ± SD.

Having confirmed the general ability of our CPP-conjugates to cross cell membranes, the internalization was tested in differentiated Caco-2 cells using different concentrations of *F\**-MPG-iCAL36. As shown in Figure 25 B, the internalization rate positively correlates with increasing concentrations of MPG-

iCAL36. Interestingly, the amount of internalized peptide at 100 μM is about 467-fold higher than the amount at 1 μM indicating a non-linear uptake. This is in accordance with common arguments that CPPs internalize via different mechanisms such as endocytosis at low concentrations and direct transduction at higher concentrations [85, 86].

### 6.5.3   Internalization of MPG-iCAL36 and Pen-iCAL36 in CFBE-ΔF cells

Previous work in our lab has shown the evidence of high variability regarding the uptake of CPPs in different cell lines [40]. We therefore tested the internalization of different CPP-conjugates in a lung epithelial cell line stably expressing ΔF508-CFTR (CFBE-ΔF cells) according to the experiments done previously with Caco-2 cells. We reduced the number of tested concentrations, omitting the 500 μM concentration due to their high potential to be cytotoxic in Caco-2 cells.

It is clearly shown that there is almost no occurring cytotoxicity for the MPG-conjugates (Figure 26 A) as well as for the Penetratin-conjugates (Figure 26 B) in 100 % confluent CFBE-ΔF cells assuming a cell viability threshold at 80 % viable cells. The only effect was observed at the final concentration of 100 μM where Pen-iCAL36 (70 %) shows a modest reduction in cell viability. Besides that, Pen-SCR (83 %), MPG-iCAL36 (87 %), MPG-SCR (93 %) as well as iCAL36 (99 %) and MPG alone (97 %) show no cytotoxicity (Figure 26)

However, it is of prime importance to also determine the potential cytotoxic influence of these conjugates on polarized cells that have grown on filter supports for reasons of comparability with Cl⁻-efflux experiments (Condition details see next chapter). Therefore, the CCK-8 assay was adapted to polarized CFBE-ΔF monolayers incubated with Pen-iCAL36 and Pen-SCR according to the experiments previously done in the 96-well format. As negative control, we used 2 % Triton X-100 that is known to be extremely cytotoxic even in low concentrations (Figure 27). Here again, we found that Pen-iCAL36 is slightly cytotoxic (70 ± 7 % cell viability) whereas Pen-SCR does not show cytotoxicity confirming the results of the viability assays in 96 well plates. The effects of Pen-iCAL36 (72 ± 2 % versus 70 ± 7 %) as well as those of Pen-SCR (83 ± 7 % versus

95 ± 7 %) are similar indicating that the results obtained by the 96-well approach are comparable to those obtained by polarized CFBE-ΔF cells on filter supports.
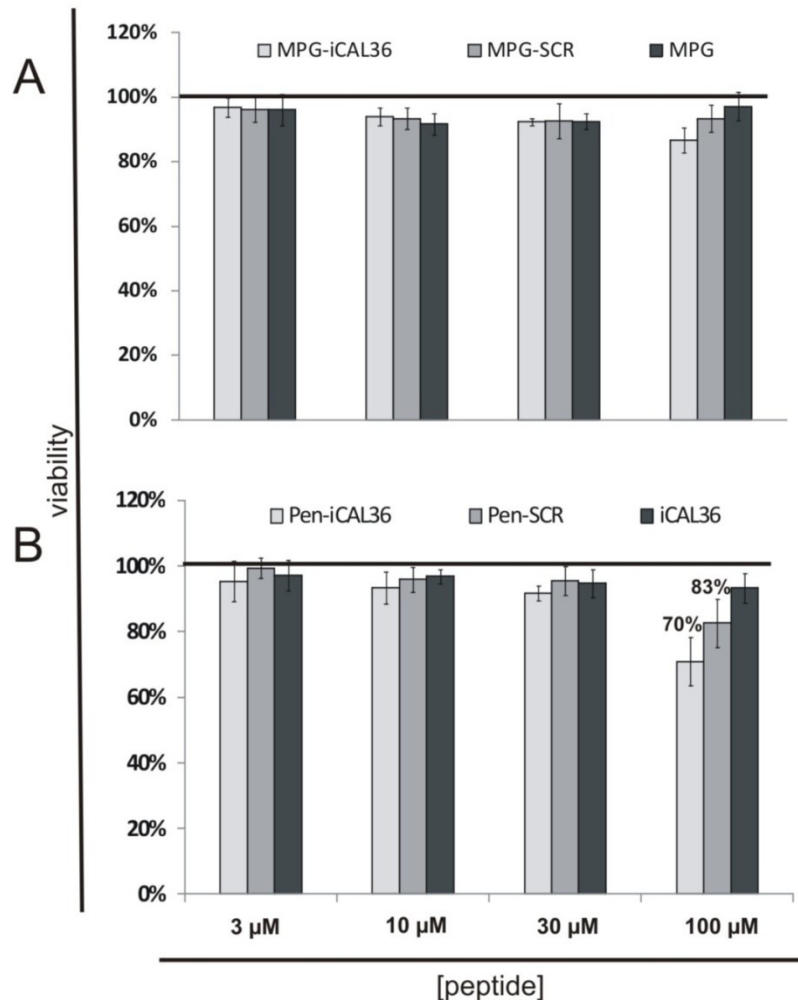


**Figure 26: Influence of CPP-iCAL conjugates on cell viability in CFBE-ΔF cells.**
Cell viability was monitored after 3.5 hr incubation of different concentrations of CPPs by detecting the level of dehydrogenases released by CFBE-ΔF cells (CCK-8 assay). Cells have grown for 6 days until they have reached confluence. Values are normalized to an untreated control (100 %). (**A**) MPG-iCAL and (**B**) Pen-iCAL conjugates are shown revealing negligible cytotoxicity under these conditions. n=6 for all experiments. Values shown are mean ± SD.

To visualize the cellular uptake of the *F\**-Pen-iCAL36 and *F\**-MPG-iCAL36 conjugates, uptake experiments on confluent CFBE-ΔF cells grown on MakTek™ dishes were performed. Cells were incubated with the respective peptide solutions of 5 µM as indicated in Figure 28. Following peptide incubation, the cell nuclei were stained with Draq5™ (cell signaling; red) and the cells were visualized by means of confocal microscopy. *F\**-iCAL36 served as negative control whereas *F\**-iCAL36 (500 µM) internalized by BioPORTER™ represents the positive control.

Fluorescence pictures represent 2D images of single cell layers as single fluorescence channel (green or red) as well as the merged image (Figure 28).
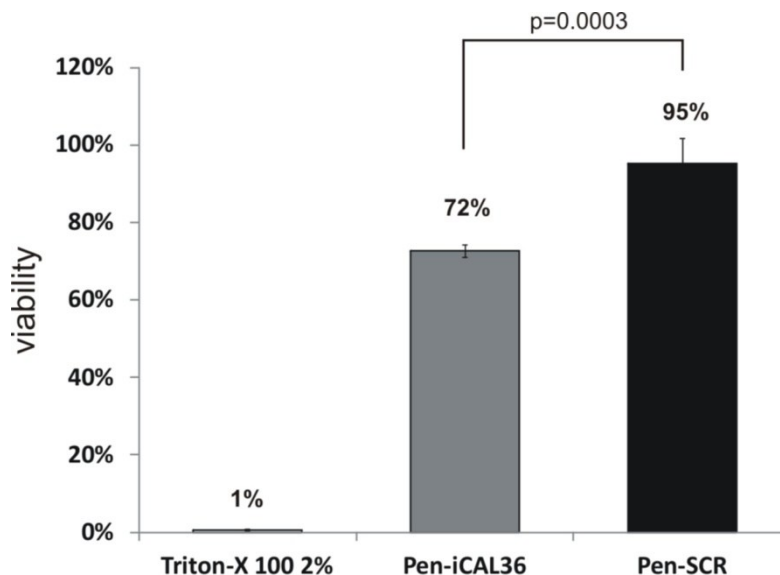


**Figure 27: Influence of CPP-iCAL conjugates on cell viability in polarized CFBE-ΔF cells.**
Cell viability was monitored after 3.5 hr incubation of 100 µM CPP by detecting the level of dehydrogenases released by CFBE-ΔF cells (CCK-8 assay). Cells were grown for 12 days on Snapwell™ filter supports until they have reached polarization. Values are normalized to an untreated control (100 %). Pen-iCAL36 and the scrambled version (Pen-SCR) are shown revealing slight cytotoxicity of Pen-iCAL36 compared to the scrambled version (p = 0.0003, T-Test). If the cells were treated with 2 % Triton X-100 as negative control, the viability value decreases to 0.58 %. n=4. Values shown are mean ± SD.

By subjectively comparing the fluorescence pictures we could clearly reproduce the results obtained by the uptake tests in Caco-2 cells. The two groups of *F\**-CPP-conjugates are clearly internalized whereas the *F\**-iCAL36 negative control is not. Generally, the green fluorescence of peptides is distributed all over the cytosol of the CFBE-ΔF cells. In all cases, the images show an additional somewhat punctuate distribution of the *F\**-peptides which was already seen for the internalization with BioPORTER™ indicating (I) aggregation of the peptide within the cell or (II) localization to specific compartments such as endosomal vesicles. The bright field images have shown that the cells grew till they reached confluence and always retained a planar shape (data not shown).

In some cases (*F*-MPG-SCR and BioPORTER™/*F*-iCAL36) the *F*-peptides seem to be stuck to the membrane which can lead to a reduced cytosolic concentration of the *F*-peptide.
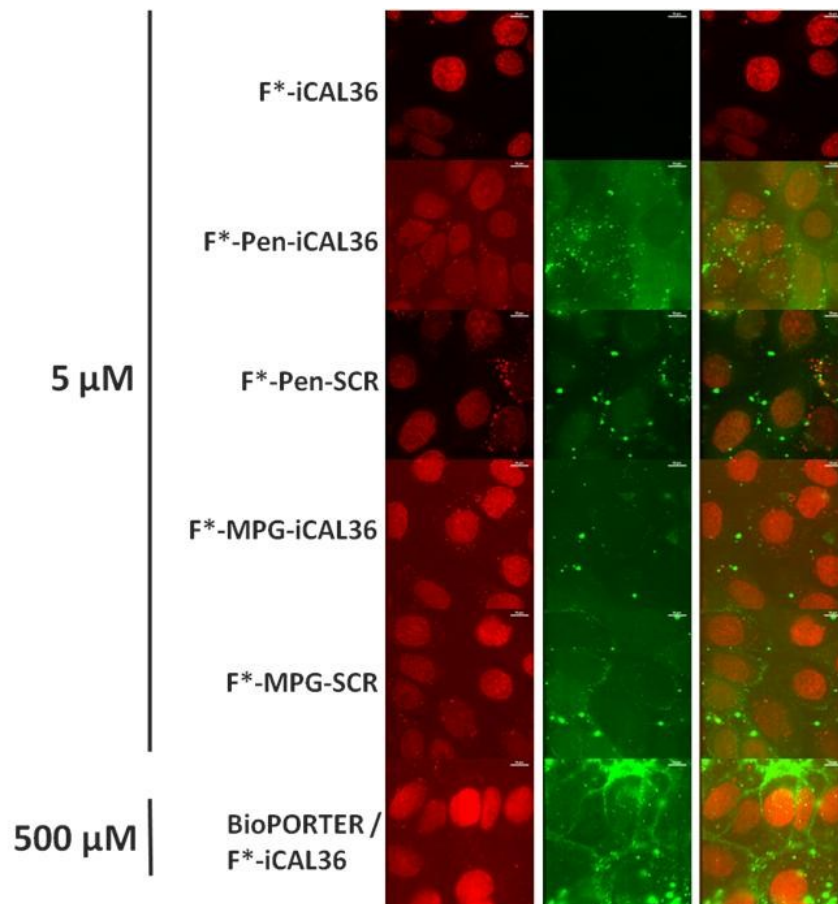


**Figure 28: Cellular uptake of CPP-iCAL36 conjugates in CFBE ΔF-cells.**
Interior sections of single layers are shown for living CFBE-ΔF cells grown on MakTek™ dishes for 4 days till they reached confluence. ICAL36 or the scrambled version of iCAL36 (SCR) peptides have been conjugated to F*-MPG or F*-Penetratin (Pen) for visualization (green florescence). Cell nuclei were stained with Draq5™ (Cell signalling, 1:1000, red fluorescence). Single *F*-iCAL36 as well as BioPORTER™/*F*-iCAL36 (500 µM) mix serve as negative and positive controls, respectively. Cells were treated with 5 µM of the *F*-labeled peptide or BioPORTER™/*F*-iCAL36 (500 µM) mix for 3.5 hr. For each condition, the Draq5™ staining (655 nm), the *F* staining (488 nm), and the merged images are shown from left to right. Scale = 10 µm.

Furthermore, for a better comparison of the internalization mode between the BioPORTER™/*F*-iCAL36 (500µM) mixture and 5 µM *F*-Pen-iCAL36, Z-stack images were taken of incubated CFBE-ΔF cells for 3D image reconstruction (Figure 29). Hereby, we were able to show the distribution of internalized peptides along all three axes. This confirms that the peptides are indeed localized within the cell and not stacking in or on the cell membrane.

Interestingly, the microscopic visualization of the internalized peptide do not obviously differ between both samples even at 100-fold lower concentration, indicating a more effective intracellular transfer by Penetratin compared to BioPORTER™ in confluent CFBE-ΔF cells.
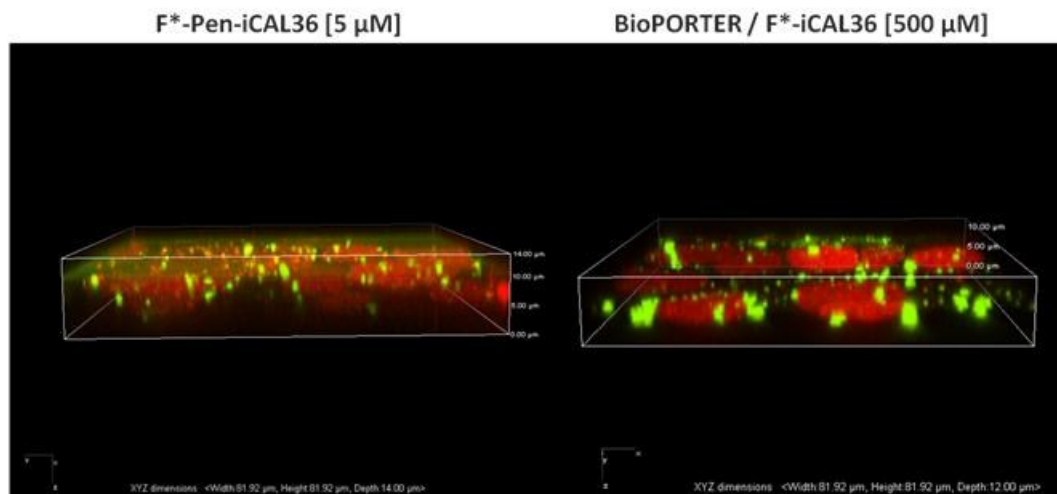


**Figure 29: Comparison of the cellular uptake of Pen-iCAL36 and BioPORTER™ in CFBE ΔF-cells.**
3D images of Z-stacks are shown for *F\**-Pen-iCAL36 as well as for the BioPORTER™/*F\**-iCAL36 mix in living CFBE-ΔF cells. Peptides carry an (5,6) carboxyflurescein (*F\**) moiety on their C-terminus appeared as green florescence. Cell nuclei were stained with Draq5™ (Cell signalling, red). Cells were treated with 5 μM *F\**-Pen-iCAL36 or BioPORTER™/500 μM *F\**-iCAL36 mix for 3.5 hr followed by Draq5™ treatment (1:1,000). The merged images of the *F\** staining (488 nm) and the Draq5™ staining (655 nm) are shown. XYZ dimensions: Width = 81.92 μm; Depth = 81.92 μm; Height = 12 μm/14 μm.

### 6.5.4   Penetratin-iCAL36 enhances ΔF508-CFTR-mediated Cl⁻-secretion

Having confirmed low cytotoxicity as well as successful internalization in confluent and polarized CFBE-ΔF cells, the proof of biological functionality is the necessary step in terms of therapeutic drug development. Since we have shown that *F\**-iCAL36 internalized by BioPORTER™ rescues Cl⁻-efflux to 25 % in CFBE-ΔF cells (Figure 15), we performed similar experiments with MPG and Penetratin as transfection vector in order to verify biological functionality (0.03 % final DMSO concentration).

CFBE-ΔF cells were treated with 100 μM MPG-iCAL36 conjugate and the respective scrambled negative controls (MPG-SCR). Unfortunately, both peptides

did not reveal significant differences excluding them for further investigations (Figure 30 A).
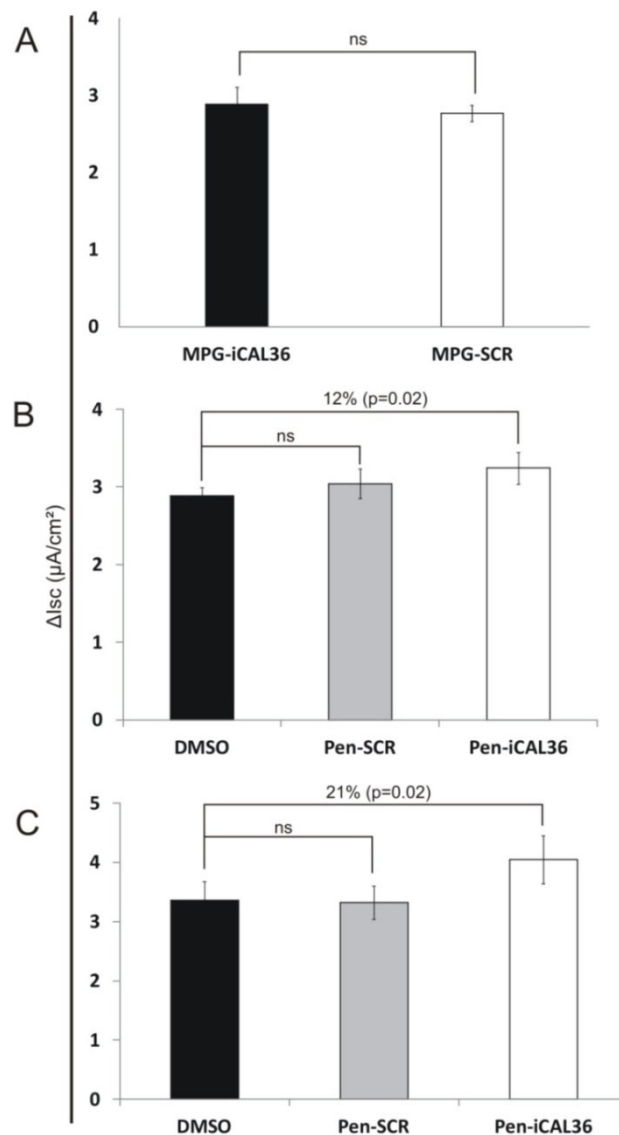


**Figure 30: Pen-iCAL36 enhances chloride efflux in polarized CFBE-ΔF cells.**
(**A**) Polarized CFBE-ΔF monolayers were treated with 100 µM *F\**-MPG-SCR or *F\**-MPG-iCAL36. Following channel activation, the change in short-circuit currents (ΔIsc) was monitored upon application of the CFTR-specific inhibitor $CFTR_{inh}172$ [73]. MPG-iCAL-36 and MPG-SCR do not differ regarding the ΔIsc. (**B, C**) Polarized CFBE-ΔF monolayers were treated with 50 µM (**B**) or 100 µM (**C**) *F\**-Pen-SCR or *F\**-Pen-iCAL36. Following channel activation, ΔIsc was monitored upon application of the CFTR-specific inhibitor $CFTR_{inh}172$. Vehicle (DMSO) was used as negative control. 50 µM Pen-iCAL36 enhances chloride efflux by 12 % and 100 µM Pen-iCAL36 by 21 %. P-values are shown for pair wise comparisons (n = 4 for A, n = 9 for B, n = 5 for C). Values shown are mean ± SEM.

In the next set of experiments, Pen-iCAL36 and Pen-SCR (50 µM or 100 µM) were analyzed compared to the vehicle (DMSO/buffer) as second negative

control to determine baseline activity. Treatment with 50 µM Pen-iCAL36 revealed a significant 12 % increase compared to cells treated with DMSO (p = 0.02, n = 9). However, treatment with 50 µM Pen-SCR did not reveal a significant difference to cells incubated with 50 µM Pen-iCAL36 (7 % increase; p = 0.1; Figure 30 B).Therefore, we treated CFBE-ΔF cells with 100 µM Pen-conjugates even if this concentration has shown slight cytotoxicity (~30 % reduction in cell viability; Figure 26 and Figure 28). In this experiment, cells treated with Pen-iCAL36 exhibited a 21 % increase (p = 0.02) in the magnitude of $CFTR_{inh}172$ $\Delta I_{SC}$ compared to Pen-SCR and vehicle control that do not show significant differences (Figure 30 C).

Thus, the resulting $\Delta I_{SC}$ of iCAL36 delivered by Penetratin  is almost as high as *F\**-iCAL36 delivered by BioPORTER™ (25 %). However, given the even 5-fold lower concentration of Pen-iCAL36 compared to BioPORTER™/*F\**-iCAL36 (500 µM), Penetratin appears to be 4-fold more effective than BioPORTER™.

Taken together, these results clearly indicate the high potential of CPP delivery in epithelial cells, thus underlining their applicability as delivery vectors for a pharmacological application.

# 7        Discussion

## 7.1   Engineering peptide inhibitors with biological functionality

Cystic fibrosis is the most common autosomal hereditary disease among Caucasians. Besides compounds that target the primary folding and gating defects of the most abundant CF inducing allele ΔF508, "stabilizers" that target the trafficking of the CFTR to the plasmamebrane are barely known. Therefore, a key therapeutic goal to reduce CF-patient mortality is the restoration of sufficient ⬚F508-CFTR activity to ameliorate the occurring chronic lung infections [87].

Here, we presented the development of a peptide based approach to identify competitive inhibitors of the CAL PDZ domain (Figure 5) in order to achieve post-endocytic stabilization of the CFTR. Thus, the idea was to mimic the functional rescue of Cl⁻-ion transport across the cellular membrane of CFBE-ΔF508 cells that have been seen previously by a CAL-specific RNA interference approach [13]. The enhanced Cl⁻-ion concentration of the lung mucus may decrease its viscosity and may therefore help to reduce the pathogenicity of cystic fibrosis.
The PDZ proteins CAL and its antagonist NHERF1 and NHERF2 are the engine of the CFTR trafficking machinery [1] but PDZ domains often have overlapping binding specificities exacerbating it to find selective inhibitors of just one PDZ domain. Therefore, we selected the high affinity sequence of the C-terminus of the somatostatin receptor type 5 (SSR5) as starting point for the CAL PDZ inhibitor engineering. It is the strongest binder among a series of known binding sequences ($K_i$ = 24.3 ± 1.7 μM) [59] – an important feature of a future CAL inhibitor. Thus, we decided to exploit the robust inherent affinity of PDZ domains for peptide ligands [55] along with the potential of inverted peptide arrays for high-throughput screening of sequence space [61] to drive a thermodynamic wedge between CAL and the other binding partners, despite their target overlap. First changes in the peptide sequence of SSR5 were achieved by comparing all binding motives resulting from HumLib and substitutional analysis (SubAna)

peptide array incubations. A preference for isoleucine at $P^0$ and $P^{-1}$ for CALP were clearly determined, which is not given for the NHERF PDZ domains (Figure 6 and Figure **7**). Although the four C-terminal amino acids mostly contribute to high affinity PDZ-ligand interactions [17, 20], upstream positions of an initially selective ligand may further enhance selectivity. Combinatorial libraries (CombLibs) are an appropriate tool to determine upstream positions in a pair wise manner. This is exemplarily shown for the identification of the Trp/Pro combinations on $P^{-4}$ and $P^{-5}$ which was found to be suitable for the improvement of a ligand interaction to CALP (Figure 9). Every single step of peptide array screening technologies was validated by FP polarization displacement assays in a parallel manner (Figure 5 and Table 2). By combining all results of both methods, we were able to design a highly specific CAL PDZ domain inhibitor named iCAL36 (ANSRWPTSII). For validation of interaction and specificity to the full length endogenous proteins, we performed pull down assays using iCAL36 as bait strictly confirming selectivity profiles obtained by FP polarization displacement assays.

Furthermore, the CAL-CFTR interaction is also weak compared to other CAL target interactions [59], which suggests that it may be possible to rescue ΔF508-CFTR using inhibitor concentrations that will probably not interfere with other CAL trafficking effects. Finally, CAL knockout mice are viable [88], suggesting that CAL inhibitors, particularly if delivered directly to the airway via inhalation, may be tolerated.

Furthermore, to evaluate iCAL36 as an apical-membrane stabilizer of chloride efflux activity, we established an Ussing chamber assay with polarized monolayers of CFBE-ΔF cells expressing ΔF508-CFTR. In order to determine whether CAL inhibition also has a substantial effect on ΔF508-CFTR maturation, we treated CFBE-ΔF monolayers with *F\**-iCAL36 in the presence of cycloheximide (CHX). The resulting highly significant 25 % increase in $\Delta I_{SC}$ (Figure 15) is close to the 26 % increase observed in the absence of CHX (data not shown), indicating that the effect of iCAL36 is largely independent of biogenesis. However, SSR5 also appears able to displace CFTR from its deleterious interaction with CAL (15 % increase in $\Delta I_{SC}$ compared to DMSO control; Figure 15) even if the interaction with its favorable NHERF proteins remains intact. This shows that CAL/NHERF

selectivity is clearly advantageous, but may not be strictly required to achieve functional benefit, broadening the potential spectrum of therapeutic CAL inhibitors.

Some studies have indicated that existing corrector compounds may also extend the apical-membrane half-life of rescued ΔF508-CFTR, although this effect has not been seen for corr-4a in primary human airway epithelial cells [10]. To assess the potential for complementary action, we also tested whether CAL inhibition can augment the effect of chemical correctors of the primary folding defect. CFBE-ΔF cells were treated with either the first-generation corrector corr-4A or DMSO and either *F\*-iCAL36* or *F\*-SCR* (scrambled version of iCAL36). Furthermore, we also tested whether CAL inhibition can augment the effect of chemical correctors (corr-4a) of the primary folding defect. The combination of *F\*-iCAL36* and corr-4A clearly demonstrates that the effects of small-molecule correctors (15 %) and iCAL36 (11 %) are essentially additive (25 %), again consistent with a model of CAL as a target for the stabilization of mature CFTR (Figure 16). The overall decreased level of iCAL36-mediated rescue seen in this dual-treatment (compared to Figure 15) experiment may be a result of higher background levels of DMSO delivery vehicle (0.03 % final DMSO concentration compared to 0.14 %), which is known to affect CFTR expression [89].

Since we know that Corr-4a produces greater apical membrane chloride current than low-temperature rescue did in Fischer rat thyroid (FRT) epithelial cells expressing ΔF508-CFTR [6], the level of rescue obtained by iCAL36 is promising. Furthermore, the rescue obtained by Corr-4a in CFBE-ΔF cells is substantial and comparable to the results obtained in FRT cells [90], thus indicating a potentially higher rescue obtained by iCAL36 in other cell types.

Finally, initial studies of our lab regarding the introduction of D-amino acids as well as non-natural building blocks into the iCAL36 sequence in order to prevent peptides from enzyme proteolysis seems to be promising. Further screening in this direction should be performed to confirm the first encouraging results and to analyze the contribution of these changes to a potential increase in efficacy.

In summary, the presented data provide a proof-of-principle for the engineering of selective PDZ inhibition, and, furthermore, determine the peptide

based CAL inhibitors as a new class of CFTR "stabilizers" specifically designed to reduce ΔF508-CFTR post-endocytic breakdown. A key aspect of our approach was the combination of multiple affinity determinants along the length of the peptide. By themselves, C-terminal motif-driven changes yielded a selectivity index of only ~10 (iCAL06) (Table 2). The rest was contributed by optimization of upstream elements (selectivity index of 170). As has been seen previously in other PPID systems, optimization also required alternating tradeoffs between target affinity and selectivity [91].

Overall, we have clearly achieved both our positive and negative design goals: *F*-iCAL36 has robust affinity for the CAL PDZ domain, but strong selectivity against the NHERF protein family, despite shared target specificity of the PDZ domains. This represents an important milestone in the development of peptidic inhibitors of this common class of PPIDs. In principle, this approach could be also adapted to other PPIDs having a pronounced peptide-binding pocket. These peptides potentially give the new opportunity to analyze the effects of CAL inhibition on CFTR expression in CF patient-derived bronchial epithelial cells and to explore the prospect of combination approaches aimed at parallel treatment of the biogenesis and stability defects of the most common disease associated CFTR allele.

## 7.2   Single PDZ specificity

The design of inhibitors that selectively target PDZ domains may ultimately be a requirement for potential therapeutic applications but it is critical to dissect their individual regulatory contributions. To overcome the well-known promiscuity of PDZ binding [59, 92-94], we have developed a peptide-engineering method combining high-throughput peptide-array and high-precision FP affinity techniques to target only CAL among a cluster of PDZ domains that share affinity for the CFTR C-terminus [76]. With this approach we were able to develop the CAL PDZ inhibitor iCAL36 (ANSRWPTSII). However, the direct extension of this approach to the full spectrum of PDZ domains to validate CALP specificity would potentially require the expression, purification, validation and evaluation of hundreds of recombinant proteins. In addition, if a particular cell type is targeted such an approach would ignore the tissue specificity of PDZ protein expression and regulation. Here we demonstrate that a systematic survey of target specificity can be performed *post hoc*, utilizing pull-down assays to probe cell lysates of the relevant tissue type, and mass spectrometry to identify off-target interactors.

Although our initial target set included only four negative design targets (PDZ1 and PDZ2 domains of NHERF1 and NHERF2), we detected only a single unintended PDZ interactor by pull down/mass spectrometry analyses with our first-generation CAL-selective inhibitor – TIP-1 (Figure 17). Retrospective analysis indicated that the SSR5 C-terminal sequence used as a starting point for CAL/NHERF design had weaker affinity for TIP-1 than for any of the members of the CAL, NHERF1, and NHERF2 cluster (Table 4). Thus, rather than reflecting a vestigial characteristic of the starting sequence, the TIP-1:iCAL36 affinity was substantially enhanced by our sequence modifications. Indeed, the off-target TIP-1 interaction is actually the product of countervailing effects of the peptide engineering process. The lack of TIP-1 binding of $P^{-5}$ Trp/Leu and Trp/Ala substitutions shows that the interaction depends critically on the stereochemical contributions of the Trp side chain (Figure 18 and Figure 19). It also shows that at

the positions other than $P^{-5}$, net affinity for TIP-1 was actually reduced by our substitutions, compared to the SSR5 starting sequence.

If anything, the surprise lay in the fact that only a single off-target interaction was detected, given the apparent promiscuity of PDZ binding. Furthermore, the lack of distributed affinity for TIP-1 at positions other than $P^{-5}$ suggests that our peptide engineering approach, by optimizing on-target interactions along the full-length of the peptide, efficiently minimizes the potential for broad-spectrum PDZ interactions. As a result of the stereochemical sensitivity of the single off-target interaction, our sequence-engineering protocol was easily able to eliminate it, without generating additional off-target effects. As summarized in Figure 22, our peptide-array data quickly identified the critical contribution of Trp at $P^{-5}$, and mass spectrometry showed that a Trp substitution not only eliminates TIP-1 binding, but also preserves the otherwise excellent trans-PDZ specificity of the iCAL36 sequence. In comparison with the biochemical effort that would have been required to exclude all such interactions in the design phase, *post-hoc* analysis thus permitted much more efficient elimination of off-target effects. The resulting inhibitor iCAL42 (ANSRLPTSII) binds only to CAL among epithelial PDZ proteins with high affinity ($K_i = 53 \pm 4$ μM), demonstrating for the first time single-PDZ specificity and confirming CAL as a pharmacologically relevant target for the rescue of $\Delta$F508-CFTR. However, a common problem of pull-down interaction analysis of protein domains is the unknown sensitivity threshold. Therefore, we currently are performing promising proof-of-principle studies by means of pull-down experiments with the C-terminus of the Kalirin protein (LGPGDPFSTYV)- a peptide sequence which is known to bind to a subset of different PDZ domains within a plethora of different binding affinities (Diploma thesis, Lars Vouillème).

However, it is important to note that the $P^{-5}$ Trp/Leu substitution is not the only potential solution to the problem of TIP-1 binding. On the contrary, Figure 31 B shows the extensive landscape of distinct selectivity-enhancing substitutions. When CAL versus TIP-1 preferences are evaluated for each individual substitution at residues $P^0$ through $P^{-5}$, 34 CAL-selective substitutions are identified, compared with only three TIP-1-selective substitutions (Figure

31 C). Positions $P^0$, $P^{-3}$ and $P^{-5}$ contribute most of the selective variation (Figure **31** C).
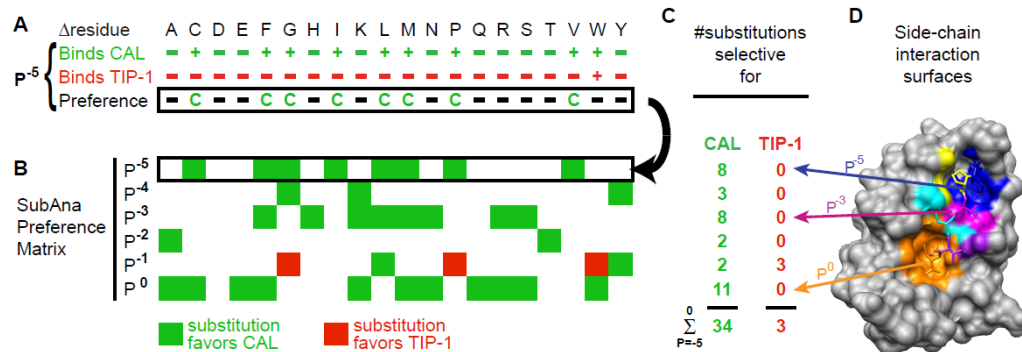


**Figure 31: Selectivity landscape of single iCAL36 substitutions.**
(**A**) For each amino-acid substitution at the $P^{-5}$ position in iCAL36, CAL and TIP-1 binding was normalized relative to the WT sequence in the SubAna shown in Fig. 2 and scored positive if $\geq 1/3$. The binding preference for each substitution was then classified as CAL (**C**), TIP-1 (T), or non-selective (-). (**B**) As illustrated for $P^{-5}$ (arrow), the binding preference described in (**A**) is encoded as a heat map (green = CAL-selective; red = TIP-1 selective; white = non-selective) for each of the last 6 residues, yielding a SubAna Preference Matrix. (**C**) The number of CAL-selective (green) and TIP-1 selective (red) substitutions is tallied for each position, and totaled across the matrix, showing a >10-fold preponderance of CAL-selective substitutions. (**D**) The interaction surfaces of each iCAL36 residue are color coded. Arrows link the positions with the most candidate CAL-selective substitutions to the corresponding interaction surfaces.

The importance of $P^0$ and $P^{-5}$ binding is correlated with the extensive stereochemical interactions seen at each position, but the role of $P^{-3}$ is more surprising, given its accessibility to solvent and relatively modest interaction surface (Figure 18 B), highlighting the importance of direct substitutional analysis of peptide binding. The differential robustness of the on-target and off-target interactions likely reflects the CAL-centric elaboration of the peptide sequence [76]: since the CAL affinity and selectivity was optimized at each position, numerous individual substitutions can be tolerated, each with a relatively modest affect on overall binding affinity. In contrast, the adventitious interaction with TIP-1 is not nearly as robust to sequence modification, and is eliminated by most of the changes that are tolerated by CAL. Thus, an ever-changing series of off-target interactions is avoided. The combinatorial diversity encoded by such a large number of target-oriented substitutions suggests that selectivity can be achieved even in cases where multiple off-target interactions are detected, or where secondary off-target interactions are introduced by an

initial substitution. In such cases, CombLib arrays are likely to be particularly powerful at handling multiple constraints in parallel.

Our success in identifying a CAL-specific inhibitor suggests that, at least in some cases, the vast stereochemical diversity encoded by a decameric peptide – $20^{10}$ combinations, corresponding to $\sim 10^{13}$ unique sequences – is sufficient to circumvent overlapping PDZ binding specificities. This idea is broadly consistent with recent reports that PDZ domains may be more widely distributed in target sequence space than had been indicated by earlier classification schemes [54, 55, 95] and that upstream residues contribute to interaction specificity [54, 55, 59, 76, 96]. However, it appears to contradict the limited sequence preferences seen in PDZ binding motifs that show preferences at only two to four amino acids, including those for CAL and NHERF1 PDZ1. It also runs counter to the recent suggestion that PDZ specificities exhibit inherently strong functional overlap [97]. Indeed, our data suggest that the extensive overlap that is found among natural PDZ binding partners may have been reinforced by evolutionary relationships and/or biological imperatives, rather than reflecting a fundamental inability of peptide sequences to distinguish among PDZ partners.

One explanation for the inability of motif analyses to report fully on protein:peptide stereochemical interactions is that motifs reveal binding preferences, but do not distinguish between residues that make no contribution and residues that are stereochemically incompatible at a given position. Neither class of side chains will be enriched among known binding sequences, but incompatible side chains can play important roles in selectivity. An example is provided by the $P^{-4}$ Pro side chain in iCAL36, which enhanced its CAL selectivity by preferentially suppressing interactions with NHERF2 PDZ domains (Table 2). Indeed, the substitution actually weakened absolute affinity for CAL $\sim$2-fold ($K_i$ WQTSII = 16.3 ± 2.1 µM ; $K_i$ WPTSII = 32.8 ± 0.3 µM), underscoring the trade-offs between inhibitor affinity and selectivity that are necessary when designing a specific inhibitor [91]. A similar trade-off was required to achieve the enhanced specificity of iCAL42 ($K_i$ iCAL36 = 17.3 ± 4 µM and $K_i$ iCAL42 = 53 ± 4 µM; Table 4). However, in Ussing chamber measurements *F*\*-iCAL36 and *F*\*-iCAL42 were tested in head-to-head measurements for efficacy versus the scrambled control

peptide, *F\**-SCR (Figure 23), where *F\**-iCAL36 increased the CFTR$_{inh}$-172-sensitive $\Delta I_{sc}$ by 10.7 % (p = 0.0016; n=10) and iCAL42 by 12.5 % (p = 0.0013; n=10). Thus, *F\**-iCAL42 was at least as efficacious as *F\**-iCAL36, suggesting that (I) TIP-1 inhibition is not a substantial component of iCAL-mediated chloride-channel rescue and (II) the decrease in binding affinity is compensated by the enhanced selectivity profile of iCAL42. Furthermore, the reduction of off-target effects clearly favors iCAL42 over iCAL36 for future applications.

Context-dependent interactions provide a second way in which binding motifs can fail to uncover stereochemical preferences. Thus, if the binding free energy contribution of an upstream residue depends on the bound conformation adopted by the C-terminus, this preference will be expressed only in a potentially small subset of sequences contributing to a global motif analysis. Even in the case of a prominent Trp-binding pocket like that found in TIP-1, the effect of a Trp/Ala substitution can vary greatly. In the context of the βCAT sequence, it shifts affinity 100-fold [80], but in the context of the iCAL36, the shift is >1500-fold (Table 4). This difference is mirrored in the different orientations of the respective P$^{-5}$ Trp side chains in the corresponding TIP-1 binding pocket (Figure 18). And together with the weak underlying affinity of the remaining positions in the iCAL36 sequence, it is enough to abrogate TIP-1 affinity of iCAL42.

The step-wise N-terminal elaboration of peptide specificity avoids both of these pitfalls. The use of SubAna arrays, which reveal substitutions that both enhance and suppress PDZ binding affinity, permits the direct detection of unfavorable interactions. Furthermore, by fixing a C-terminal core sequence, we are able to identify upstream amino-acid combinations that enhance selectivity in the relevant stereochemical framework, rather than optimizing context-independent affinity at each position to generate a global solution, which motif analysis suggests may not exist. The success of our approach, both in the initial design stage and in the specificity refinement stage reported here, suggests that meaningful affinity differentials are present at sequence positions that are invisible to motifs, and demonstrates that our protocol can identify them. Ultimately, this paradigm has not only identified a uni-selective CAL PDZ

inhibitor, but also provides a template that may be useful for interrogating the cell-biological roles and therapeutic potential of other PDZ domains.

## 7.3  Crossing biological membranes

Progress in peptide chemistry (SPOT synthesis in particular) now allows the rapid screening of peptide libraries in search for epitopes at the interface between proteins. These peptides are valuable starting points for drug development and, indeed, a number have already made their way into the clinic [98]. A major roadlock has been for long their poor intracellular delivery and bioavailability. In previously described experiments (Figure 15, Figure 16, and Figure 23), the transfection reagent BioPORTER™ was used to administrate iCAL peptide and to analyze its biological activity *in vitro* in CFBE-ΔF cells. However, this method is not suitable for a therapeutical drug delivery with clinical application.

The discovery of cell penetrating peptides (CPP) now offers the possibility of transfecting peptides or proteins (for review see [99]). Therefore, two different CPPs – MPG and Penetratin – were coupled covalently to our engineered CAL inhibitor iCAL36 in order to use their properties (amphipatic, positive net charge) to cross the plasma membrane. Evaluation of CPP-iCAL36 conjugates were done in parallel to the iCAL42 development. The presented data of CPP-iCAL36 represents the proof of concept for the new transfection strategy. Nevertheless, the proof of biological functionality for the CPP-iCAL42 peptide also is of major interest and currently under investigation.

Since we know that N-terminal elongation can affect binding affinity [59] (Table 3) we first tested the CPP-iCAL36 conjugates regarding their affinity to CALP by means of fluorescence anisotropy measurements. Generally, the coupling of CPPs to iCAL36 did not reveal major effects on binding affinity to the CAL PDZ domain. However, by looking on competitive binding assays, the coupling of Penetratin seems to have a positive effect on CAL affinity as revealed by an 8-fold increase in $K_i$ values. This is consistent with the fact that N-terminal elongation can contribute to CALP affinity [59].

Due to the versatility of CPPs to behave differently in different cell lines [40] and their different uptake modes [81, 100], we investigated (I) the uptake, (II) the cytotoxicity and (III) the biological functionality of our CPP-iCAL conjugates in two different cell lines (CFBE-ΔF cells; Caco-2 cells). In Caco-2 cells, we found that cytotoxicity of the CPP-conjugates depends on cell density. They were more cytotoxic in 80 % confluent cells than in confluent and differentiated cells (Figure 24). This is not surprising, because the free accessible cellular surface of 80 % confluent cells is bigger compared to differentiated cells with tight junction formation, allowing a more effective uptake.

The cytotoxicity of our CPP-iCAL conjugates in polarized CFBE-ΔF cells (Figure 26) is comparable to the occurring cytotoxicity observed for Caco-2 cells. Generally, the CPP-conjugates did not reveal relevant cytotoxicity up to concentrations of 100 μM in differentiated or polarized cells. Only for Pen-iCAL36, a slight cytotoxicity for confluent CFBE-ΔF cells grown on 96 well plates (70 ± 7 %) as well as for polarized monolayers grown on filter support (72 ± 2 %) could be observed. However, the fact that the cytotoxic effect of Pen-iCAL36 comes close to the estimated cytotoxicity threshold of 80 % viability, the effect of Pen-iCAL36 on cell viability seems to be of slight peculiarity.

Visualization of the impact of CPP-iCAL36 incubation on cell morphology as well as its cellular localization was performed by confocal (Figure 28) and fluorescence microscopy (Figure 14) experiments. *F\*-MPG-iCAL36* and *F\*-Pen-iCAL36* incubation induced no changes in cellular morphology. We found four different phenomena regarding the *F\*-staining* in CFBE-ΔF cells: (I) evenly distributed staining, (II) punctuate cellular staining pattern, and (III) membrane staining, whereas the latter probably reflects peptide that still remained in the lipid bilayer. However, that does not necessarily mean that the peptide is really stuck to the membrane but rather currently is in the process of getting internalized.

Punctuate intracellular pattern suggests that at least a subset of the peptide was internalized by endocytosis and is till remaining in vesicles which is consistent with recent studies about endocytic CPP internalization [39, 86]. However, this proposed mode of internalization contradicts earlier studies that

suggest a direct translocation process observed at 4 °C which prevents cells from performing endocytosis [101]. This direct translocation could be also an explanation for the evenly distributed staining. Generally, it is probable that CPP uptake shows a combination of different translocation mechanisms.

In conclusion, we have clearly demonstrated the cellular internalization of iCAL36 by a covalent CPP delivery strategy. The fact that the bright field images of the CFBE-ΔF cells (data not shown) reveal a flat cell shape and that the 3D images clearly show CPP distribution along all three axes (Figure 29) demonstrates that the CPP-conjugates are localized in the cytosol. Furthermore, the direct comparison of 5 µM Pen-iCAL36 and the BioPORTER™/*F\**-iCAL36 (500 µM) mixture (confocal microscopy) led to the assumption of high efficacy of CPP-based internalization. The 3D-images of Pen-iCAL36 and BioPORTER™/*F\**-iCAL36 (500 µM) internalization (Figure 29) do not show major differences even if a 100-fold lower Pen-iCAL36 concentration has been used. Clearly, iCAL36 peptide delivery mediated by Penetratin appears to be more effective.

Finally, the biological functionality of our internalized CPP-conjugates was measured to demonstrate that (I) internalization is functional and (II) that CPP delivery is more effective than peptide internalization reached by an uncovalent strategy using BioPORTER™ reagent.

CFBE-ΔF cells were treated with different concentrations of CPP-iCAL conjugates (MPG-iCAL36, MPG-SCR, Pen-iCAL36, Pen-SCR with 0.03 % final DMSO concentration) and the Cl⁻-efflux was determined by Ussing chamber assays. First experiments with MPG-iCAL36 revealed no significant differences in CFTR$_{inh}$172 $\Delta I_{SC}$ compared to a scrambled control (Figure 30 A) even if both constructs were internalized by CFBE-ΔF cells. MPG is a CPP which is frequently used to deliver cargoes by a non-covalent strategy via formation of nano particles [100]. Complex formation may also occur if MPG is covalently attached to its cargo resulting in an artificial masking of the cargo. This could explain that MPG-iCAL36 is not active in CFBE-ΔF cells.

In contrast, an increase in CFTR$_{inh}$172 $\Delta I_{SC}$ of 12 % and 21 % using 50 µM and 100 µM Pen-iCAL36, respectively, is shown compared to a vehicle control (Figure 30). Unfortunately, in case of the 50 µM Pen-iCAL36 incubation, a slight increase

of the scrambled control (Pen-SCR) is observed making the measured enhancement of $Cl^-$-efflux obsolete. Nevertheless, using 100 µM Pen-iCAL36 solutions, the scrambled control does not show any differences to the vehicle control. Curiously, low toxic effect of 100 µM Pen-iCAL36 (Figure 26) seems to have no influence on its activity. Pen-iCAL36 increases $CFTR_{inh}172$ $\Delta I_{SC}$ about 21 % which is in the range of the effect reached by a BioPORTER™/$F^*$-iCAL36 (500 µM) incubation (25 % $Cl^-$-efflux increase using 0.03 % final DMSO concentration; Figure 15). Due to the fact that the concentration is 5 fold lower using Pen-iCAL36, the compound is about 4-fold more effective than BioPORTER™/$F^*$-iCAL36 (500 µM). Knowing that $F^*$-iCAL36 ($K_d$ = 0.6 ± 0.1 µM) also has an even higher binding affinity to CALP than Pen-iCAL36 ($K_i$ = 2.2 ± 0.3 µM) (Table 5), Penetratin appears to be an effective vector for biological applications. However, given the high variability of the $CFTR_{inh}172$ $\Delta I_{SC}$ measurements in Ussing chambers, an even higher CALP affinity seems to be of major interest for $Cl^-$-efflux enhancement as well as for an improved manageability with regard to biochemical analyses.

Thinking about the lack of activity of 100 µM MPG-iCAL36 and 50 µM Pen-iCAL36, different explanations could be considered. Endocytotic machinery induced by MPG-cargo internalization could artificially increase the number of CFTR-channels at the plasma membrane, probably by reducing the CFTR-endocytosis itself. Furthermore, it is always possible that the CPP-majority (I) is stuck to the membrane, (II) aggregates, or (III) did not escape endosomal vesicles which would also prevent the CPP-conjugate from reaching the working concentration.

For 100 µM Pen-iCAL36, the internalization is likely to be driven by direct translocation, an effect which is observed at higher concentration [86]. The prevention of endocytotic pathway via transduction may eliminate the endosomal entrapment of Pen-iCAL36 and may result in a higher cytosolic availability of the compound for its therapeutical activity.

However, the high variability of the experimental setup to measure the $Cl^-$-efflux combined with the low total values of $CFTR_{inh}172$ $\Delta I_{SC}$ in CFBE-ΔF cells (2 µA versus 20 µA in wt-CFBE cells) complicated the acquirement of suitable

data. Furthermore, a 21 % increase in Cl$^-$-efflux is remarkable but could probably be further increased by using a co-administration with correctors and/or potentiators to restore enough ΔF508-CFTR-channels to significantly attenuate CF symptoms.

The efficacy of a drug is mainly described by (I) the internalization rate, (II) the affinity to the target molecule, (III) the stability against enzyme proteolysis, and (IV) low immunogenicity. Given the different behavior of CPPs with regard to their target cell [40] others CPPs should be evaluated especially in terms of tissue specificity (e.g. using *homing peptides*).

In sum, this work shows the potential of peptide based inhibitors as well as a proof-of-principle for a suitable working tool for future therapeutical approaches to enhance CF-patients life quality.

# 8 Conclusion

Restoring ΔF508-CFTR activity by using a combined therapeutical approach utilizing different biomolecules is one of the main objectives of CF research to ameliorate the symptoms of CF patients [87]. The here presented data suggest that optimal rescue will involve a combination of corrector and stabilizer activities targeting distinct protein networks. Small-molecule correctors are currently in late-stage clinical trials [102, 103]. Since only 10-35 % of wild-type channel activity may be required for significant therapeutic benefit [5], and although pharmaceutical stabilizers are not currently available, the high-affinity peptide ligands (iCAL36 and iCAL42) developed in this project provided essential progress in CF-drug development.

However, additional work should take in account to (I) increase the CALP affinity, (II) increase protease stability (for mucus resistance) and (III) reduce immunogenicity of CALP inhibitors. Here again, our engineering approach has high potential to be advantageous. The introduction e.g. of D-amino acids, non-natural peptide building blocks, or polyethylene glycol into the iCAL36 and iCAL42 sequences (while retaining it affinity and activity profiles) may protect the peptide from enzyme proteolysis. First results from ongoing iCAL development are promising (data not shown).

Furthermore, peptides are attracting increasing attention as therapeutics. Predictions have placed the value of peptides used for clinical applications at more than $13.4 billion in 2010 [104]. The increasing interest by the pharmaceutical industry in developing peptides as drugs is at least partially a consequence of increased acceptance of injected drugs on the market, the availability of new formulation and delivery technologies, and the relatively high approval success rates. This indicates the high potential of peptide based drug development.

# 9       Acknowledgements

Ussing chamber and fluorescence spectroscopy. Dr. D. Mierke (Dartmouth College) for access to NMR spectroscopic facilities and B. Coutermarsh, R. Barnaby and A. Fellows for technical assistance. Furthermore I want to thank Sahar Lemira, Christopher D. Bahl, Jessica D. St. Laurent, PRC, Jeanine F. Amacher (JFA), Yu Zhao and Kelli L. Hvorecny for their support and numerous fruitful discussions and for giving me the feeling to be part of their group. Mass spectrometry data were kindly provided by Dr. Bin Deng (Vermont Genetics Network, UVM).

Finally, I want to thank Prof. Dr. Dean R. Madden (DRM) for giving me the opportunity to work in his group. The always excellent scientific advice had definitely a share regarding my development as a scientist as well as the creation of this work.

# 10      Contributions

Dr. Prisca Boisguerin, Dr. Rudolf Volkmer (RV), Prof. Dr. Dean R. Madden (DRM) and Prof. Dr. Christian Freund initiated and supervised the project. Lars Vouilleme, Dr. Patrick R. Cushing (PRC), Jeanine F. Amacher (JFA), Maria Pelligrini, DRM and PB contributed to the experimental design. Lars Vouilleme developed and performed cell-viability assays, fluorescence microscopy experiments and peptide array studies. Furthermore Lars Vouilleme performed fluorescence polarization binding and chloride-secretion assays. PRC developed and performed the pull-down, fluorescence polarization, NMR spectroscopy, and chloride-secretion assays. JFA determined crystal structures. All contributed to data analysis and interpretation.

# 11 References

[1] W. B. Guggino, B. A. Stanton, *Nat Rev Mol Cell Biol* **2006**, *7*, 426.

[2] S. H. Cheng, R. J. Gregory, J. Marshall, S. Paul, D. W. Souza, G. A. White, C. R. O'Riordan, A. E. Smith, *Cell* **1990**, *63*, 827.

[3] B. Kerem, J. M. Rommens, J. A. Buchanan, D. Markiewicz, T. K. Cox, A. Chakravarti, M. Buchwald, L. C. Tsui, *Science* **1989**, *245*, 1073.

[4] W. Dalemans, P. Barbry, G. Champigny, S. Jallat, K. Dott, D. Dreyer, R. G. Crystal, A. Pavirani, J. P. Lecocq, M. Lazdunski, *Nature* **1991**, *354*, 526.

[5] E. Kerem, *Curr Opin Pulm Med* **2004**, *10*, 547.

[6] N. Pedemonte, G. L. Lukacs, K. Du, E. Caci, O. Zegarra-Moran, L. J. Galietta, A. S. Verkman, *J Clin Invest* **2005**, *115*, 2564.

[7] F. Van Goor, K. S. Straley, D. Cao, J. Gonzalez, S. Hadida, A. Hazlewood, J. Joubran, T. Knapp, L. R. Makings, M. Miller, T. Neuberger, E. Olson, V. Panchenko, J. Rader, A. Singh, J. H. Stack, R. Tung, P. D. Grootenhuis, P. Negulescu, *Am J Physiol Lung Cell Mol Physiol* **2006**, *290*, L1117.

[8] B. Illek, H. Fischer, G. F. Santos, J. H. Widdicombe, T. E. Machen, W. W. Reenstra, *Am J Physiol* **1995**, *268*, C886.

[9] Y. Wang, M. C. Bartlett, T. W. Loo, D. M. Clarke, *Mol Pharmacol* **2006**, *70*, 297.

[10] D. M. Cholon, W. K. O'Neal, S. H. Randell, J. R. Riordan, M. Gentzsch, *Am J Physiol Lung Cell Mol Physiol* **2010**, *298*, L304.

[11] G. L. Lukacs, X. B. Chang, C. Bear, N. Kartner, A. Mohamed, J. R. Riordan, S. Grinstein, *J Biol Chem* **1993**, *268*, 21592.

[12] A. Swiatecka-Urban, A. Brown, S. Moreau-Marquis, J. Renuka, B. Coutermarsh, R. Barnaby, K. H. Karlson, T. R. Flotte, M. Fukuda, G. M. Langford, B. A. Stanton, *J Biol Chem* **2005**, *280*, 36762.

[13] M. Wolde, A. Fellows, J. Cheng, A. Kivenson, B. Coutermarsh, L. Talebian, K. Karlson, A. Piserchio, D. F. Mierke, B. A. Stanton, W. B. Guggino, D. R. Madden, *J Biol Chem* **2007**, *282*, 8099.

[14] L. Guerra, T. Fanelli, M. Favia, S. M. Riccardi, G. Busco, R. A. Cardone, S. Carrabino, E. J. Weinman, S. J. Reshkin, M. Conese, V. Casavola, *J Biol Chem* **2005**, *280*, 40925.

[15]   F. Sun, M. J. Hug, C. M. Lewarchik, C. H. Yun, N. A. Bradbury, R. A. Frizzell, *J Biol Chem* **2000**, *275*, 29539.

[16]   S. Wang, H. Yue, R. B. Derin, W. B. Guggino, M. Li, *Cell* **2000**, *103*, 169.

[17]   D. A. Doyle, A. Lee, J. Lewis, E. Kim, M. Sheng, R. MacKinnon, *Cell* **1996**, *85*, 1067.

[18]   Z. Songyang, A. S. Fanning, C. Fu, J. Xu, S. M. Marfatia, A. H. Chishti, A. Crompton, A. C. Chan, J. M. Anderson, L. C. Cantley, *Science* **1997**, *275*, 73.

[19]   M. van Ham, W. Hendriks, *Mol Biol Rep* **2003**, *30*, 69.

[20]   J. H. Morais Cabral, C. Petosa, M. J. Sutcliffe, S. Raza, O. Byron, F. Poy, S. M. Marfatia, A. H. Chishti, R. C. Liddington, *Nature* **1996**, *382*, 649.

[21]   Y. Zhang, J. Dasgupta, R. Z. Ma, L. Banks, M. Thomas, X. S. Chen, *J Virol* **2007**, *81*, 3618.

[22]   X. Li, J. Zhang, Z. Cao, J. Wu, Y. Shi, *Protein Sci* **2006**, *15*, 2149.

[23]   M. P. Stumpf, T. Thorne, E. de Silva, R. Stewart, H. J. An, M. Lappe, C. Wiuf, *Proc Natl Acad Sci U S A* **2008**, *105*, 6959.

[24]   R. Frank, *J Immunol Methods* **2002**, *267*, 13.

[25]   J. Petschnigg, O. W. Moe, I. Stagljar, *Curr Opin Nephrol Hypertens* **2011**, *20*, 425.

[26]   G. Castel, M. Chteoui, B. Heyd, N. Tordo, *Molecules* **2011**, *16*, 3499.

[27]   Y. Oda, T. Owa, T. Sato, B. Boucher, S. Daniels, H. Yamanaka, Y. Shinohara, A. Yokoi, J. Kuromitsu, T. Nagasu, *Anal Chem* **2003**, *75*, 2159.

[28]   D. Ponsel, J. Neugebauer, K. Ladetzki-Baehs, K. Tissot, *Molecules* **2011**, *16*, 3675.

[29]   R. Frank, *Tetrahedron* **1992**, *48*, 9217.

[30]   K. Hilpert, D. F. Winkler, R. E. Hancock, *Nat Protoc* **2007**, *2*, 1333.

[31]   R. Volkmer, *Chembiochem* **2009**, *10*, 1431.

[32]   G. P. Dietz, *Curr Pharm Biotechnol* **2010**, *11*, 167.

[33]   M. Mae, U. Langel, *Curr Opin Pharmacol* **2006**, *6*, 509.

[34]   V. P. Torchilin, *Biopolymers* **2008**, *90*, 604.

[35]   S. El-Andaloussi, P. Jarver, H. J. Johansson, U. Langel, *Biochem J* **2007**, *407*, 285.

[36]   M. Fotin-Mleczek, S. Welte, O. Mader, F. Duchardt, R. Fischer, H. Hufnagel, P. Scheurich, R. Brock, *J Cell Sci* **2005**, *118*, 3339.

[37]   B. Gupta, T. S. Levchenko, V. P. Torchilin, *Adv Drug Deliv Rev* **2005**, *57*, 637.

[38] A. Joliot, A. Prochiantz, *Nat Cell Biol* **2004**, *6*, 189.

[39] J. R. Maiolo, M. Ferrer, E. A. Ottinger, *Biochim Biophys Acta* **2005**, *1712*, 161.

[40] J. Mueller, I. Kretzschmar, R. Volkmer, P. Boisguerin, *Bioconjug Chem* **2008**, *19*, 2363.

[41] J. Mueller, J. Triebus, I. Kretzschmar, R. Volkmer, P. Boisguerin, *J Con Rel* **2010**.

[42] M. C. Morris, P. Vidal, L. Chaloin, F. Heitz, G. Divita, *Nucleic Acids Res* **1997**, *25*, 2730.

[43] D. Derossi, A. H. Joliot, G. Chassaing, A. Prochiantz, *J Biol Chem* **1994**, *269*, 10444.

[44] M. C. Morris, L. Chaloin, J. Mery, F. Heitz, G. Divita, *Nucleic Acids Res* **1999**, *27*, 3510.

[45] L. Crombez, G. Aldrian-Herrada, K. Konate, Q. N. Nguyen, G. K. McMaster, R. Brasseur, F. Heitz, G. Divita, *Mol Ther* **2009**, *17*, 95.

[46] L. Crombez, M. C. Morris, S. Deshayes, F. Heitz, G. Divita, *Curr Pharm Des* **2008**, *14*, 3656.

[47] S. Deshayes, M. Morris, F. Heitz, G. Divita, *Adv Drug Deliv Rev* **2008**, *60*, 537.

[48] E. Dupont, A. Prochiantz, A. Joliot, *J Biol Chem* **2007**, *282*, 8994.

[49] M. Magzoub, K. Kilk, L. E. Eriksson, U. Langel, A. Graslund, *Biochim Biophys Acta* **2001**, *1512*, 77.

[50] W. Zhang, S. O. Smith, *Biochemistry* **2005**, *44*, 10110.

[51] R. M. Johnson, S. D. Harrison, D. Maclean, *Methods Mol Biol* **2011**, *683*, 535.

[52] C. Nourry, S. G. Grant, J. P. Borg, *Sci STKE* **2003**, *2003*, RE7.

[53] U. Wiedemann, P. Boisguerin, R. Leben, D. Leitner, G. Krause, K. Moelling, R. Volkmer-Engert, H. Oschkinat, *J Mol Biol* **2004**, *343*, 703.

[54] M. A. Stiffler, J. R. Chen, V. P. Grantcharova, Y. Lei, D. Fuchs, J. E. Allen, L. A. Zaslavskaia, G. MacBeath, *Science* **2007**, *317*, 364.

[55] R. Tonikian, Y. Zhang, S. L. Sazinsky, B. Currell, J. H. Yeh, B. Reva, H. A. Held, B. A. Appleton, M. Evangelista, Y. Wu, X. Xin, A. C. Chan, S. Seshagiri, L. A. Lasky, C. Sander, C. Boone, G. D. Bader, S. S. Sidhu, *PLoS Biol* **2008**, *6*, e239.

[56] J. Li, Z. Dai, D. Jana, D. J. Callaway, Z. Bu, *J Biol Chem* **2005**, *280*, 37634.

[57] M. Favia, T. Fanelli, A. Bagorda, F. Di Sole, S. J. Reshkin, P. G. Suh, L. Guerra, V. Casavola, *Biochem Biophys Res Commun* **2006**, *347*, 452.

[58] L. Vouilleme, P. R. Cushing, R. Volkmer, D. R. Madden, P. Boisguerin, *Angew. Chem. Int. Ed.* **2010**, *17;49*, 9912.

[59] P. R. Cushing, A. Fellows, D. Villone, P. Boisguerin, D. R. Madden, *Biochemistry* **2008**, *47*, 10084.

[60] R. Fischer, O. Mader, G. Jung, R. Brock, *Bioconjug Chem* **2003**, *14*, 653.

[61] P. Boisguerin, B. Ay, G. Radziwill, R. D. Fritz, K. Moelling, R. Volkmer, *Chembiochem* **2007**, *8*, 2302.

[62] A. Piserchio, A. Fellows, D. R. Madden, D. F. Mierke, *Biochemistry* **2005**, *44*, 16158.

[63] W. L. DeLano, **2002**.

[64] E. Bruscia, F. Sangiuolo, P. Sinibaldi, K. K. Goncz, G. Novelli, D. C. Gruenert, *Gene Ther* **2002**, *9*, 683.

[65] Y. Li, W. Wang, W. Parker, J. P. Clancy, *Am J Respir Cell Mol Biol* **2006**, *34*, 600.

[66] A. Swiatecka-Urban, M. Duhaime, B. Coutermarsh, K. H. Karlson, J. Collawn, M. Milewski, G. R. Cutting, W. B. Guggino, G. Langford, B. A. Stanton, *J Biol Chem* **2002**, *277*, 40099.

[67] S. Maudsley, A. M. Zamah, N. Rahman, J. T. Blitzer, L. M. Luttrell, R. J. Lefkowitz, R. A. Hall, *Mol Cell Biol* **2000**, *20*, 8352.

[68] R. A. Hall, L. S. Ostedgaard, R. T. Premont, J. T. Blitzer, N. Rahman, M. J. Welsh, R. J. Lefkowitz, *Proc Natl Acad Sci U S A* **1998**, *95*, 8496.

[69] T. Shibata, M. Chuma, A. Kokubu, M. Sakamoto, S. Hirohashi, *Hepatology* **2003**, *38*, 178.

[70] G. E. Crooks, G. Hon, J. M. Chandonia, S. E. Brenner, *Genome Res* **2004**, *14*, 1188.

[71] S. H. Joo, D. Pei, *Biochemistry* **2008**, *47*, 3061.

[72] A. K. Singh, B. Riederer, A. Krabbenhoft, B. Rausch, J. Bonhagen, U. Lehmann, H. R. de Jonge, M. Donowitz, C. Yun, E. J. Weinman, O. Kocher, B. M. Hogema, U. Seidler, *J Clin Invest* **2009**, *119*, 540.

[73] T. Ma, J. R. Thiagarajah, H. Yang, N. D. Sonawane, C. Folli, L. J. Galietta, A. S. Verkman, *J Clin Invest* **2002**, *110*, 1651.

[74] A. Taddei, C. Folli, O. Zegarra-Moran, P. Fanen, A. S. Verkman, L. J. Galietta, *FEBS Lett* **2004**, *558*, 52.

[75]    A. Jurkuvenaite, L. Chen, R. Bartoszewski, R. Goldstein, Z. Bebok, S. Matalon, J. F. Collawn, *Am J Respir Cell Mol Biol* **2010**, *42*, 363.

[76]    L. Vouilleme, Cushing, P.R., Volkmer, R., Madden, D.R., Boisguerin, P., *Angew Chem Int Ed Engl* **2010**, *in press*.

[77]    P. R. Cushing, Vouilleme, L.,Pellegrini, M., Boisguerin, P., Madden, D.R., *Angew Chem Int Ed Engl* **2010**, *in press*.

[78]    M. Kanamori, P. Sandy, S. Marzinotto, R. Benetti, C. Kai, Y. Hayashizaki, C. Schneider, H. Suzuki, *J Biol Chem* **2003**, *278*, 38758.

[79]    C. Alewine, O. Olsen, J. B. Wade, P. A. Welling, *Mol Biol Cell* **2006**, *17*, 4200.

[80]    J. Zhang, X. Yan, C. Shi, X. Yang, Y. Guo, C. Tian, J. Long, Y. Shen, *J Mol Biol* **2008**, *384*, 255.

[81]    T. Letoha, S. Gaal, C. Somlai, A. Czajlik, A. Perczel, B. Penke, *J Mol Recognit* **2003**, *16*, 272.

[82]    B. Press, D. Di Grandi, *Curr Drug Metab* **2008**, *9*, 893.

[83]    S. Laohapitakworn, J. Thongbunchoo, L. I. Nakkrasae, N. Krishnamra, N. Charoenphandhu, *Am J Physiol Cell Physiol* **2011**, *301*, C137.

[84]    P. R. Cushing, L. Vouilleme, M. Pellegrini, P. Boisguerin, D. R. Madden, *Angew Chem Int Ed Engl* **2010**, *17;49*, 9907.

[85]    G. Tunnemann, G. Ter-Avetisyan, R. M. Martin, M. Stockl, A. Herrmann, M. C. Cardoso, *J Pept Sci* **2007**.

[86]    F. Duchardt, M. Fotin-Mleczek, H. Schwarz, R. Fischer, R. Brock, *Traffic* **2007**, *8*, 848.

[87]    J. B. Lyczak, C. L. Cannon, G. B. Pier, *Clin Microbiol Rev* **2002**, *15*, 194.

[88]    R. Yao, C. Ito, Y. Natsume, Y. Sugitani, H. Yamanaka, S. Kuretake, K. Yanagida, A. Sato, K. Toshimori, T. Noda, *Proc Natl Acad Sci U S A* **2002**, *99*, 11211.

[89]    T. Arakawa, D. Ejima, Y. Kita, K. Tsumoto, *Biochim Biophys Acta* **2006**, *1764*, 1677.

[90]    S. M. Rowe, L. C. Pyle, A. Jurkevante, K. Varga, J. Collawn, P. A. Sloane, B. Woodworth, M. Mazur, J. Fulton, L. Fan, Y. Li, J. Fortenberry, E. J. Sorscher, J. P. Clancy, *Pulm Pharmacol Ther* **2010**, *23*, 268.

[91]    G. Grigoryan, A. W. Reinke, A. E. Keating, *Nature* **2009**, *458*, 859.

[92]    U. Hoffmüller, M. Russwurm, F. Kleinjung, J. Ashurst, H. Oschkinat, R. Volkmer-Engert, D. Koesling, J. Schneider-Mergener, *Angewandte Chemie International Edition* **1999**, *38*, 2000.

[93]    B. Z. Harris, W. A. Lim, *J Cell Sci* **2001**, *114*, 3219.

[94]    Z. Songyang, A. S. Fanning, C. Fu, J. Xu, S. M. Marfatia, A. H. Chishti, A. Crompton, A. C. Chan, J. M. Anderson, L. C. Cantley, *Science* **1997**, *275*, 73.

[95]    N. J. Skelton, M. F. Koehler, K. Zobel, W. L. Wong, S. Yeh, M. T. Pisabarro, J. P. Yin, L. A. Lasky, S. S. Sidhu, *J Biol Chem* **2003**, *278*, 7645.

[96]    Y. Zhang, S. Yeh, B. A. Appleton, H. A. Held, P. J. Kausalya, D. C. Phua, W. L. Wong, L. A. Lasky, C. Wiesmann, W. Hunziker, S. S. Sidhu, *J Biol Chem* **2006**, *281*, 22299.

[97]    A. J. te Velthuis, P. A. Sakalis, D. A. Fowler, C. P. Bagowski, *PLoS One* **2011**, *6*, e16047.

[98]    A. Loffet, *J Pept Sci* **2002**, *8*, 1.

[99]    J. M. Gump, S. F. Dowdy, *Trends Mol Med* **2007**, *13*, 443.

[100]   S. Deshayes, K. Konate, G. Aldrian, L. Crombez, F. Heitz, G. Divita, *Biochim Biophys Acta* **2010**, *1798*, 2304.

[101]   A. Joliot, C. Pernelle, H. Deagostini-Bazin, A. Prochiantz, *Proc Natl Acad Sci U S A* **1991**, *88*, 1864.

[102]   E. L. Turnbull, M. F. Rosser, D. M. Cyr, *BMC Biochem* **2007**, *8 Suppl 1*, S11.

[103]   M. Wilschanski, *Proc Am Thorac Soc* **2010**, *7*, 399.

[104]   V. Glaser, *Genetic Engineering & Biotechnology News* **2007**, *29*.

# 12      Appendix
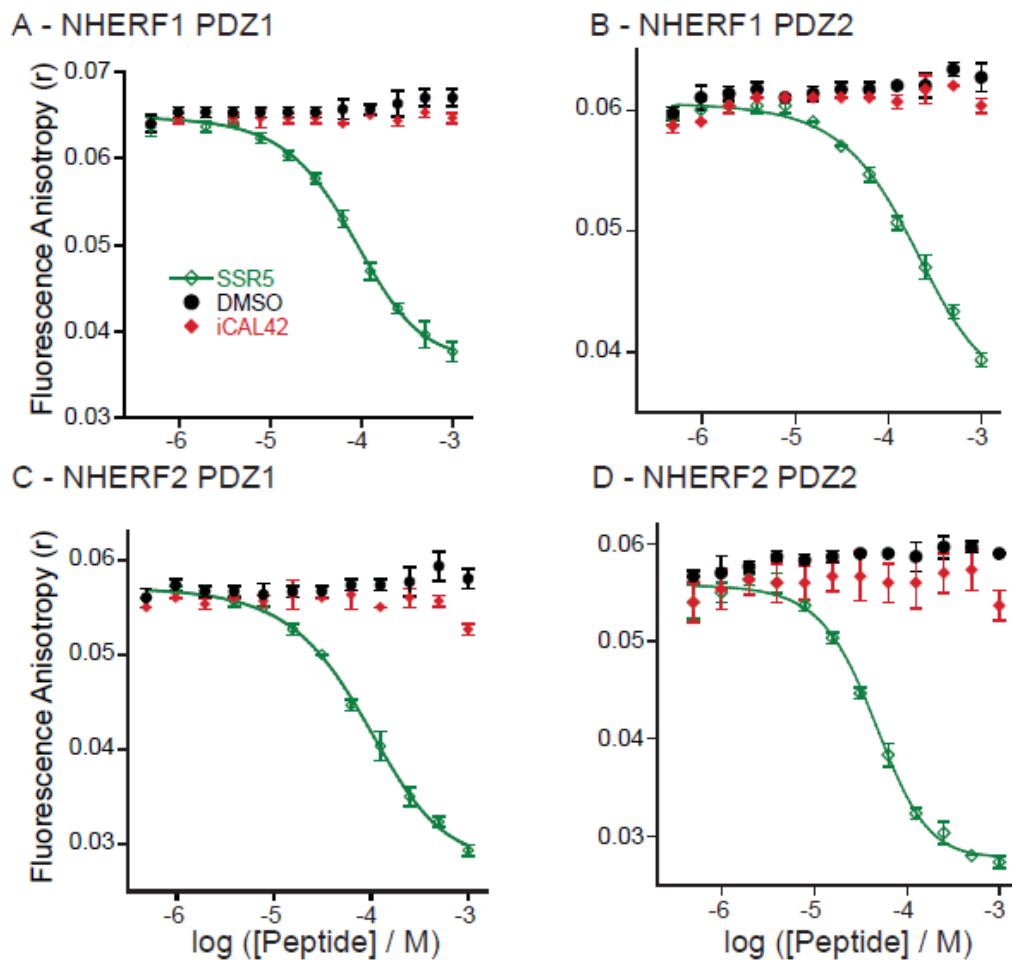


**Figure A1 appendix: Affinity measurements of iCAL42 with the PDZ domains of NHERF1 and NHERF2.**

Fluorescence anisotropy values are shown for a fluorescent reporter incubated with (**A**) the first PDZ domain of NHERF1, (**B**) the second PDZ domain of NHERF1 (**C**) the first PDZ domain of NHERF2 (**D**), and the second PDZ domain of NHERF2 in the presence of increasing concentrations of iCAL42 (red), SSR5 (green) compared to DMSO (black). A four-parameter logistic fit is shown to reflect $IC_{50}$ values (n = 3).

**Table A1:** - Data collection and refinement statistics

| | TIP-1:iCAL36 crystal |
|---|---|
| **Data collection** | |
| Space group | *P* 1 |
| Cell dimensions | |
| *a*, *b*, *c* (Å) | 26.97, 34.09, 66.86 |
| $\alpha$, $\beta$, $\gamma$ (°) | 79.64, 87.15, 89.97 |
| Resolution (Å) | 19.11-1.24 (1.31-1.24)* |
| $R_{sym}$ | 0.04 (0.27) |
| $I / \sigma I$ | 27.63 (4.29) |
| Completeness (%) | 91.3 (70.0) |
| Redundancy | 6.1 (3.6) |
| | |
| **Refinement** | |
| Resolution (Å) | 19.11 – 1.24 |
| No. reflections | 60,539 |
| $R_{work}$ / $R_{free}$ | 0.180/0.193 |
| No. atoms | |
| Protein | 1,739 |
| Ligand/ion | 184 |
| Water | 256 |
| *B*-factors | |
| Protein | 19.47 |
| Ligand/ion | 22.44 |
| Water | 28.01 |
| R.m.s. deviations | |
| Bond lengths (Å) | 0.005 |
| Bond angles (°) | 0.985 |

*Values in parentheses are for highest-resolution shell.

**Table A2: 80 best binding sequences of the 6223-HumLib incubation with CALP**

| Spot | BLU | Sequence | ID |
|------|------|-----------|------|
| 23 | 144120 | QAEEDWTC | P009 |
| 131 | 80217 | KRNTLYFSTD | Q129 |
| 232 | 107439 | TIKVIKAKKKT | O148 |
| 332 | 76930 | QKVKEKLKID | P026 |
| 439 | 73965 | GSPIHSLETSL | Q018 |
| 456 | 102531 | RVAFKLRINK | P144 |
| 465 | 116107 | SNVKIVKVKK | P563 |
| 542 | 72848 | KRQSILFSTE | P112 |
| 619 | 92449 | LFLVLASRTQ | Q105 |
| 668 | 98814 | NVISERNSTT | Q165 |
| 681 | 71152 | FGFDVGPVC | P024 |
| 683 | 68469 | FGVDVGPVC | P024 |
| 699 | 98936 | FGVEIGPVCF | P059 |
| 799 | 97400 | SSIKVVLRKE | P565 |
| 834 | 106809 | LQDSRVYVS | Q139 |
| 835 | 122709 | LADEMICITT | Q016 |
| 849 | 107942 | NNPANRRTT | O603 |
| 962 | 103406 | ETEEEVQDT | P135 |
| 1099 | 122169 | EQSDVRFSS | Q995 |
| 1106 | 82568 | KGGALQSCTI | P095 |
| 1168 | 86001 | KINLSQKETSI | P536 |
| 1253 | 233260 | NSRPHTNET | P235 |
| 1257 | 152494 | SFHSIKQSTA | P349 |
| 1300 | 83064 | SNQLAWFDT | P352 |
| 1309 | 99732 | QVNKVWDQ | O145 |
| 1329 | 94806 | RPRDHVKKTI | O953 |
| 1351 | 68116 | IGTMFLRETS | P334 |
| 1391 | 87919 | DMMLEMLC | P518 |
| 1451 | 101596 | WGMGSQSC | P484 |
| 1557 | 82301 | TENFPLKLCR | O149 |
| 1616 | 101678 | KELKTVTFSK | Q130 |
| 1620 | 84380 | QSLAGSPSSK | Q084 |
| 1805 | 73874 | RELLKELRTQ | Q005 |
| 1806 | 117487 | FRTSLPKSCD | O152 |
| 1850 | 117990 | SVKYRLKFRF | P120 |
| 1952 | 70639 | GPGWLLSW | O755 |
| 2054 | 244862 | FREKKFFCTIL | P501 |
| 2055 | 128534 | PFRPQKVCS | P306 |
| 2177 | 163083 | LRLCIPSTGPL | P227 |
| 2395 | 73447 | HSEASGMVT | P059 |

| Spot | BLU | Sequence | ID |
|------|------|-----------|------|
| 2577 | 154368 | EQQRAEDIT | P090 |
| 2585 | 70828 | RLPEAPKLTH | P312 |
| 2595 | 192017 | VACRLAQLT | P527 |
| 2611 | 76290 | GGKGGLCQS | O959 |
| 2653 | 74938 | RHSRSSLNTV | P981 |
| 2744 | 151871 | GSSSGHTSTT | P250 |
| 2839 | 100826 | LRTLLLQQSN | Q997 |
| 2926 | 107169 | RRVRKLPSTT | Q154 |
| 2927 | 78837 | RGMKRLTST | Q153 |
| 2928 | 75629 | RGIKKITSTAL | P518 |
| 3214 | 66823 | SQKVAVYST | P079 |
| 3340 | 80125 | TLDSQIQETS | P278 |
| 3666 | 73802 | WCIQFNRGS | Q149 |
| 3731 | 77071 | FVPWIKSVT | P567 |
| 3842 | 129725 | DWAKEKQH | Q149 |
| 3843 | 98912 | ALPAHHNAT | Q064 |
| 3845 | 97639 | EWAKERKLT | O004 |
| 3874 | 289032 | NALEEPKGT | O605 |
| 3969 | 147564 | HHHHTLPGS | Q030 |
| 4109 | 79085 | ARLVKGERT | O148 |
| 4233 | 187987 | NWIKRRPQT | O607 |
| 4268 | 80178 | IAKADAQES | Q007 |
| 4336 | 77065 | ENLIEFIRSRL | Q151 |
| 4481 | 68498 | DEDQHTQIT | O006 |
| 4833 | 104909 | TERRSKSCTIL | Q928 |
| 5028 | 212567 | SSTCILQETSL | Q9Y2 |
| 5185 | 75304 | AANGLMQT | P353 |
| 5529 | 66775 | IHQNPGEFC | P235 |
| 5578 | 84892 | IHFTRRAITD | P130 |
| 5615 | 201912 | DGQEEQVTT | Q9UL |
| 5634 | 98102 | QISEEYMQT | P164 |
| 5840 | 67977 | QSFLQTETSV | P415 |
| 5873 | 69941 | RVVTRPCQC | O149 |
| 5945 | 139137 | SYRRPPSATC | Q141 |
| 5960 | 72701 | FIPTLFCLCRL | Q141 |
| 5977 | 70518 | NFIFDEFRTV | Q127 |
| 5999 | 122101 | PWSPRLESS | O150 |
| 6010 | 88885 | SRLERIESTEI | O602 |
| 6121 | 117998 | CGKGFSYSSV | Q9UJ |
| 6214 | 77093 | DGYDWGPA | O950 |

**Footnotes:** The table is sorted by the spot numbers. The signal intensities are revealed in Biochemical Light Units (BLU). The IDs are taken from the Uniprot database (http://www.uniprot.org/).

**Table A3: 80 best binding sequences of the 6223-HumLib incubation with N1P1**

| Spot | BLU | Sequences | ID |
|------|-----|-----------|-----|
| 7 | 118369 | DEAEAGEGGE | P2931 |
| 237 | 361617 | AQWVDSYYTSL | Q926 |
| 314 | 153424 | CSLAPNIISQL | P3004 |
| 383 | 113716 | EWLVETLKSRQ | P4061 |
| 431 | 717705 | GDFREDDDTAL | Q046 |
| 438 | 689416 | GSPLHSLETSL | P2002 |
| 439 | 1,32E+09 | GSPIHSLETSL | Q018 |
| 495 | 306764 | GRNCSTNDSLL | P0755 |
| 613 | 213959 | GPHSFVTSSYL | Q9UL |
| 731 | 327978 | EMGAIKNLTSF | Q112 |
| 785 | 252824 | NRVGFAEAARL | P0733 |
| 834 | 273824 | LQDSRVYVSSL | Q139 |
| 857 | 235510 | ESENATSLTTF | P3230 |
| 962 | 900453 | ETEEEVQDTRL | P1356 |
| 1021 | 96967 | SLQERGGASLK | Q929 |
| 1121 | 193479 | PKNPATKQQK | O751 |
| 1151 | 180466 | SGPASETLDCS | P0735 |
| 1244 | 708189 | GPQAQAENTA | P1227 |
| 1253 | 226959 | NSRPHTNETSL | P2350 |
| 1320 | 173276 | SSKARSDDLSV | P3638 |
| 1367 | 341425 | NKAKHDELTYF | P0408 |
| 1451 | 766293 | WGMGSQSCTL | P4844 |
| 1609 | 297994 | DTISFTQTSQF | P4300 |
| 1619 | 116034 | VEKRKANFKDQ | P3008 |
| 1621 | 437554 | NISSTSEPKEE | Q166 |
| 1652 | 211784 | VSLAPVVTTCA | Q068 |
| 1674 | 97595 | LSSMPSASKTG | Q142 |
| 1694 | 392037 | SIVAWTGMLIA | P5685 |
| 1820 | 791638 | KMHIFFTTFAL | P9809 |
| 2099 | 105908 | WNLSIKKEWTE | P5256 |
| 2216 | 247906 | RSLSNINSEML | Q143 |
| 2237 | 460143 | LPWIKRTMKRL | P2071 |
| 2253 | 850143 | SDSEEELPTRL | P4325 |
| 2280 | 103686 | SLEEARKIFRF | P0826 |
| 2282 | 345404 | ALEEARKIFRF | Q167 |
| 2380 | 611788 | NIAVAGYSTRL | Q132 |
| 2395 | 432324 | HSEASGMVTQ | P0598 |
| 2500 | 330231 | LNTTDKESTYF | P2509 |
| 2577 | 1,05E+09 | EQQRAEDITRL | P0901 |
| 2586 | 252642 | AKDHHTDLTTL | P0901 |

| Spot | BLU | Sequences | ID |
|------|-----|-----------|-----|
| 2717 | 568030 | VRGLLLLKTRL | P2080 |
| 2914 | 1,56E+09 | TCGASTTGSRF | O760 |
| 2926 | 127012 | RRVRKLPSTTL | Q154 |
| 2927 | 868983 | RGMKRLTSTRL | Q153 |
| 2928 | 319489 | RGIKKITSTAL | P5181 |
| 2985 | 101761 | LSRRRSAQMRV | Q127 |
| 3043 | 97390 | SAAGPGFSLKF | P2112 |
| 3103 | 123931 | FGQGTKVQIKR | P0443 |
| 3111 | 840374 | FGQGTRLEIKR | P0161 |
| 3173 | 130587 | LSMDHVCLGH | Q995 |
| 3304 | 896686 | FKSREDCCTKF | Q134 |
| 3368 | 192178 | LTVTGKTVRLL | P3399 |
| 3389 | 127588 | SLQASSEKTQQ | Q020 |
| 3427 | 135695 | REVVDSTTSSL | Q144 |
| 3428 | 175974 | REVLDSTTSSL | Q148 |
| 3656 | 142450 | SVKVEAEASRQ | Q157 |
| 3767 | 116099 | NNRSSGCCSGC | Q9UG |
| 3780 | 205302 | GRRLTTSTSTF | Q129 |
| 3797 | 399542 | FIMLTRLVLNS | Q074 |
| 3854 | 99576 | LHSCKTSVGKE | Q154 |
| 4027 | 280313 | VVLTSVTTVLP | O436 |
| 4232 | 163466 | DSSDLVEDSFL | P1623 |
| 4268 | 591867 | IAKADAQESRL | Q007 |
| 4282 | 519925 | DSESQEENTQL | Q019 |
| 4336 | 127743 | ENLIEFIRSRL | Q151 |
| 4639 | 102047 | KTMVTRFNEA | P9817 |
| 4774 | 180442 | SDEDMGFGLF | P0538 |
| 4833 | 213646 | TERRSKSCTIL | Q928 |
| 4891 | 313131 | DNITLLQSVSN | P0857 |
| 4978 | 109960 | QHVTEAFQFHF | O431 |
| 5028 | 643529 | SSTCILQETSL | Q9Y2 |
| 5053 | 242094 | MGRGNIFQKR | P4333 |
| 5098 | 146131 | DRNYVPGKVR | Q9U |
| 5130 | 320192 | HYKTHLVTKNL | Q020 |
| 5134 | 134498 | PGNIPPPPPTN | Q154 |
| 5183 | 182538 | EKSSTMRISYL | P3274 |
| 5184 | 264079 | KRIPLTRTTTF | P3139 |
| 5185 | 410199 | AANGLMQTSK | P3534 |
| 5498 | 193265 | FAPSRKLNTEI | Q130 |
| 5778 | 129473 | GLAYLEETKPL | P3193 |

**Footnotes:** The table is sorted by the spot numbers. The signal intensities are revealed in Biochemical Light Units (BLU). The IDs are taken from the Uniprot database (http://www.uniprot.org/).

**Table A4: 80 best binding sequences of the 6223-HumLib incubation with N1P2**

| Spot | BLU | Sequence | ID |
|------|-----|----------|-----|
| 23 | 125693 | QAEEDWTCTIL | P0097 |
| 412 | 137807 | EQELLDFTNWF | P5055 |
| 431 | 292201 | GDFREDDDTAL | Q046 |
| 438 | 425624 | GSPLHSLETSL | P2002 |
| 439 | 268057 | GSPIHSLETSL | Q018 |
| 481 | 87430 | SSCNLAKETLL | Q9UK |
| 658 | 129919 | ETLHSLQTAFT | Q9NV |
| 788 | 221802 | FKLLDQMETPL | P0831 |
| 835 | 114087 | LADEMICITTL | Q016 |
| 857 | 108432 | ESENATSLTTF | P3230 |
| 906 | 145891 | TSSCDKSDTCF | P4208 |
| 962 | 446304 | ETEEEVQDTRL | P1356 |
| 1018 | 173540 | LCLDTSRETDL | P2246 |
| 1043 | 153547 | VEAETTTTFSP | P3224 |
| 1244 | 255989 | GPQAQAENTA | P1227 |
| 1253 | 165470 | NSRPHTNETSL | P2350 |
| 1300 | 164935 | SNQLAWFDTD | P3522 |
| 1351 | 84434 | IGTMFLRETSL | P3340 |
| 1609 | 144853 | DTISFTQTSQF | P4300 |
| 1703 | 106791 | MENGSLDTFLR | P2932 |
| 2054 | 156441 | FREKKFFCTIL | P5015 |
| 2148 | 104362 | AWLQEKLSFFR | O602 |
| 2170 | 116978 | NIKRKLDTYLQ | P4697 |
| 2253 | 221649 | SDSEEELPTRL | P4325 |
| 2380 | 151652 | NIAVAGYSTRL | Q132 |
| 2395 | 385985 | HSEASGMVTQ | P0598 |
| 2500 | 421373 | LNTTDKESTYF | P2509 |
| 2559 | 233032 | RIQEAPKLTHL | O433 |
| 2577 | 603340 | EQQRAEDITRL | P0901 |
| 2585 | 125873 | RLPEAPKLTHL | P3124 |
| 2743 | 111295 | TSSSVNVSSNL | P2502 |
| 2744 | 369911 | GSSSGHTSTTL | P2502 |
| 2881 | 91123 | GVEISCWSVEL | Q146 |
| 2926 | 88679 | RRVRKLPSTTL | Q154 |
| 2927 | 169804 | RGMKRLTSTRL | Q153 |
| 2928 | 274912 | RGIKKITSTAL | P5181 |
| 3214 | 101913 | SQKVAVYSTCL | P0794 |
| 3251 | 98795 | LRNGLVKDKRF | P2754 |
| 3304 | 100506 | FKSREDCCTKF | Q134 |
| 3372 | 158891 | ETHREVKFTSL | P1552 |

| Spot | BLU | Sequence | ID |
|------|-----|----------|-----|
| 3427 | 118680 | REVVDSTTSSL | Q144 |
| 3454 | 272445 | LGARVSKETPL | P5377 |
| 3486 | 368367 | FGCAEPANTFL | P2434 |
| 3545 | 97662 | AGIENVNSTKF | Q928 |
| 3547 | 238183 | PSTLTIFETAL | O154 |
| 3780 | 182790 | GRRLTTSTSTF | Q129 |
| 3842 | 455484 | DWAKEKQHTR | Q149 |
| 3843 | 147278 | ALPAHHNATRL | Q064 |
| 3845 | 188248 | EWAKERKLTRL | O004 |
| 3874 | 614907 | NALEEPKGTRL | O605 |
| 3882 | 86667 | GLIAGEKETHL | P4806 |
| 3891 | 87727 | IAAITEKETHF | P4806 |
| 3965 | 152072 | ERPTILKSTAF | O760 |
| 3969 | 218941 | HHHHTLPGSV | Q030 |
| 3970 | 155476 | DMIQLMNSTH | Q9UK |
| 4055 | 100339 | AGSENTKDIRL | P4123 |
| 4068 | 340068 | PEFKQNGDTSL | P4790 |
| 4231 | 117110 | APRAEAEDSFL | P0961 |
| 4232 | 105254 | DSSDLVEDSFL | P1623 |
| 4267 | 211686 | DIPGKEFDTPL | Q9NQ |
| 4268 | 183227 | IAKADAQESRL | Q007 |
| 4282 | 278332 | DSESQEENTQL | Q019 |
| 4575 | 140290 | VKKPGKKCTVF | O146 |
| 4788 | 147855 | LERGLESATSL | O757 |
| 4833 | 131699 | TERRSKSCTIL | Q928 |
| 5027 | 333030 | DGGRDQQETN | Q929 |
| 5028 | 335845 | SSTCILQETSL | Q9Y2 |
| 5181 | 239239 | NGTCTSRITTL | P3087 |
| 5184 | 178038 | KRIPLTRTTTF | P3139 |
| 5218 | 236013 | KINKTEICSQL | Q9UH |
| 5592 | 127653 | PLLEACEFLRK | P0278 |
| 5648 | 449104 | QNQELPSCSSR | P5380 |
| 5663 | 82641 | MEGAWSMSA | Q156 |
| 5744 | 129921 | NLGHTPFVDEL | P2269 |
| 5838 | 110671 | LRWVRKTPWY | P1820 |
| 5934 | 82897 | VREIGTVTYLM | P5399 |
| 6010 | 215090 | SRLERIESTEI | O602 |
| 6016 | 134307 | LTYHQRIHNVT | Q9Y2 |
| 6059 | 199932 | KEGSRSYCTDS | Q9UF |
| 6175 | 289592 | TGEKPYSCKVC | P1702 |

**Footnotes:** The table is sorted by the spot numbers. The signal intensities are revealed in Biochemical Light Units (BLU). The IDs are taken from the Uniprot database (http://www.uniprot.org/).

**Table A5: 80 best binding sequences of the 6223-HumLib incubation with N1P2**

| Spot | BLU | Sequence | ID | Spot | BLU | Sequence | ID |
|---|---|---|---|---|---|---|---|
| 23 | 221540 | QAEEDWTCTIL | P0097 | 3666 | 67778 | WCIQFNRGSRL | Q149 |
| 237 | 60319 | AQWVDSYYTSL | Q926 | 3842 | 247921 | DWAKEKQHTR | Q149 |
| 431 | 65006 | GDFREDDDTAL | Q046 | 3843 | 284083 | ALPAHHNATRL | Q064 |
| 438 | 127482 | GSPLHSLETSL | P2002 | 3845 | 193825 | EWAKERKLTRL | O004 |
| 439 | 102836 | GSPIHSLETSL | Q018 | 3874 | 467173 | NALEEPKGTRL | O605 |
| 481 | 74125 | SSCNLAKETLL | Q9UK | 3954 | 63484 | VLKDDELKTKL | P4672 |
| 495 | 83383 | GRNCSTNDSLL | P0755 | 3965 | 57579 | ERPTILKSTAF | O760 |
| 613 | 109367 | GPHSFVTSSYL | Q9UL | 3970 | 59040 | DMIQLMNSTH | Q9UK |
| 834 | 102611 | LQDSRVYVSSL | Q139 | 4176 | 116708 | DPEIVVQATVL | O007 |
| 835 | 84873 | LADEMICITTL | Q016 | 4231 | 173209 | APRAEAEDSFL | P0961 |
| 962 | 673632 | ETEEEVQDTRL | P1356 | 4232 | 206536 | DSSDLVEDSFL | P1623 |
| 1244 | 86588 | GPQAQAENTA | P1227 | 4233 | 99584 | NWIKRRPQTKL | O607 |
| 1253 | 93570 | NSRPHTNETSL | P2350 | 4267 | 261096 | DIPGKEFDTPL | Q9NQ |
| 1351 | 57725 | IGTMFLRETSL | P3340 | 4268 | 227828 | IAKADAQESRL | Q007 |
| 1367 | 82523 | NKAKHDELTYF | P0408 | 4282 | 142404 | DSESQEENTQL | Q019 |
| 1450 | 317744 | MEAQGCSCTLL | P4335 | 4336 | 118677 | ENLIEFIRSRL | Q151 |
| 1451 | 204560 | WGMGSQSCTL | P4844 | 4575 | 63417 | VKKPGKKCTVF | O146 |
| 1495 | 70760 | GGAPVSAGTIF | Q076 | 4599 | 67124 | GGACGGYCSVL | Q9NP |
| 1514 | 302063 | IGKIGTVMTFL | P3004 | 4742 | 137918 | RFTTKRPNTFF | Q025 |
| 1609 | 104190 | DTISFTQTSQF | P4300 | 4781 | 94426 | VWRSKRTDTLL | O608 |
| 1703 | 70712 | MENGSLDTFLR | P2932 | 4833 | 65288 | TERRSKSCTIL | Q928 |
| 1954 | 68522 | LQDWASVGAF | Q929 | 5028 | 90063 | SSTCILQETSL | Q9Y2 |
| 2053 | 77188 | FREKKFFCALL | P2979 | 5120 | 99861 | YRPRRKTKTLL | P3571 |
| 2054 | 278356 | FREKKFFCTIL | P5015 | 5176 | 105162 | QRDRYSHWTK | Q050 |
| 2055 | 88081 | PFRPQKVCSFL | P3067 | 5181 | 100643 | NGTCTSRITTL | P3087 |
| 2110 | 78999 | KSKSCHDLSVL | P5504 | 5183 | 149106 | EKSSTMRISYL | P3274 |
| 2246 | 84725 | FFNVIYWSIYL | P4816 | 5184 | 189672 | KRIPLTRTTTF | P3139 |
| 2253 | 138475 | SDSEEELPTRL | P4325 | 5218 | 95242 | KINKTEICSQL | Q9UH |
| 2380 | 234812 | NIAVAGYSTRL | Q132 | 5560 | 209474 | LDQTLLELNNM | P0949 |
| 2395 | 106255 | HSEASGMVTQ | P0598 | 5616 | 383595 | SMEPNQEETN | Q9Y2 |
| 2500 | 181616 | LNTTDKESTYF | P2509 | 5635 | 68321 | IVSMYLYCNLQ | O606 |
| 2577 | 247967 | EQQRAEDITRL | P0901 | 5662 | 174863 | LFGSGTTLVVT | P0397 |
| 2927 | 194460 | RGMKRLTSTRL | Q153 | 5691 | 80647 | RDRTVQSPQSK | Q156 |
| 2928 | 76003 | RGIKKITSTAL | P5181 | 5783 | 86757 | GTMFYWSRIEY | O758 |
| 3257 | 71173 | FGGGTQLTVLR | P0170 | 5806 | 58892 | SEFYPRDSAKH | P2128 |
| 3304 | 334371 | FKSREDCCTKF | Q134 | 5978 | 314534 | QPLRKDKDKKN | Q925 |
| 3413 | 79397 | NFTSLTWISTL | O434 | 5984 | 216916 | YTDDIPLLKEA | Q925 |
| 3486 | 170629 | FGCAEPANTFL | P2434 | 6027 | 133431 | SAPEAEQGGAE | P1699 |
| 3545 | 178819 | AGIENVNSTKF | Q928 | 6143 | 218017 | FSLWSHEQTH | Q9ULJ |
| 3547 | 450681 | PSTLTIFETAL | O154 | 6159 | 62284 | IMRHHKEVGLP | P1701 |

**Footnotes:** The table is sorted by the spot numbers. The signal intensities are revealed in Biochemical Light Units (BLU). The IDs are taken from the Uniprot database (http://www.uniprot.org/).

**Table A6: 80 best binding sequences of the 6223-HumLib incubation with N2P2**

| Spot | BLU | Sequence | ID |
|------|------|----------|-----|
| 23 | 221540 | QAEEDWTCTIL | P0097 |
| 237 | 60319 | AQWVDSYYTSL | Q926 |
| 431 | 65006 | GDFREDDDTAL | Q046 |
| 438 | 127482 | GSPLHSLETSL | P2002 |
| 439 | 102836 | GSPIHSLETSL | Q018 |
| 481 | 74125 | SSCNLAKETLL | Q9UK |
| 495 | 83383 | GRNCSTNDSLL | P0755 |
| 613 | 109367 | GPHSFVTSSYL | Q9UL |
| 834 | 102611 | LQDSRVYVSSL | Q139 |
| 835 | 84873 | LADEMICITTL | Q016 |
| 962 | 673632 | ETEEEVQDTRL | P1356 |
| 1244 | 86588 | GPQAQAENTA | P1227 |
| 1253 | 93570 | NSRPHTNETSL | P2350 |
| 1351 | 57725 | IGTMFLRETSL | P3340 |
| 1367 | 82523 | NKAKHDELTYF | P0408 |
| 1450 | 317744 | MEAQGCSCTLL | P4335 |
| 1451 | 204560 | WGMGSQSCTL | P4844 |
| 1495 | 70760 | GGAPVSAGTIF | Q076 |
| 1514 | 302063 | IGKIGTVMTFL | P3004 |
| 1609 | 104190 | DTISFTQTSQF | P4300 |
| 1703 | 70712 | MENGSLDTFLR | P2932 |
| 1954 | 68522 | LQDWASVGAF | Q929 |
| 2053 | 77188 | FREKKFFCALL | P2979 |
| 2054 | 278356 | FREKKFFCTIL | P5015 |
| 2055 | 88081 | PFRPQKVCSFL | P3067 |
| 2110 | 78999 | KSKSCHDLSVL | P5504 |
| 2246 | 84725 | FFNVIYWSIYL | P4816 |
| 2253 | 138475 | SDSEEELPTRL | P4325 |
| 2380 | 234812 | NIAVAGYSTRL | Q132 |
| 2395 | 106255 | HSEASGMVTQ | P0598 |
| 2500 | 181616 | LNTTDKESTYF | P2509 |
| 2577 | 247967 | EQQRAEDITRL | P0901 |
| 2927 | 194460 | RGMKRLTSTRL | Q153 |
| 2928 | 76003 | RGIKKITSTAL | P5181 |
| 3257 | 71173 | FGGGTQLTVLR | P0170 |
| 3304 | 334371 | FKSREDCCTKF | Q134 |
| 3413 | 79397 | NFTSLTWISTL | O434 |
| 3486 | 170629 | FGCAEPANTFL | P2434 |
| 3545 | 178819 | AGIENVNSTKF | Q928 |
| 3547 | 450681 | PSTLTIFETAL | O154 |

| Spot | BLU | Sequence | ID |
|------|------|----------|-----|
| 3666 | 67778 | WCIQFNRGSRL | Q149 |
| 3842 | 247921 | DWAKEKQHTR | Q149 |
| 3843 | 284083 | ALPAHHNATRL | Q064 |
| 3845 | 193825 | EWAKERKLTRL | O004 |
| 3874 | 467173 | NALEEPKGTRL | O605 |
| 3954 | 63484 | VLKDDELKTKL | P4672 |
| 3965 | 57579 | ERPTILKSTAF | O760 |
| 3970 | 59040 | DMIQLMNSTH | Q9UK |
| 4176 | 116708 | DPEIVVQATVL | O007 |
| 4231 | 173209 | APRAEAEDSFL | P0961 |
| 4232 | 206536 | DSSDLVEDSFL | P1623 |
| 4233 | 99584 | NWIKRRPQTKL | O607 |
| 4267 | 261096 | DIPGKEFDTPL | Q9NQ |
| 4268 | 227828 | IAKADAQESRL | Q007 |
| 4282 | 142404 | DSESQEENTQL | Q019 |
| 4336 | 118677 | ENLIEFIRSRL | Q151 |
| 4575 | 63417 | VKKPGKKCTVF | O146 |
| 4599 | 67124 | GGACGGYCSVL | Q9NP |
| 4742 | 137918 | RFTTKRPNTFF | Q025 |
| 4781 | 94426 | VWRSKRTDTLL | O608 |
| 4833 | 65288 | TERRSKSCTIL | Q928 |
| 5028 | 90063 | SSTCILQETSL | Q9Y2 |
| 5120 | 99861 | YRPRRKTKTLL | P3571 |
| 5176 | 105162 | QRDRYSHWTK | Q050 |
| 5181 | 100643 | NGTCTSRITTL | P3087 |
| 5183 | 149106 | EKSSTMRISYL | P3274 |
| 5184 | 189672 | KRIPLTRTTTF | P3139 |
| 5218 | 95242 | KINKTEICSQL | Q9UH |
| 5560 | 209474 | LDQTLLELNNM | P0949 |
| 5616 | 383595 | SMEPNQEETN | Q9Y2 |
| 5635 | 68321 | IVSMYLYCNLQ | O606 |
| 5662 | 174863 | LFGSGTTLVVT | P0397 |
| 5691 | 80647 | RDRTVQSPQSK | Q156 |
| 5783 | 86757 | GTMFYWSRIEY | O758 |
| 5806 | 58892 | SEFYPRDSAKH | P2128 |
| 5978 | 314534 | QPLRKDKDKKN | Q925 |
| 5984 | 216916 | YTDDIPLLKEA | Q925 |
| 6027 | 133431 | SAPEAEQGGAE | P1699 |
| 6143 | 218017 | FSLWSHEQTH | Q9ULJ |
| 6159 | 62284 | IMRHHKEVGLP | P1701 |

**Footnotes:** The table is sorted by the spot numbers. The signal intensities are revealed in Biochemical Light Units (BLU). The IDs are taken from the Uniprot database (http://www.uniprot.org/).

# 13 Eidesstattliche Erklärung

Hiermit versichere ich, die vorliegende Dissertation selbstständig und ohne unerlaubte Hilfe angefertigt zu haben.

Bei der Verfassung der Dissertation wurden keine anderen als die im Text aufgeführten Hilfsmittel verwendet.

Ein Promotionsverfahren wurde zu keinem früheren Zeitpunkt an einer anderen Hochschule oder bei einem anderen Fachbereich beantragt.

Berlin, 12.02.2007

Lars Vouilleme

# 14      Curriculum Vitae and scientific contributions

**Work Experience**

| | |
|---|---|
| since 07/2008 | **PhD Thesis**<br><br>AG Molekulare Bibliotheken<br><br>Institut für Medizinische Immunologie<br><br>Charité – Universitätsmedizin Berlin<br><br>   ▪  Engineering Peptide Inhibitors to reduce the pathogenicity of cystic fibrosis |
| 05/2011 to 11/2011 | **Visiting Scientist**<br><br>Lab of Dean R. Madden, Ph.D. (Professor of Biochemistry)<br><br>Department of Biochemistry<br><br>Dartmouth Medical School (Dartmouth College) |
| 07/2007 to 03/2008 | **Diploma Thesis**<br><br>AG Molekulare Bibliotheken<br><br>Institut für Medizinische Immunologie<br><br>Charité – Universitätsmedizin Berlin<br><br>   ▪  Synthese eines selektiven, proteasestabilen Inhibitors der CAL-PDZ-Domäne zur Reduktion der Pathogenität von Mukoviszidose |

## Education

| 04/2003 to 03/2008 | Freie Universität Berlin |
| | Course of studies: Diploma Biology |
| | Main subject: Genetics/Physiology/Zoology |
| | Grade: 1.0 |
| 04/2002 to 03/2003 | TU Berlin |
| | Course of studies: Business management |
| 1994 to 2001 | Werner-von-Siemens Gymnasium |
| | Berlin-Zehlendorf (Schlachtensee) |
| | Degree: Abitur 2.3 |

## Alternative Service

| 09/2001 to 02/2002 | Behring Klinikum |
| | Berlin-Zehlendorf |

## Teaching

| 2005 to 2007 | Biochemistry for biologist („Grundpraktikum") |
| | AG Kuhl |
| | Freie Universität Berlin |

## Languages

| | German (native) |
| | English (fluent) |
| | Spanish (basics) |
| | French (basics) |

**SCIENTIFIC CONTRIBUTIONS**

**Publications**

**(peer-review)**

| | |
|---|---|
| 2012 | Cushing, P.R., **Vouilleme, L.**, Amacher, J.F., Boisguerin, P., Madden, D.R., Engineering a CAL Inhibitor with Single-PDZ Specificity to Stabilize ΔF508-CFTR.Ssubmitted to **Proceedings of the National Academy of Sciences** (PNAS) |
| 2012 | Weski, J., Meltzer, M., Spaan, L., Mönig, T., Oeljeklaus, J., Hauske, P., **Vouilleme, L.**, Volkmer, R., Boisguerin, P., Boyd, D., Huber, R., Kaiser, M., Chemical Biology Approaches Reveal Conserved Features of a C-Terminal Processing PDZ Protease. **Chembiochem**. 2012 Feb 13;13(3):402-8. |
| 2010 | Cushing, P.R., **Vouilleme, L.**, Pellegrini, M., Boisguerin, P., Madden, D.R., A Stabilizing Influence: CAL PDZ Inhibition Extends the Half-Life of ΔF508-CFTR. **Angew Chem Int Ed Engl.** 2010 Dec 17;49(51):9907-11. |
| 2010 | **Vouilleme, L**., Cushing, P.R., Volkmer, R., Madden, D.R., Boisguerin, P. Engineering Peptide Inhibitors to Overcome PDZ Binding Promiscuity. **Angew Chem Int Ed Engl.** 2010 Dec 17;49(51):9912-6**.** |

**Conference Poster Presentations**

| | |
|---|---|
| 2010 | **Vouilleme, L.**, Cushing, P.R., Madden, D.R., Volkmer, R., Boisguerin, P., CAL-selective PDZ Inhibitors to Treat Cystic Fibrosis: A SPOT Synthesis Based Study, 31th European Peptide Symposium, 2010, Copenhagen (Denmark). |
| 2009 | **Vouilleme, L.**, Cushing, P.R., Madden, D.R., Volkmer, R., Boisguerin, P., Using SPOT Synthesis for drug design: a peptide based approach to reduce the pathogenicity of cystic fibrosis, 9th German Peptide Symposium, 2009, Göttingen (Germany). |
| 2009 | **Vouilleme, L.**, Cushing, P.R., Madden, D.R., Volkmer, R., Boisguerin, P., Using SPOT Synthesis for drug design: A peptide based approach to design CAL selective PDZ inhibitors, 3rd European Cystic Fibrosis Young Investigators Meeting, 2009, Lille (France) |

**Oral Presentations**

| | |
|---|---|
| 05/07/10 | Using Spot-Synthesis for drug design: A peptide based approach to design CAL selective PDZ inhibitors, 12th Naples Workshop on Bioactive Peptides, Naples (Italy). |
| 28/08/2009 | Using SPOT Synthesis for drug design: A peptide based approach to design CAL selective PDZ inhibitors, 3rd European Cystic Fibrosis Young Investigators Meeting, Lille (France). |

**Abstracts**

| | |
|---|---|
| 2010 | 31st European Peptide Symposium, Copenhagen, Denmark |
| 2009 | 12th Naples Workshop on Bioactive Peptides, Naples, Italy |
| 2009 | 9th German Peptide Symposium, Göttingen, Germany |
| 2009 | 23rd NACFC, Minneapolis, Minnesota |

| | |
|---|---|
| **Patent** | PCT/US2009/061246 |